

12-2013

# Engineering Beta-Cell Spheroids for Type 1 Diabetes Treatment

Xiaoyan Liu

Clemson University, liu9832129@gmail.com

Follow this and additional works at: [https://tigerprints.clemson.edu/all\\_dissertations](https://tigerprints.clemson.edu/all_dissertations)



Part of the [Biomedical Engineering and Bioengineering Commons](#)

---

## Recommended Citation

Liu, Xiaoyan, "Engineering Beta-Cell Spheroids for Type 1 Diabetes Treatment" (2013). *All Dissertations*. 1225.  
[https://tigerprints.clemson.edu/all\\_dissertations/1225](https://tigerprints.clemson.edu/all_dissertations/1225)

This Dissertation is brought to you for free and open access by the Dissertations at TigerPrints. It has been accepted for inclusion in All Dissertations by an authorized administrator of TigerPrints. For more information, please contact [kokeefe@clemson.edu](mailto:kokeefe@clemson.edu).

ENGINEERING BETA-CELL SPHEROIDS FOR TYPE I DIABETES TREATMENT

---

A Dissertation  
Presented to  
the Graduate School of  
Clemson University

---

In Partial Fulfillment  
of the Requirements for the Degree  
Doctor of Philosophy  
Bioengineering

---

by  
Xiaoyan Liu  
December 2013

---

Accepted by:  
Martine LaBerge, PhD, Committee Chair  
Xuejun Wen, PhD  
Ning Zhang, PhD  
Ken Webb, PhD

## ABSTRACT

Diabetes mellitus, the third most common disease in the world, is a chronic metabolic disorder caused by a failure of insulin production and/or an inability to respond to insulin. Specifically, type 1 diabetes is a disorder characterized by targeted autoimmune-directed destruction of a patient's  $\beta$ -cell population within the pancreatic islets of Langerhans. The current primary treatment for type 1 diabetes is daily multiple insulin injections. However, this treatment cannot provide sustained physiological release, and the insulin amount is not finely tuned to glycemia. Pancreatic transplants or islet transplants would be the preferred treatment method but the lack of donor tissue and immunoincompatibility has been shown to be a roadblock to their widespread use.

The objective of this project is to develop an effective strategy for the treatment of type 1 diabetes using  $\beta$ -cells based replacement therapy. To improve the viability of transplanted  $\beta$ -cells, one novel approach is to transplant optimal size range of  $\beta$ -cell spheroids rather than cell suspension. Uniform sized multicellular spheroids can be coated with a thin layer of non-degradable hydrogel for immunoisolation. In addition, the survival of spheroids of optimized size can be further improved with a novel coating of multiple layers of human mesenchymal stem cells (hMSCs), a cell type that has profound immunoregulatory effect, to prevent graft rejection. To prevent hMSC migrate away from spheroids, another layer of non-degradable hydrogel can be added. To further improve the viability and suppress the immune rejection, spheroids will be encapsulated with nanoparticles loaded with angiogenic and immune regulatory molecules. By this means

the spheroid will passively evade the complications of stressors in addition to actively modulating the immune microenvironment for regulatory tolerance and long-term engraftment.

Firstly, through optimizing our hydrogel systems based on poly (ethylene glycol) (PEG), we have created specific niche for  $\beta$ -cells to form artificial islets *in vitro*. We have found that the optimal condition is the concentration of PEG at 5% and the ratios of 4-arm thiolated PEG to 4-arm PEG acrylate at 1:2. Conjugated with adhesive peptides, especially, RGD at 0.2 mM, can significantly promote the glucose stimulated insulin secretion of encapsulated  $\beta$ -cells. Secondly, we have fabricated different sizes of uniformed  $\beta$ -cells spheroids through our designed high-throughput automatic spheroids maker. Beta-cells in the spheroids of 200  $\mu\text{m}$  exhibited largest insulin secretion based on glucose stimulus when compared to others with sizes of 100, 300, 400 and 500  $\mu\text{m}$ . The novel core-shell structured spheroids-hMSCs complex was successfully achieved. Methylcellulose hydrogel was applied as physical barrier on the surface of  $\beta$ -cells spheroids to inhibit invasion of hMSCs. Human MSCs prevented apoptosis of  $\beta$ -cells spheroids and benefited insulin secretion when exposed to pro-inflammatory cytokines. Thirdly, immune regulatory molecules [leukemia inhibitory factor (LIF) and interleukin 10 (IL-10)] and angiogenic molecule [vascular endothelial growth factor (VEGF)] loaded poly (lactic-co-glycolic acid) (PLGA) nanoparticles have been successfully fabricated through solvent extraction/evaporation technique. These growth factors can be controlled release about 6 weeks. The bioactivity of released VEGF has been confirmed by the *in vitro* HAEC proliferation assay. Finally,  $\beta$ -cells spheroids were transplanted under the



kidney capsule to treat diabetic mice. Beta-cells spheroids kept the glucose level of diabetic mice constant. Co-transplanted hMSCs suppressed the host inflammation response, activated the regulatory T cells and also promoted angiogenesis at the transplantation site. The  $\beta$ -cells spheroids/hMSCs/hydrogel complex initiated a mild inflammatory response. The LIF and IL-10, and VEGF loaded complex can further inhibited this response and promoted blood vessel network formation at the transplantation site. Our approach holds a great potential to treat type 1 diabetes

## DEDICATION

This thesis is dedicated to my family and friends for their generous support. Especially, I would like to thank my husband, Xiaowei Li, for always being there for me. I could not have made it through graduate school without him.

## ACKNOWLEDGMENTS

Foremost, I would like to express my sincere gratitude to my advisor Prof. Xuejun Wen for the continuous support of my PhD study and research, for his patience, motivation, enthusiasm, and immense knowledge. His guidance helped me in all the time of research and writing of this thesis. I could not have imagined having a better advisor and mentor for my PhD study.

Besides my advisor, I would also like to acknowledge the help and support of my dissertation committee members, Prof. Ning Zhang, Prof. Martin LaBerge, and Prof. Ken Webb. Your encouragement, insightful comments, and hard questions made this dissertation become a reality. Additionally, I would like to thank Dr. Hongjun Wang and Dr. Qian Kang, as they both had a great influence on my research and provided me with a lot of guidance as well.

This work would not have been completed without the help of the entire Clemson-MUSC bioengineering program. I would like to thank all the members of the Wen Regenerative Medicine Laboratory, for their friendship and assistance. I would also like to thank Dr. Huangsheng Dong, for his assistance in my animal experiments.

## TABLE OF CONTENTS

	Page
Title Page .....	i
ABSTRACT .....	ii
DEDICATION .....	v
ACKNOWLEDGMENTS .....	vi
LIST OF TABLES .....	xi
LIST OF FIGURES .....	xii
CHAPTER	
1. INTRODUCTION .....	1
1.1 Type 1 diabetes and current treatments .....	1
1.2 Study objectives and specific aims .....	2
1.3 Dissertation organization .....	3
2. BIOENGINEERING STRATEGIES FOR TYPE 1 DIABETES TREATMENT .....	5
2.1 Introduction .....	5
2.2 Diabetes types and current treatments .....	7
2.2.1 Diabetes types .....	7
2.2.2 Current clinical treatments for type 1 diabetes .....	8
2.2.3 New treatments under clinical trial and development .....	9
2.3 Bioengineering strategies for type 1 diabetes treatment .....	11
2.3.1 Insulin control release .....	11
2.3.2 Islets transplantation .....	21
2.3.3 Beta cells transplantation .....	31
2.3.4 Cell sources for $\beta$ -cell regeneration .....	42
2.4 Conclusion remarks .....	46
2.5 References .....	47
3. DEVELOPING HYDROGELS SYSTEMS FOR THE FORMATION OF ISLETS OF LANGERHAM FROM SINGLE BETA-CELLS .....	65
3.1 Introduction .....	65
3.2 Materials and methods .....	67

## Table of Contents (Continued)

	Page
3.2.1	Materials ..... 67
3.2.2	Synthesis of thiolated multi-arm PEG ..... 67
3.2.3	Preparation of hydrogels ..... 68
3.2.4	Rheological characterization of hydrogels ..... 68
3.2.5	Swelling of hydrogels ..... 70
3.2.6	Peptide conjugated to hydrogels ..... 70
3.2.7	Cell culture and encapsulation ..... 71
3.2.8	Cell viability ..... 71
3.2.9	Glucose-stimulated insulin secretion ..... 72
3.2.10	Statistical analysis ..... 72
3.3	Results ..... 72
3.3.1	Hydrogel characterization ..... 72
3.3.2	Effects of PEG hydrogels with different ratios on $\beta$ -cell clusters formation ..... 77
3.3.3	Effects of PEG hydrogels with different ratios on glucose-stimulated insulin secretion ..... 78
3.3.4	Effects of peptides on $\beta$ -cell survival and clusters formation ..... 79
3.3.5	Effects of peptides on $\beta$ -cell based on glucose-stimulated insulin secretion ..... 81
3.4	Discussion ..... 82
3.5	Conclusion ..... 86
3.6	References ..... 86
4	AUTOMATIC ROBOTIC FABRICATION OF BETA-CELL SPHEROIDS AND MSC MICROENCAPSULATION IN A CORE-SHELL CONFIGURATION FOR IMMUNOMODULATION ..... 88
4.1	Introduction ..... 88
4.2	Materials and Methods ..... 91
4.2.1	Materials ..... 91
4.2.2	Cell culture ..... 92
4.2.3	Beta-cells spheroids fabrication ..... 92
4.2.4	Viability of cells in microwells ..... 93
4.2.5	Morphology of spheroids ..... 94
4.2.6	Co-culture RIN-m cells and hMSCs ..... 94
4.2.7	Co-culture $\beta$ -cells spheroids and hMSCs ..... 94
4.2.8	Core/shell structure RIN-m/hMSCs complex fabrication ..... 95
4.2.9	Insulin release from hMSCs coated $\beta$ -cells spheroids ..... 96
4.2.10	Bioactivation of hMSCs to pro-inflammatory cytokines ..... 97
4.2.11	Analysis of $\beta$ -cells apoptosis by TUNEL assay ..... 97

## Table of Contents (Continued)

	Page
4.2.12 Statistical analysis.....	98
4.3 Results.....	98
4.3.1 Fabrication of $\beta$ -cells spheroids with uniform size.....	98
4.3.2 Glucose-stimulated insulin secretion.....	100
4.3.3 Human MSCs invasion into $\beta$ -cells spheroids.....	102
4.3.4 Construction of unique RIN-m/hMSCs complex with core/shell structure .....	103
4.3.5 Insulin secretion from RIN-m/hMSCs hybrid spheroids.....	105
4.3.6 Effects of hMSCs on $\beta$ -cells spheroids.....	107
4.3.7 Agarose hydrogel coating.....	109
4.4 Discussion.....	109
4.5 Conclusion.....	112
4.6 References.....	113
5 LIF, IL-10 AND VEGF-LOADED NANOPARTICLES COATED MSC MICROENCAPSULATED BETA-CELL SPHEROIDS.....	116
5.1 Introduction.....	116
5.2 Materials and methods.....	119
5.2.1 Materials.....	119
5.2.2 Cell culture.....	119
5.2.3 Fabrication of IL-10, LIF and VEGF-loaded PLGA nanoparticles.....	120
5.2.4 IL-10, LIF and VEGF release from PLGA nanoparticles.....	120
5.2.5 Bioactivity of LIF and IL-10 nanoparticles to pro-inflammatory cytokines .....	121
5.2.6 Analysis of $\beta$ -cells apoptosis by TUNEL assay.....	121
5.2.7 Bioactivity of VEGF released from nanoparticles.....	122
5.2.8 Loaded nanoparticles in RIN-m/hMSCs hybrid spheroids.....	122
5.2.9 Statistical analysis.....	123
5.3 Results and discussion.....	123
5.3.1 LIF and IL-10 nanoparticles.....	123
5.3.2 Bioactivity of released IL-10 and LIF to pro-inflammatory cytokines...	125
5.3.3 Bioactivity of released VEGF on HAECs.....	127
5.3.4 Loaded nanoparticles in RIN-m/hMSCs hybrid spheroids.....	130
5.4 Conclusion.....	130
5.5 References.....	131
6 IN VIVO EVALUATION OF BETA-CELLS/MSC HYBRID SPHERIODS FOR THE TREATMENT OF TYPE 1 DIABETES.....	133

## Table of Contents (Continued)

	Page
6.1 Introduction .....	133
6.2 Materials and Methods .....	134
6.2.1 Materials .....	134
6.2.2 Animals .....	134
6.2.3 Animal model and spheroids transplantation.....	135
6.2.4 Tissue processing, histology and immunohistochemistry .....	135
6.3 Results and discussion.....	136
6.3.1 Macro-inspection of transplantation of spheroids.....	136
6.3.2 Glucose level investigation .....	137
6.3.3 Survived hMSCs at the transplantation site .....	139
6.3.4 Macrophages .....	140
6.3.5 Regulatory T cells .....	142
6.3.6 Blood vessels .....	144
6.4 Conclusion.....	145
6.5 References .....	146
7 OVERALL CONCLUSIONS AND FUTURE DIRECTIONS .....	149
7.1 Overall conclusions .....	149
7.2 Future directions.....	151
7.2.1 Hydrogels conjugated with functional peptides.....	151
7.2.2 Adjusting the structure of $\beta$ -cells spheroids-hMSCs complex .....	152
7.2.3 Clinical use of our approaches.....	153
7.3 References .....	154

## LIST OF TABLES

Table	Page
Table 2. 1 Insulin analogs by amino acid substitutions [33].....	13
Table 2. 2 Peptide conjugated PEG hydrogels for $\beta$ -cells encapsulation. ....	35
Table 3. 1 Mesh size of hydrogels with various concentrations of PEG and different ratios of 4arm thiolated PEG to PEGTA. ....	83



## LIST OF FIGURES

Figure	Page
Figure 2. 1 Islet transplantation for the treatment of type 1 diabetes in clinical [21].	10
Figure 2. 2 Insulin loading and release from pH/thermo-sensitive hydrogels. (A) The polymer solution in sol state at 10 °C and pH 7.0 with the ionic complex between insulin and PAE–PCL–PEG–PCL–PAE. (B) The gel formed by insulin free PAE–PCL–PEG–PCL–PAE after injection to human body (37 °C and pH 7.4). (C) Insulin release from gel by polymer degradation [65].	19
Figure 2. 3 Microencapsulation of islets with alginate-polylysine [111].	25
Figure 2. 4 Modification of cell surface with synthetic polymers: Covalent bonding, hydrophobic interaction, electrostatic interaction, and the layer-by-layer method [125].	28
Figure 2. 5 Encapsulation of islets with living cells. (A) Hamster islets modified with polyA20-PEG-lipid were treated with (a-1, FITC) FITC-labeled polyT20. (a-2) Naked islets were treated with FITC-labeled polyT20. (B) Attachment of polyT20-PEG-lipid modified GFP-HEK cells onto the surface of polyA20-PEG-lipid modified hamster islets. An islet was observed by a confocal laser scanning microscope for (b-1, GFP) and a phase contrast microscope (b-2). (C) GFP-HEK cells-immobilized islets were cultured for 1, 3, and 5 days. Islets were observed by a phase contrast microscope (left panels) and a confocal laser scanning microscope (right panels, GFP). Scale bars: 200 μm [140].	29
Figure 2. 6 Construction of a bioartificial pancreas module. (A) A piece of non-woven fabric with a backing of rayon cloth was covered with 550 hollow fibers. (B) The fibers and cloth were rolled together and the spaces between the hollow fibers were sealed with urethane, and the roll was inserted into a polycarbonate casing with dimensions as shown [100].	32
Figure 2. 7 Schematic illustrating the formation of polymer coatings initiated by glucose oxidase (GOx). (A) Cell-laden PEG hydrogels are swollen in a glucose-containing media and then (B) dipped into a pre-polymer solution containing acryl-PEG, GOx, Fe <sup>2+</sup> , and thiolated signaling molecules. Glucose diffuses out of the gel, reacts with GOx and initiates polymerization at the surface of the hydrogel. (C) Reactive coating results in conformal PEG layers. (D) Confocal micrograph of PEG hydrogel (green) with GOx mediated polymer coating (red). Scale: 200 μm [169].	36
Figure 2. 8 Schematic depiction of the <i>in vitro</i> cultivation of dispersed islet single cells, formation of islet cell-spheroids using concave microwell arrays, and the process of spheroids encapsulation within collagen-alginate composite [155].	38

List of Figures (Continued)

Figure	Page
Figure 2. 9 Three-dimensional structure of alginate/polylysine microspheroid encapsulating $\beta$ -cells and gadolinium chelates [174].	39
Figure 3. 1 Evolution of shear storage moduli, ( $G'$ ) of hydrogels as a function of time. Inserted pictures: (1) $G'$ at 1 hr and (2) gelation time as a function of PEG concentrations.	73
Figure 3. 2 (A) Frequency sweep of hydrogels of various PEG concentrations. (B) Oscillatory stress sweep of hydrogels of various PEG concentrations.	74
Figure 3. 3 Frequency sweep and oscillatory stress sweep of hydrogels of various ratios of different concentrations of (A) 5% and (B) 2.5%.	75
Figure 3. 4 Dynamic swelling of the hydrogels in PBS. (A) Degree swelling of hydrogels as the function of concentration. (B and C) Degree swelling of hydrogels as the function of ratios of PEGTA to 4arm PEGSH at the concentration of (B) 5% and (C) 2.5%.	76
Figure 3. 5 LIVE/DEAD (Green/Red) staining of MIN6 cells 3D cultured in 5% PEG hydrogels of different ratios of 4-arm thiolated PEG to PEGTA.	77
Figure 3. 6 The size of artificial islets of MIN6 cells in 5% PEG hydrogels of different ratios of 4-arm thiolated PEG to PEGTA.	78
Figure 3. 7 Insulin release response to glucose from MIN6 cells cultured in 5% PEG hydrogels of different ratios of 4-arm thiolated PEG to PEGTA at the day 1, 4 and 7....	79
Figure 3. 8 LIVE/DEAD (Green/Red) staining of MIN6 cells cultured in 5% PEG hydrogels of 4-arm thiolated PEG to PEGTA at the ratio of 1:2 conjugated with different peptides: IKVAV, RGD, and YIGSR at the day 4.	79
Figure 3. 9 The size of artificial islets of MIN6 cells cultured in 5% PEG hydrogels of 4-arm thiolated PEG to PEGTA at the ratio of 1:2 conjugated with different peptides: IKVAV, RGD, and YIGSR at the day 4.	80
Figure 3. 10 Insulin release response to glucose from MIN6 cells cultured in 5% PEG hydrogels of different peptides at the day 4.	81
Figure 4. 1 (A) The computer controlled spheroid maker. (B and C) The fabrication process of microwells. (D) Agarose microwells.	99

List of Figures (Continued)

Figure	Page
Figure 4. 2 (A) Beta-cells formed aggregates of different diameters of 200, 300, and 400 $\mu\text{m}$ in microwells. (B) LIVE/DEAD staining of $\beta$ -cells aggregates in microwells. Live cells stained with green and dead with red. (C) The relationship between cell seeding concentrations and spheroid diameters. ....	99
Figure 4. 3 Beta-cells formed spheroids with different diameters of (A) 100, (B) 200, (C) 300, (D) 400, and (E) 500 $\mu\text{m}$ transferred into a suspension flask for culture 1 week with high viability. Live cells stained with green and dead with red. Scale bar = 200 $\mu\text{m}$ . ...	100
Figure 4. 4 Insulin (green) staining of $\beta$ -cells spheroids with different diameters of (A) 200, (B) 300, and (C) 500 $\mu\text{m}$ . Nuclei were stained with DAPI (blue). Scale bar = 100 $\mu\text{m}$ . ....	101
Figure 4. 5 Insulin release from $\beta$ -cells spheroids with different diameters of 100, 200, 300, 400, and 500 $\mu\text{m}$ . (A) Insulin release from spheroids of total number of 270. Spheroids of diameter of 200 $\mu\text{m}$ released significant larger amount of insulin than those with diameter of 100 $\mu\text{m}$ (* $P < 0.05$ ). (B) Insulin release from the single cell in the spheroids. Cells from spheroids of 200 $\mu\text{m}$ released larger amount of insulin compared to those from spheroid of 300 $\mu\text{m}$ (* $P < 0.05$ ). ....	101
Figure 4. 6 (A) Co-culture of $\beta$ -cells and hMSCs. (B) Co-culture of $\beta$ -cells spheroids with hMSCs. Beta-cells were stained with insulin with green. Human MSCs were identified by human mitochondria with red. Scale bar = 100 $\mu\text{m}$ . ....	103
Figure 4. 7 Methylcellulose was coated on the surface of $\beta$ -cell spheroid. Methylcellulose was conjugated with Cy3 NHS ester (red) and DAPI for nuclei (blue). Scale bar = 100 $\mu\text{m}$ . ....	104
Figure 4. 8 Human MSCs of different concentrations of (A) 0.4, (B) 0.8, (C) 1.6, and (D) 3.2 million/mL were coated on the surface of $\beta$ -cell spheroid. Human MSCs were stained with human mitochondria antibody with red, $\beta$ -cell spheroid was identified by insulin antibody (green) and DAPI for nuclei (blue). Scale bar = 100 $\mu\text{m}$ . ....	105
Figure 4. 9 Insulin release from $\beta$ -cells spheroids with diameter of 200 $\mu\text{m}$ coated with different concentrations of hMSCs. Spheroids of diameter of 200 $\mu\text{m}$ coated with the concentration of hMSCs of 0.8 million cells/mL released significant larger amount of insulin than those with 1.6 million cells/mL (* $P < 0.05$ ). ....	106

## List of Figures (Continued)

Figure	Page
Figure 4. 10 Beta-cells spheroids with the diameter of 200 $\mu\text{m}$ co-cultured with different concentrations of hMSCs. (A) Insulin release from $\beta$ -cells spheroids co-culture with hMSCs of different concentrations at 24 hr. (B) Percentage change of insulin release after exposing to the pro-inflammatory cytokines after 24 hr (* $P < 0.05$ ). .....	107
Figure 4. 11 Apoptosis of $\beta$ -cells with the diameter of 200 $\mu\text{m}$ co-cultured with hMSCs of different concentrations: (A) 0, (B) 0.4, (C) 0.8, (D) 1.6, (E) 3.2, and (F) 6.4 million/mL after exposing to the pro-inflammatory cytokines. AlexaFluor 488 labeled anti-BrdU antibody was used for detection of apoptotic cells and propidium iodide staining for all the cells. Scale bar = 100 $\mu\text{m}$ .....	108
Figure 4. 12 Agarose was coated on the surface of complex. Through controlling the stirring rate, hydrogel outlayer of different thicknesses of (A) 5, (B) 20, and (C) 60 $\mu\text{m}$ can be formed on the surface of $\beta$ -cell spheroid-hMSCs complex. Scale bar = 100 $\mu\text{m}$ . .....	109
Figure 5. 1 (A) The scheme of our core-shell structured $\beta$ -cells/hMSCs/hydrogels complex. (B and C) The $\beta$ -cells spheroids/hMSCs complex coated with agarose hydrogel mixed with LIF, VEGF and IL-10 loaded nanoparticles. Scale bar = 100 $\mu\text{m}$ .....	118
Figure 5. 2 (A) LIF-loaded PLGA nanoparticles. (B) The average particle size is 400 nm. ....	124
Figure 5. 3 Cumulative <i>in vitro</i> LIF (A) percentage release from PLGA nanoparticles and (B) release amounts from 3.5 mg nanoparticles during the first 7 days. ....	124
Figure 5. 4 Cumulative <i>in vitro</i> IL-10 cumulative percentage release from PLGA nanoparticles. ....	125
Figure 5. 5 Beta-cells spheroids with the diameter of 200 $\mu\text{m}$ cultured with LIF and IL-10 loaded nanoparticles with a cocktail of cytokines of interferon- $\gamma$ , tumor necrosis factor- $\alpha$ , and interferon 1 $\beta$ . ....	127
Figure 5. 6 Apoptosis of $\beta$ -cells with the diameter of 200 $\mu\text{m}$ cultured (A) with LIF and IL-10 loaded nanoparticles and (B) blank nanoparticles with a cocktail of cytokines of interferon- $\gamma$ , tumor necrosis factor- $\alpha$ , and interferon 1 $\beta$ . AlexaFluor 488 labeled anti-BrdU antibody was used for detection of apoptotic cells and propidium iodide staining for all the cells. Scale bar = 100 $\mu\text{m}$ . ....	128

List of Figures (Continued)

Figure	Page
Figure 5. 7 Cumulative <i>in vitro</i> VEGF cumulative percentage release from PLGA nanoparticles. ....	129
Figure 5. 8 The bioactivity of the VEGF assessed using an <i>in vitro</i> HAEC proliferation assay. (A) The proliferation of HAEC affected by the concentration of VEGF. (B) Comparison of VEGF solution and VEGF released from nanoparticles on the proliferation of HAEC. ....	129
Figure 5. 9 The $\beta$ -cells spheroids/hMSCs complex coated with agarose hydrogel mixed with LIF, VEGF and IL-10 loaded nanoparticles. Scale bar = 100 $\mu$ m. ....	130
Figure 6. 1 Macro inspection of spheroids transplantation. (A) The kidney has been exposed for $\beta$ -cells spheroids transplantation. (B) Beta-cells spheroids have been transplanted under the kidney capsule. (C) Inspection of the $\beta$ -cells spheroids after 3 days post-transplantation .....	136
Figure 6. 2 Glucose level after transplanted different groups of $\beta$ -cells spheroids at the day 1 and 2. ....	137
Figure 6. 3 Glucose level after transplanted different groups of $\beta$ -cells spheroids. ....	139
Figure 6. 4 Human MSCs at the transplantation sites at the day of 3 (A-D), 9 (E-H) and 30 (I-L). (A, E and I) Beta-cells spheroids. (B, F and J) Beta-cells spheroids/hMSCs. (C, G and K) Beta-cells spheroids/hMSCs coated with agarose hydrogel. (D, H and L) Beta-cells spheroid/hMSCs coated with porous hydrogel mixed with IL-10, LIF and VEGF loaded-nanoparticles. Human MSCs were identified by mitochondria and nuclei by DAPI. Scale bar: 100 $\mu$ m. ....	140
Figure 6. 5 Macrophages at the transplantation sites at the day 3 (A-D), 9 (E-H) and 30 (I-L). (A, E and I) Beta-cells spheroids. (B, F and J) Beta-cells spheroids/ hMSCs. (C, G and K) Beta-cells spheroids/hMSCs coated with agarose hydrogel. (D, H and L) Beta-cells spheroids/hMSCs coated porous hydrogel mixed with IL-10, LIF and VEGF loaded-nanoparticles. Macrophages were identified by F40/80 and nuclei by DAPI. Scale bar: 100 $\mu$ m. ....	142

List of Figures (Continued)

Figure	Page
Figure 6. 6 Regulatory T cells at the transplantation sites at the day 3 (A, B, C and D), 9 (E, F, G, and H) and 30 (I, J, K and L). (A, E and I) Beta-cells spheroids. (B, F and J) Beta-cells spheroids/hMSCs. (C, G and K) Beta-cells spheroids/hMSCs coated with agarose hydrogel. (D, H and L) Beta-cells spheroids/hMSCs coated with porous hydrogel mixed with IL-10, LIF and VEGF loaded-nanoparticles. T cells were identified by FOXP3 and nuclei by DAPI. Scale bar: 100 $\mu$ m. ....	143
Figure 6. 7 Blood vessels inspected at the transplantation sites at the day 3 (A-D), 9 (E-H) and 30 (I-L). (A, E and I) Beta-cells spheroids. (B, F and J) Beta-cells spheroids/hMSCs. (C, G and K) Beta-cells spheroids/hMSCs coated with agarose hydrogel. (D, H and L) Beta-cells spheroid/hMSCs coated with porous hydrogel mixed with IL-10, LIF and VEGF loaded-nanoparticles. Blood vessels were identified by CD-31 and nuclei by DAPI. Scale bar: 100 $\mu$ m. ....	145

## CHAPTER ONE

### 1. INTRODUCTION

#### 1.1 Type 1 diabetes and current treatments

Diabetes mellitus is one of the most common metabolic diseases, which has become the third most common disease in the world. Around 285 million people worldwide suffer from various types of diabetes in 2012, and the number of people with diabetes will reach to 439 million by 2030. And the complications followed by diabetes mellitus include coronary heart disease, kidney failure, blindness, limb amputations, and premature death.

Type 1 diabetes, referred to insulin-dependent diabetes mellitus, is an autoimmune disease resulting from the destruction of  $\beta$ -cells located in the islets of Langerhans of pancreas by autoantigen-reactive T lymphocytes which produce immune factors to attack and destroy  $\beta$ -cells in the pancreas. Once  $\beta$ -cells are destroyed, the ability to secrete insulin in response to control the blood glucose level is inhibited, and then leading to hyperglycaemia at clinical diagnosis. In the United States there are 30,000 new cases annually with 1 in 300 children affected.

To date, no effective treatment is available for type 1 diabetes in clinical settings. The exogenous insulin injection therapy is the current main treatment. However, the multiple injections are inconvenient and painful and may lead to infection at the site of injection. Pancreas transplantation is a clinical option available to cure type 1 diabetes. But complications are followed immediately after surgery including thrombosis, pancreatitis, infection, bleeding, and rejection. Rejection is a serious condition and ought

to be treated immediately. Patients must take a long-term immunosuppressive therapy. Transplantation of islets, the parts of the pancreas that can make insulin, can avoid a delicate surgical procedure and reduce the risk followed by the transplantation. However, for decades, the clinical application of islet transplantation is also limited by the shortcoming of immunosuppression therapy and the shortage of donor tissues. In pancreatic islet transplantation, while efforts have been centered on systematic modulation of host immune responses for transplantation tolerance, strategies that render the allograft itself resistant to host immune insult have not been adequately explored. Islet encapsulation has been attempted as an immunoisolation device to facilitate the transplantation of islets without the need for immunosuppression for decades. Immunoisolation of islets aims to overcome the immune-mediated destruction of the donor tissues without requiring toxic immunosuppression agents. The strategy of immunoisolation means encapsulating islets within a semi-permeable structure made of biomaterials with good biocompatibility. Immunoisolation of islets also offers a possibility of using islets gained from animals, or insulin-producing cells induced from stem cells or pancreatic precursor cells, thus enlarging the potential sources of donor tissues. However, an optimal encapsulation device that allows sufficient oxygen and nutrient exchange while protecting from immune rejection response and promoting vascularization is still lacking.

## 1.2 Study objectives and specific aims

In this study, we will develop a comprehensive strategy for the treatment of type 1 diabetes using  $\beta$ -cell based replacement therapy. To improve the viability of transplanted



$\beta$ -cells, one novel approach is to transplant optimal size range of  $\beta$ -cell spheroids. We will focus on a novel and unique automatic robotic fabrication/microencapsulation system that can produce uniform-sized multicellular spheroid ranging anywhere between 100  $\mu\text{m}$  to 1000  $\mu\text{m}$ . It can also allow coating of the islets or islet-like spheroids with multiple layers for immunoisolation and immunomodulation. We will coat the islets or spheroids with a non-degradable methylcellulose first, then with multiple layers of human mesenchymal stem cells (hMSCs), which demonstrated anti-immune and anti-inflammatory effects. Lastly, we will have a porous non-degradable polymer layer for further protection and promoting vascular formation surrounding the encapsulated islets. Porous layer will be loaded with nanoparticles impregnated with angiogenic factors and immune regulatory molecules to enhance blood vessel formation around the encapsulated spheroids and in the same time further suppress the host immune response (Schematic 1). By this means the islets will passively evade the complications of stressors in addition to actively modulating the immune microenvironment for regulatory tolerance and long-term engraftment. Islet microencapsulation can not only serve as a physical barrier deterring host immune recognition, but also function as a cargo carrier slowly releasing immune-modulatory molecules that accommodate the allograft into a local permissive cytokine milieu for long-term engraftment.

### 1.3 Dissertation organization

The following manuscript is arranged in chapters that highlight individual studies that relate to the overall aims of the project. Chapter 2 focuses on highlighting existing

strategies currently being investigated for type 1 diabetes treatment. In Chapter 3, we have created specific niche for  $\beta$ -cells through developing a series of hydrogels based on polyethelene glycol (PEG) and addehisve peptides RGD, YIGSR and IKVAV. In Chapter 4, we developed a fully robotic biofabrication method to produce uniform size multicellular  $\beta$ -cells spheroids in large scale. Furthermore, we have constructed the complex of islet-like spheroids with multiple layers of hydrogels and hMSCs for immunoisolation and immunomodulation. To further improve the viability and suppress the immune rejection, in Chapter 5, we have loaded angiogenic and immune regulatory molecules like VEGF, IL-10 and LIF, into degradable poly (lactic-co-glycolic acid) (PLGA) nanoparticles and loaded nanoparticles into last layer hydrogels coating, for sustained release; we then inspected the biological activities of released IL-10 and LIF on survival and function of  $\beta$ -cells spheroids against pro-inflammatory cytokines, and the bioactivity of VEGF released from nanoparticles. In Chapter 6, we have evaluated of  $\beta$ -cells/MSK hybrid spheroids for the treatment of type 1 diabetes *in vivo*. Chapter 8 summarizes overall conclusions drawn from the body of work and discusses developments related to the presented research.

## CHAPTER TWO

### 2. BIOENGINEERING STRATEGIES FOR TYPE 1 DIABETES TREATMENT

#### 2.1 Introduction

Diabetes mellitus is a chronic endocrine disease that is attributed to insulin deficiency. Type 1 diabetes mellitus, occurring in children or young people, is an autoimmune disorder in which  $\beta$ -cells located in pancreatic islets are damaged and no longer able to secrete insulin. Every year around 15,000 patients are diagnosed with type 1 diabetes in the United States, adding to the three million existing type I diabetes patients.

The current clinical treatments for type 1 diabetes include exogenous insulin administration therapy and pancreas transplantation. Even though routine glucose monitoring and exogenous insulin therapy has been the common treatment, the lack of precise control of blood glucose with this therapy results in many complications, such as retinopathy (loss of vision), nephropathy (renal failure), and neuropathy (foot ulcers with the risk of amputation, even cardiovascular symptoms) [1]. Pancreas transplantation is an option of clinically available  $\beta$ -cells replacement to cure the disease. However, the procedure involves major surgery and long-term immunosuppression therapy which will lead to severe side effects [2]. Pancreas transplantation is not an optimal therapeutic option for the vast majority of diabetic patients [3].

Many new strategies for type 1 diabetes are under clinical trials. In order to reduce the risks of developing diabetes-related complications, novel methods in the insulin formulations and delivery systems have been investigated to improve the blood

glucose level control. Islet transplantation has also been studied as a potential option for the treatment of type 1 diabetes. Compared to pancreas transplantation, islet transplantation is more effective and less invasive. But islet transplantation cannot avoid similar problems to pancreas transplantation such as the limitation of donor tissue and long-term immunosuppression therapy if naked islets are used. An immunoisolated bioartificial pancreas (BAP) has been developed based on bioengineering strategies for avoiding immunosuppression. BAP allows the passage of oxygen, glucose, nutrients, waste products, and insulin, but blocks the penetration of immunocompetent cells and immune response associated biologics, such as antibodies and complements [4]. Immunoisolation technology offers a possibility for cell-based therapy to transplant  $\beta$ -cells or islets from animal sources, or new insulin-producing  $\beta$ -cells induced from other sources like stem cells and pancreatic precursor cells, thus expanding the sources of donor tissues. The generation of insulin-producing  $\beta$ -cells through *in vivo* regeneration or *in vitro* differentiation from stem cells has been investigated [5, 6].

There are several excellent review articles that offer a very detailed and comprehensive overview regarding the use of islet encapsulation and cell-based therapy for type 1 diabetes treatment [7-10]. Here, we will present a more detailed overview on bioengineering strategies for type 1 diabetes treatment. We will have a comprehensive review on bioengineering strategies with a focus on insulin delivery systems, BAP fabrication, transplantation of  $\beta$ -cells and inducing  $\beta$ -cells from other cell sources, and so on. Finally, we will also discuss major challenges using existing strategies and future directions for type 1 diabetes treatment.

## 2.2 Diabetes types and current treatments

Diabetes mellitus is one of the most common metabolic diseases and has become the third most common disease following cardiovascular diseases and cancers. Around 347 million people worldwide suffered from various types of diabetes in 2012, and the projected number of diabetes patients will reach to 439 million by 2030 [11]. The complications followed by diabetes mellitus include coronary heart disease, kidney failure, blindness, limb amputations, and premature death [12]. About 25.8 million Americans have diabetes and a total cost of diagnosed diabetes is \$245 billion in 2012.

### 2.2.1 Diabetes types

Diabetes mellitus is a group of chronic metabolic diseases characterized by a deficit in  $\beta$ -cells mass and a dysregulation of glucose metabolism, resulting in many complications. The classical symptoms include polyuria, polydipsia and polyphagia. There are three types of diabetes mellitus: type 1 diabetes, type 2 diabetes, and gestational diabetes. Type 1 diabetes is an insulin-dependent diabetes mellitus, which is believed to be an autoimmune disease leading to the destruction of  $\beta$ -cells in the islets of Langerhans. Once  $\beta$ -cells are destroyed by autoantigen-reactive T lymphocytes, the ability to secrete insulin in response to blood glucose increase is compromised, leading to hyperglycaemia. Type 2 diabetes is a non-insulin-dependent diabetes mellitus or an adult-onset diabetes. It is characterized as insulin resistance, meaning cells fail to use insulin properly, leading to hyperglycaemia. The development of type 2 diabetes is caused by a combination of lifestyle and genetic factors. Obesity is the primary cause of type 2

diabetes in people who are genetically predisposed to the disease. Exercise and dietary modification are the first steps of disease management. If blood glucose levels are still high by these measures, medications such as Metformin or insulin may be needed. Gestational diabetes is a condition in which pregnant women, who have never had diabetes before, reveal high blood glucose level during pregnancy. Pregnancy hormones lead to insulin resistance and then hyperglycaemia. Gestational diabetes generally has few symptoms. It is commonly diagnosed by a screening test during pregnancy. Around 3-10% pregnant women will have gestational diabetes depending on the population [13]. Women with gestational diabetes are at increased risk of developing type 2 diabetes after pregnancy. Most patients are treated only with diet modification and moderate exercise, but some will have to take anti-diabetic drugs, such as insulin, if the blood glucose level is too high [14].

### 2.2.2 Current clinical treatments for type 1 diabetes

Exogenous insulin injection therapy is the current main treatment for type 1 diabetes. It includes multiple/daily injections and insulin pump therapy (chronic subcutaneous injection). The multiples injections are inconvenient and painful and may lead to infection at the site of injection, giving rise for the increased research for new methods of treatment. For insulin pump therapy, the long-term injection at the same place can result in lipodystrophy. Although insulin-based therapy allows a monitor of the control of blood glucose levels through daily glucose monitoring, strict control of blood glucose levels can be difficult to achieve due to environmental variations, such as

exercise, diet, pregnancy, or age. The exogenous insulin injection therapy may lead to long-term complications, such as retinopathy, nephropathy, and neuropathy [15].

Currently, pancreas transplantation is a clinical option available to treat type 1 diabetes. In this procedure, the recipient's native pancreas is left in place to prevent the rejection of the donor pancreas which would lead to life-threatening diabetes quickly, thus the donor pancreas is placed in a different location [16]. In patients with type 1 diabetes who have suffered the destruction of their kidney, the pancreas transplantation usually is performed along with kidney transplantation [17]. More than 90% of pancreas transplantations are simultaneous pancreas-kidney transplants. Complications immediately following surgery include thrombosis, pancreatitis, infection, bleeding, and rejection. Rejection is a serious condition and ought to be treated immediately. Patients must undergo a long-term immunosuppressive therapy [18].

### 2.2.3 New treatments under clinical trial and development

The development of insulin administration by alternative routes has made remarkable progress over the last decade. The ultimate goal is to better simulate the physiological fluctuations of endogenous insulin release and thus leading to a better blood glucose metabolism and control. The current main alternatives for insulin delivery include nasal, pulmonary, dermal, rectal, and oral routes [19].

Islet cell transplantation is an experimental procedure that only transplants the islet parts that can make insulin. Islet transplantation has the potential to be widely used for type 1 diabetes, since this procedure can avoid a delicate surgical procedure and

reduce the risk followed by the whole pancreas transplantation [2, 20]. Islet transplantation includes two steps: the isolation of islets from donor pancreas tissue and the transplantation. The transplantation procedure is shown in Figure 2.1 [21]. Islets are injected into the hepatic portal vein, from where islets will flow into liver sinuses, which are well perfused. In this case, islets are not transplanted in the recipient's pancreas because the pancreas is highly sensitive to any injury, which may lead to severe pancreatitis with accompanying pain and tissue destruction.

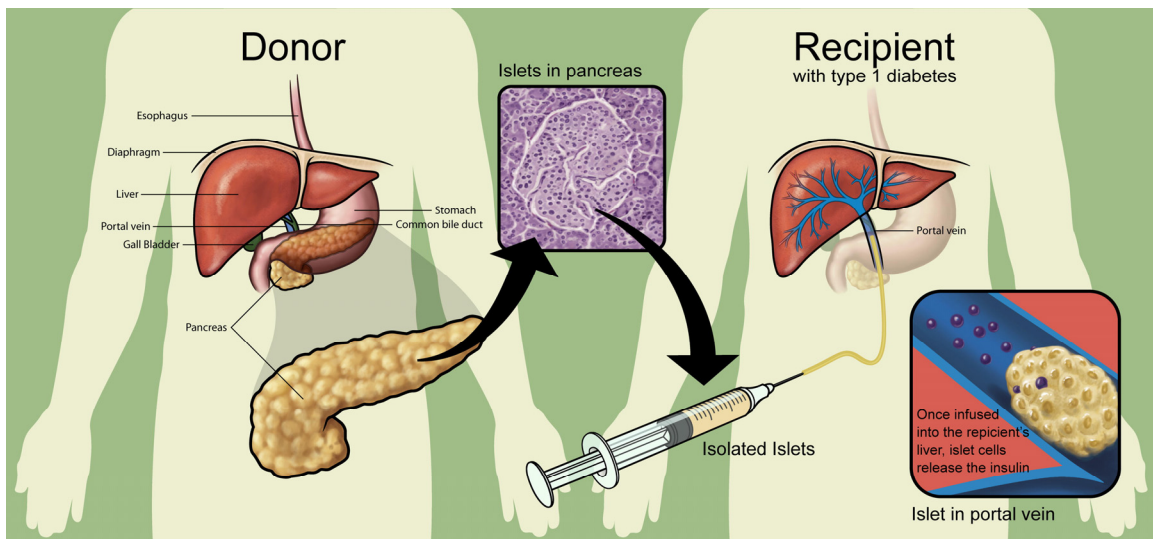


**Figure 2. 1** Islet transplantation for the treatment of type 1 diabetes in clinical [21].

For decades, the clinical application of islets transplantation was also limited by the shortcoming of immunosuppression therapy and the shortage of donor tissues. Using biomaterial, scientists paid attention to immunoisolating islets from host immune systems based on various bioengineering approaches [22]. Using immunoisolated islets for transplantation can minimize, and even eliminate immunosuppressive needs theoretically



[23, 24]. Immunoisolation of islets offers a possibility of using islets derived from animals, or insulin-producing cells obtained from stem cells or pancreatic precursor cells, thus enlarging the potential sources of donor tissues. To this end, the generation of new insulin-producing cells by *in vivo* regeneration or by *in vitro* differentiation of stem cells has become a major effort in diabetes research [25, 26].

Since type 1 diabetes is one of the most common autoimmune diseases, considerable experimental and clinical progress has been made in understanding of its immunopathogenesis [27]. This knowledge has been used to develop immunopreventive and immunomodulatory treatments for type 1 diabetes [28, 29].

### 2.3 Bioengineering strategies for type 1 diabetes treatment

Several novel bioengineering approaches are applied in insulin administration, islets transplantation, and cell-based therapy for type 1 diabetes treatment, such as microspheres and nanoparticles for insulin controlled release systems, hollow fibers and chamber diffusion device for islets immunoisolation, and hydrogels for  $\beta$ -cells transplantation.

#### 2.3.1 Insulin control release

Insulin was firstly discovered by Banting and Best in 1922 [30]. The role of insulin is to change extra glucose into two storage forms, glycogen and triacylglycerols, and maintain blood glucose levels. The main method for insulin administration is subcutaneous injection because of insulin's large molecular size, hydrophilicity and low

permeability. However, injection therapy is burdensome and has a low efficiency for insulin targeting to the liver, which is the primary organ of action. Only about 20% of the insulin reaches the liver after injection [31]. Various technologies have been investigated for replacing the insulin injections. Therefore, drug delivery systems have been paid attention to for the development of non-injectable routes. The main alternative routes studied for insulin deliveries include nasal, pulmonary, dermal, rectal and oral routes. In this section we will discuss the different drug delivery strategies available (molecular, formulation, and device) and their current and potential applications with respect to the different insulin delivery routes.

#### 2.3.1.1 Molecular engineering

Insulin is a polypeptide (molecular weight: 5800 Da) secreted by  $\beta$ -cells which consists of a 21-amino acid A chain and a 30-amino acid B chain, linked by two disulfide bonds, and a third disulfide bond occurs within the A chain [32]. Molecular engineering strategies are to modify insulin to improve its pharmacodynamic properties (insulin analogs) and prevent it from proteolytic degradation (insulin conjugates). An insulin analog is another form of insulin which results from changing the amino acid sequence of insulin. The characteristics of insulin such as absorption, distribution, metabolism and excretion are optimized for improving pharmacodynamic properties of the applied insulin by adjusting the amino acid sequence of insulin. Insulin conjugates is the chemically modified formation of insulin for protecting the insulin from proteolytic degradation or improving its properties such as solubility, permeability, stability and circulation half-

life.

### 2.3.1.1.1 Insulin analogs

Through the molecular engineering approaches, the amino acid sequences of insulin are altered to fabricate two types of insulin analogs. One is rapid-acting insulin analogs which are designed to provide a bolus level of insulin; another is long-acting analogs which are required to supply a basal level of insulin. Three rapid-acting analogs and two long-acting analogs are shown in Table 2.1. Aspart, Lispro and Glulisine insulin are rapid-acting analogs [33]; Glargine and Detemir analogs are long-acting analogs [34]. Compared to human insulin, the different amino acids of insulin analogs are labeled. Long-acting analogs with the slowing absorption property can last 20-24 hrs in the body after injection and decrease nocturnal hypoglycemia. Rapid-acting analogs increase the rate of absorption after injection and last longer than regular insulin.

**Table 2. 1** Insulin analogs by amino acid substitutions [33].

Types	A21	B3	B28	B29	B30	B31 & B32
Human	Asn	Asn	Pro	Lys	Thr	
Aspart	Asn	Asn	Asp	Lys	Thr	
Lispro	Asn	Asn	Lys	Pro	Thr	
Glulisine	Asn	Lys	Pro	Glu	Thr	
Glargine	Gly	Asn	Pro	Lys	Thr	Arg
Detemir	Asn	Asn	Pro	Lys	Myristic acid	

#### 2.3.1.1.2 Insulin conjugates

Insulin conjugates have been investigated with several macromolecules such as poly (ethylene glycol) (PEG) [35, 36], polysialic acids [37, 38], albumin [39, 40], and chitosan [41]. For example, one of the most important modifications of insulin is the hexyl-insulin mono-conjugate 2 (HIM2), which has been introduced by the NOBEX corporation [35]. The HIM2 molecule was made by covalently linking a single, low molecular weight amphiphilic oligomer to the free amino acid group on the Lys-B29 residue of recombinant human insulin through an amide bond. The oligomer was synthesized by binding a lipophilic alkyl unit to a hydrophilic PEG unit. This conjugation conferred many advantageous properties to the insulin molecule, such as more lipid and water solubility. These properties can be used to manufacture more varieties of formulation than ordinary insulin [42, 43]. Moreover, an insulin prodrug was designed by conjugating insulin to a PEG (40 kDa) containing sulfhydryl moiety. After subcutaneous injection, the insulin prodrug could extend glucose-lowering effects compared to the native hormone [44]. Bile acids [45, 46] or fatty acids [47] were also bonded with insulin to improve the stability of insulin.

#### 2.3.1.2 Formulation engineering

The insulin administration routes and the required pharmacokinetic property decide the formulation of insulin. Formulation engineering aims to reach the required delivery profile. Hydrogels, patches, dry powders, microspheres, and nanoparticles have been applied to control the release of insulin for novel delivery routes such as nasal, oral,

pulmonary, and rectal.

#### 2.3.1.2.1 Hydrogels

Hydrogels are three-dimensional (3D) networks of hydrophilic polymers that can entrap drugs and biomolecules under certain conditions and then releases the drugs or biomolecules in a controlled slow release manner. Thus, a higher concentration of the drugs and biomolecules can be loaded inside the hydrogels, which can be formulated to respond to various environmental signals such as pH [48], temperature [49], light [50], glucose [51], antigens [52], ultrasound, and so on, to release the drugs or biomolecules. These stimuli-responsive polymeric hydrogels have been extensively studied and used as “smart” carriers for the control release of insulin.

##### 2.3.1.2.1.1 pH-sensitive hydrogels

All the pH-sensitive hydrogels include acids, such as sulfuric and carboxylic acids, or bases, such as ammonium salts group, for gaining or releasing protons in response to changes in environmental pH. Acidic hydrogels accept protons, swell at high pH, and shrink at low pH. In contrast, basic hydrogels exhibit opposite swelling behaviors in response to pH. The pH-sensitive hydrogels have shown the potential for the application as oral delivery of insulin [53-55]. Through controlling the swelling/shrinking properties, encapsulated insulin can be protected from degradation in the acidic environment in stomach (pH 1-2) [56, 57] and then be released in the basic environment of intestine (pH 6-7) [58, 59]. For example, hydrogels containing poly(methacrylic acid) grafted with PEG were investigated for their potential as oral insulin carriers [54]. The

results showed insulin loaded hydrogels induced a hypoglycemic effect and an increase in insulin levels, proving that insulin was still biologically active. Tuesca et al. [60] demonstrated the feasibility of combining insulin PEGylation with pH-sensitive hydrogels for oral insulin delivery.

#### 2.3.1.2.1.2 Thermosensitive hydrogels

Polymers comprising both hydrophobic and hydrophilic parts in their molecular structure exhibit thermo-sensitive properties. The thermo-sensitive hydrogel is usually designed for application as an injectable local drug delivery system. The insulin-loaded hydrogel is a flowing solution at ambient temperature and turns into a non-flowing gel at body temperature after being injected into body, and starts to release insulin at local sites [61, 62]. A study was aimed at developing a delivery system for the controlled slow release of insulin, based on chitosan-zinc-insulin complex incorporated into a poly(lactic acid)-poly(ethylene glycol)-poly(lactic acid) (4500 Da) thermo-sensitive polymer [63]. The addition of zinc to insulin reduced the initial burst, stabilized the insulin as compared with its monomeric state by forming reversible complex through a zinc-coordinated insulin hexamer, and controlled the overall release rate.

#### 2.3.1.2.1.3 pH/thermo-sensitive hydrogels

The pure thermo-sensitive hydrogel is not suitable for the deep injection into the tissue because of the gelation formation inside the needle during the injection procedure. The pH/thermo-sensitive hydrogels can solve this problem. The polymer requires the

stimulation of both pH and temperature for the gelation process [64]. As Figure 2.2 shown, a pH- and thermo-sensitive hydrogel was prepared by adding pH-sensitive sulfamethazine oligomers to either end of a thermosensitive poly( $\epsilon$ -caprolactone-co-lactide)-poly(ethylene glycol)-poly( $\epsilon$ -caprolactone-co-lactide) block copolymer, which exhibited a pH-sensitivity around pH 7.4 as well as a temperature-sensitivity around 37 °C [65]. Another study used poly( $\beta$ -amino ester) as a duo-functional group for controlled drug/protein delivery when responding to pH and thermal stimulations [66].

#### 2.3.1.2.1.4 Glucose-sensitive hydrogels

Glucose-sensitive hydrogels attracted lots of attention due to their glucose sensing ability, which may allow for automatic initiation or shut-off the insulin delivery. One series of glucose-sensitive hydrogels was prepared by mixing glucose-containing polymers with PEGylated concanavalin A (conA). Tang et al. [67] reported a polymer produced by crosslinking two dextrans of different molecular weights. The smaller dextran was covalently grafted with conA. This material was then mixed with the larger unfunctionalized dextran, allowing easy control of the overall amount of grafted conA in the material. Insulin was initially bound to the conA, which was used to control the delivery of glycosylated insulin. The affinity of conA for dextran provided additional affinity crosslinks, which were competitively inhibited by free glucose, resulting in a decrease in total crosslink density and increase in permeability to proteins. Moreover, Kim's et al [68] demonstrated that glucose could be incorporated into the polymer backbone by copolymerization of allyl glucose with comonomers, such as 3-sulfopropylacrylate, potassium salt, N-vinyl pyrrolidone, and acrylamide. ConA was

grafted with five PEG molecules to improve its stability. Although all of the glucose-sensitive hydrogels are used to develop modulated insulin delivery systems, many improvements need to be achieved before they become clinically useful. The response of these hydrogels to changes in the environmental glucose concentration needs to be improved; also the speed for hydrogels returning to their original states needs to be increased after responding to the changing glucose concentration.

#### 2.3.1.2.2 Microspheres

Polymer microspheres are small (less than 2  $\mu\text{m}$  in size), thermoplastic spheres, which can be used in controlled release of insulin because of their ability to increase the stability of insulin and the protection of encapsulated insulin from enzymatic degradation. Microspheres improve the insulin absorption due to the distribution of microspheres in the body. Microspheres are expected to accumulate in the liver where insulin can efficiently suppress elevated glucose production.

Since 1986, Damge et al. [69] fabricated insulin loaded isobutyl 2-cyanoacrylate microspheres to treat streptozotocin-induced diabetic rats. Significant reductions in blood glucose levels were observed following administration of these microspheres [70, 71]. Since administration of insulin requires repeated dosing, the use of non-biodegradable microspheres posed a question with regard to the toxic effects of their accumulation in the body. Hence biodegradable microspheres such as ones made from a blend of poly(lactic acid) [72], poly( $\epsilon$ -caprolactone) [73], chitosan [74], and poly (lactide-co-glycolide) (PLGA) [75], were investigated. The water/oil/water (w/o/w) double emulsion



technique has been widely used for encapsulation of hydrophilic macromolecules in microparticles [76]. The microsphere drug delivery system has been investigated to increase the poor permeability across intestinal epithelia and avoid destruction by proteolytic intestinal enzymes.

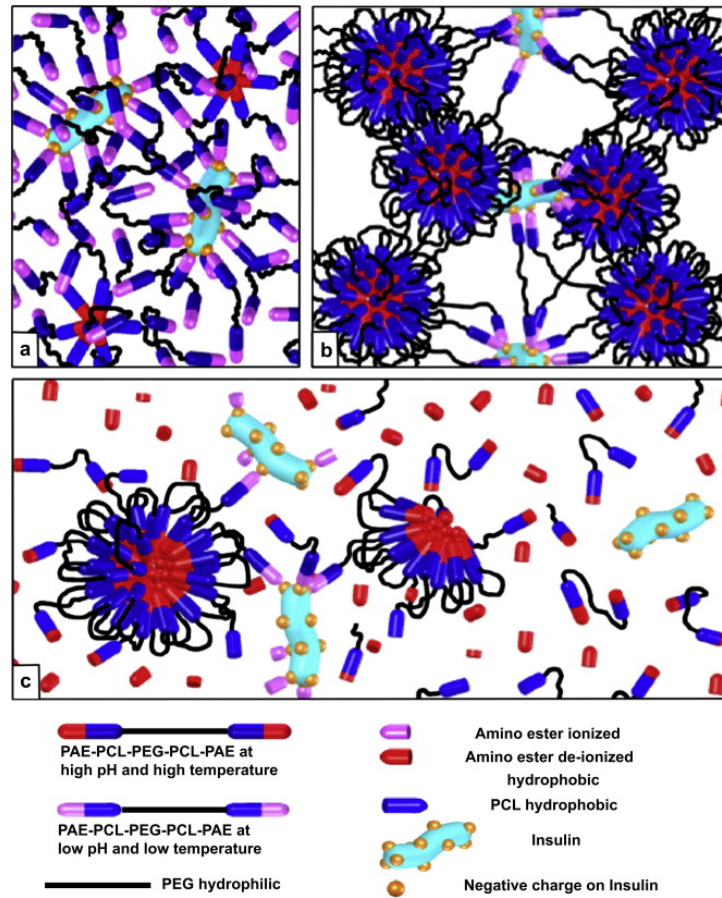


**Figure 2. 2** Insulin loading and release from pH/thermo-sensitive hydrogels. (A)The polymer solution in sol state at 10 °C and pH 7.0 with the ionic complex between insulin and PAE–PCL–PEG–PCL–PAE. (B) The gel formed by insulin free PAE–PCL–PEG–PCL–PAE after injection to human body (37 °C and pH 7.4). (C) Insulin release from gel by polymer degradation [65].

As discussed earlier, stimuli-responsive “smart” hydrogels have attracted a great

deal of interest [77]. A pH-sensitive copolymeric hydrogel microspheres were prepared from N-vinylcaprolactam and methacrylic acid monomers by free radical polymerization offered 52% encapsulation efficiency and evaluated for oral delivery of human insulin [78]. Kumar et al. [79] prepared pH-sensitive hydrogel microparticles based on poly(methacrylic acid), and the result was shown that insulin dose released from microparticles were sufficient to control the blood glucose level of fed diabetic rats between 100 and 300 mg/dL.

#### 2.3.1.2.3 Nanoparticles

Nanoparticles are defined as colloidal particles ranging in sizes less than 1000 nm. A variety of nanoparticulate systems including nanospheres, nanovesicles, nanoplexes, nanocapsules, liposomes, and a wide array of polymers were developed in nanoparticulate systems. The choice of polymers should be based on the required release profile, administration route, drug to be loaded, and the degradation property. Common polymers used for the insulin delivery system include PLGA [80, 81], chitosan, alginate [82], poly( $\epsilon$ -caprolactone) [83], polyalkylacrylates [84, 85], and polymethacrylic acid/acrylates [86]. Using a double-emulsion/solvent technique, insulin was encapsulated in PLGA nanoparticles [87]. Insulin loaded in PLGA-Pluronic F68 can overcome the gastrointestinal barrier which can be used as an oral administration of insulin [81]. *In vivo* experiments showed that the insulin loaded PLGA nanoparticles could decrease animal blood glucose. Insulin loaded chitosan nanoparticles were tested in nasal and oral delivery routes. As a nasal delivery system, insulin loaded PEG-g-chitosan nanoparticles

in rabbits improved the absorption of insulin compared to control insulin solution and mix of insulin and PEG-g-chitosan [88]. The insulin loaded chitosan nanoparticles have been tested in oral administration [89-91].

### 2.3.1.3 Device engineering

Some insulin release device designs, such as insulin pumps, insulin pen injectors, inhalation, and transdermal patches are used as a straightforward approach to increase patient acceptance and compliance [92, 93]. Delivery systems are being engineered for reproducible dose delivery. Inhalation devices are designed to delivery insulin powder through the pulmonary system. A blister pack of insulin powder is loaded into the inhaler and then the powder is dispersed into a standing cloud within the transparent chamber for the patients [94, 95]. Insulin pen, insulin jet injectors, and insulin pumps are non-needle injectors for people who prefer not to use a regular needle and syringe. Insulin pumps can deliver insulin constantly and can help to control glucose level all the time, even when patients are sleeping, which may avoid glucose swings and overall provide tighter control of glucose levels. In addition, pumps will allow patients to have a more flexible meal and activity schedule [96]. Glucometers are designed to monitor the blood glucose levels and are currently widely used by patients [97].

### 2.3.2 Islets transplantation

The transplantation of islets of Langerhans is a potential option for curing type 1 diabetes. The procedure can avoid the complications followed by major surgery

compared to whole pancreas transplantation. However, islets transplantation still faces the problems of the long-term administration of immunosuppressive agents with severe side effects, and the shortage of donor tissues. To solve these issues, the immunoisolation of islets with a semi-permeable membrane, or bioartificial pancreas (BAP), has been attempted. Using novel bioengineering approaches, a bioartificial pancreas has been fabricated for immunoisolating islets away from the host immune systems. Many groups have reported that BAP functions very well in small animal models. In this review, we overview the current techniques for the islets immunoisolation such as macro/micro encapsulation and conformal coating, and discuss some novel techniques for the modification of islets, such as chemical and cell modification.

#### 2.3.2.1 Islets immunoisolation

Immunoisolation of islets is a technology becoming accepted to overcome the immune-mediated destruction of the donor tissues without requiring toxic immunosuppression agents. The strategy of immunoisolation means encapsulating islets within a semi-permeable membrane made of biomaterials with good biocompatibility. Immunoisolation devices include three different types of encapsulated systems based on different encapsulation techniques: macro-scale encapsulation, micro-scale encapsulation, and nano-scale encapsulation [22].

#### 2.3.2.1.1 Macro-scale encapsulation

Macro-scale encapsulation includes two categories: intravascular and extravascular. The intravascular devices usually contain hollow fibers, which are perfused with blood. Extravascular devices such as hollow fibers, diffusion chambers, and hydrogels sheets, are implanted outside of the vasculature.

##### 2.3.2.1.1.1 Intravascular devices

In the intravascular devices, the islets are encapsulated in hollow fibers sealed with semi-permeable membranes. The device is similar to a dialysis device in which blood is perfused in the hollow fiber and islets are placed around the fibers. The device is directly connected to the host systemic circulation, resulting in improving the diffusive exchange rate [98-100]. Ikada et al. [100] designed a BAP based on poly(ethylene-vinyl alcohol) (PVA), which was properly controlled in response to glucose in pancreatectomized pigs. However, these devices are hard to implant into a body and require some anticoagulation treatment.

##### 2.3.2.1.1.2 Extravascular devices

Extra vascular devices entrap islets in a space surrounded by a semi-permeable membrane. Compared to intravascular devices, these devices are easily implantable and have the advantage of biocompatibility. Islets are contained in a diffusion chamber surrounded by semi-permeable membranes [101, 102]. The structure of the diffusion chamber is rather simple and the optimal membrane with desired pore size can be chosen.

However, islets tend to clump up with each other and undergo central necrosis. Seeding islets within hydrogels can avoid this clumping and improve islets function [4]. Macro-encapsulation encapsulates islets in hydrogels such as agarose, alginate [103, 104], polyurethane, PVA, and chitosan-polyvinylpyrrolidone hydrogel. For example, a unique continuous amphiphilic network membrane created for macroencapsulation and immunoisolation of porcine islet cells has been studied based on hydrophilic poly (N, N-dimethyl acrylamide) and hydrophobic/oxyphilic polydimethylsiloxane chains [105].

#### 2.3.2.1.2 Micro-scale encapsulation

In micro-scale encapsulation, generally one or a few islets are encapsulated within a microcapsules surrounded by semi-permeable membrane. Microcapsules are smaller than macrocapsules and are spherical in shape, which offers a large volume-to-surface area ratio. They can be implanted into patients through simple procedures without major surgery. Generally, microcapsules are fabricated from polymers that form hydrogels under certain conditions. They are derived either naturally or through synthetic routes. The polymers include the natural biomaterials such as alginate, agarose, and the synthetic biomaterials including polyacrylates [106, 107] and PEG [108, 109].

##### 2.3.2.1.2.1 Alginate

Alginate microcapsules are made by  $\text{Ca}^{2+}$  or  $\text{Ba}^{2+}$  cross-linked gel formation. The traditional type of alginate microcapsules is alginate-poly-L-lysine alginate (APA) microcapsules. APA microencapsulation of islets, first reported by Lim and Sun [110], of

encapsulation devices from the macro- to nano-scale has shown that islets encapsulated in APA microcapsules survived well and resulted in long term normoglycemia [111, 112].

Figure 2.3 shows the protocols of islets microencapsulation with APA [11].

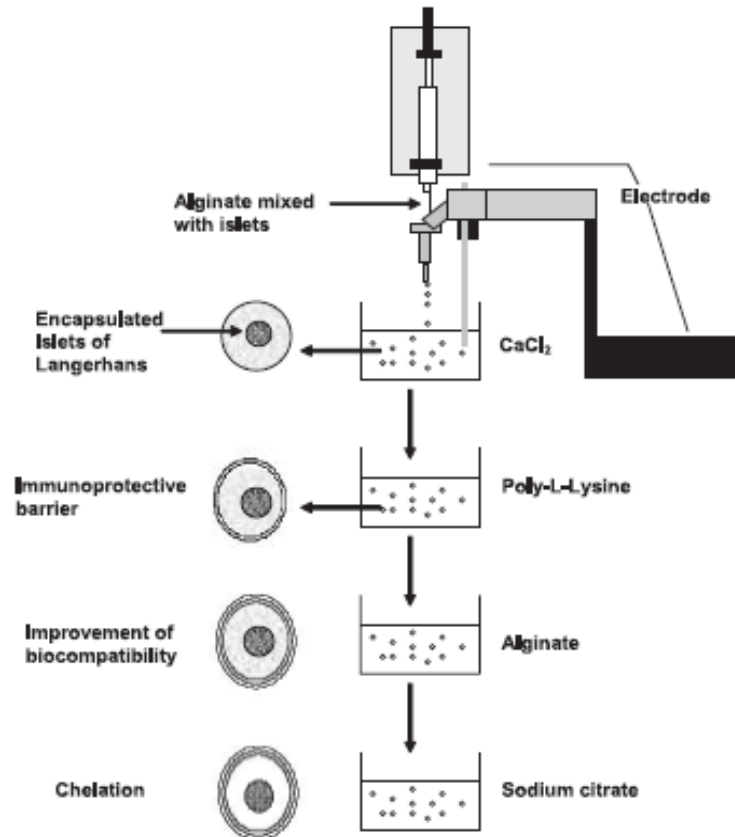


**Figure 2. 3** Microencapsulation of islets with alginate-polylysine [111].

The shortcomings of APA microcapsules are that they are immunogenic and highly bio-incompatible due to the PLL coating. PLL coating degrades over time, consequently leading to alginate matrix destabilization [113-115]. To overcome the drawback associated with APA microcapsules, many people tried to crosslink alginate with barium ions instead of calcium and without PLL to make barium alginate

microcapsules [116]. Morch et al. [117] showed that the gelation ion  $Ba^{2+}$  rather than  $Ca^{2+}$  yielded microcapsules of higher strength and stability when used with high G alginate compared to APA microcapsules. Tuch et al. [118] is processing a product of barium alginate microcapsules in phase I clinical study.

#### 2.3.2.1.2.2 Agarose

Agarose microcapsules are made by gel formation in response to low temperatures. Agarose microcapsules have been investigated as a stable and durable immunoisolation membrane in human body [119-121]. Highly purified islets isolated from non-obese diabetic (NOD) mice were microencapsulated in 5% agarose hydrogel as a semi-permeable membrane to examine the feasibility of the immunoisolation. The size range of agarose microcapsules was 100 to 400  $\mu m$ . Islets encapsulated in agarose microcapsules were transplanted into NOD spontaneously mice. Agarose microcapsules were able to completely protect NOD islet isografts from autoimmune destruction [121].

#### 2.3.2.1.3 Nano-scale encapsulation

The design of nano-scale encapsulation is similar to microcapsules. The difference of nanoencapsulation compared to microencapsulation is to decrease the thickness of the coating covering around the islets for forming the conformal coating. The conformal coating can decrease the size of encapsulated islets, advance the passage of nutrient, waste and insulin secretion between the implanted islets and extracellular matrix (ECM), and improve the viability of islets. The ultimate goal of the BAP is the



immunoisolation property for protecting implanted islets from host immune systems, while at the same time still keeping cell function and viability as well as normal islets. Islets with a thin coating can be transplanted into the liver through the portal veins. In the following, some new techniques for surface modification of islets will be introduced.

#### 2.3.2.1.3.1 Polymers coating

Surface modification with ultra thin polymer membranes was reported by chemically treating red blood cells to enclose surface antigen [122-124]. The surface modification of islets with thin polymer membranes has been investigated by using amphiphilic polymers, such as PEG-conjugated phospholipid (PEG-lipid), polyvinyl alcohol (PVA, carrying long alkyl chains), and cationic polymers like poly (ethyleneimine) (PEI) (Fig. 2.4) [125].

PEI as a cationic polymer can be coated on the islets surface by the layer-by-layer method. The negatively charged cell surface bond with positively charged PEI, and then the surface is further exposed to a negatively charged polymer to form a layer-by-layer membrane based on the electrostatic binding theory [126].

The PEG chain can be anchored to the cell surface through the hydrophobic portion of the PEG-lipid and incorporated into the lipid layer of the cell membrane [127-129]. The thickness of the PEG layer on the cell surface is several nanometers, which depends on the molecular weight of the PEG used [130]. The layer-by-layer method was used to improve the stability of the PEG-lipid membrane on the cell surface. Functional groups, such as biotin and maleimide, can be easily bonded to the end of the PEG chain

of PEG-lipid [131, 132]. Teramura et al. [127] formed a layer-by-layer membrane of PVA with thiol groups on a PEG-lipid with a maleimide group on the surface of islets using the reaction between the thiol and maleimide groups. Moreover, PEG carrying an N-hydroxyl-succinimidyl ester (NHS), activated ester group at one end was employed to react with an amino group of the membrane proteins or collagen layer on the islet surface [133, 134]. Byun's group reported that normoglycemia was maintained for 1 year after islets with a PEG-NHS modified surface were transplanted into recipient rats treated with low dose of cyclosporine A [135, 136].

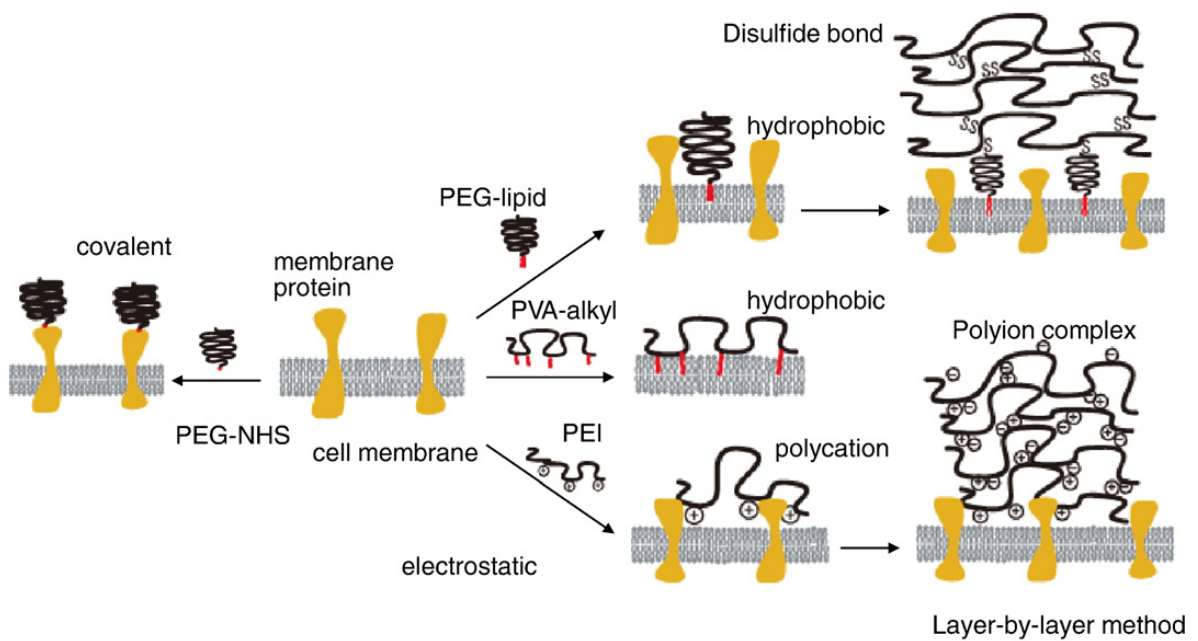


**Figure 2. 4** Modification of cell surface with synthetic polymers: Covalent bonding, hydrophobic interaction, electrostatic interaction, and the layer-by-layer method [125].

### 2.3.2.1.3.2 Living cells coating

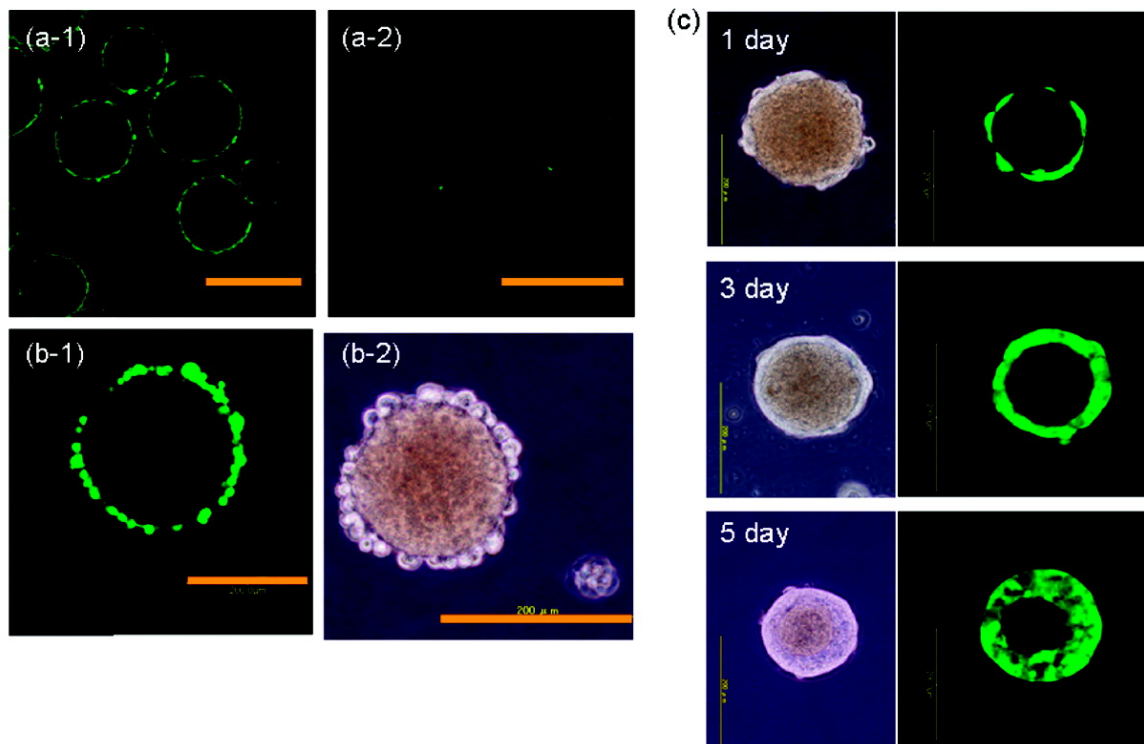


**Figure 2. 5** Encapsulation of islets with living cells. (A) Hamster islets modified with polyA20-PEG-lipid were treated with (a-1, FITC) FITC-labeled polyT20. (a-2) Naked islets were treated with FITC-labeled polyT20. (B) Attachment of polyT20-PEG-lipid modified GFP-HEK cells onto the surface of polyA20-PEG-lipid modified hamster islets. An islet was observed by a confocal laser scanning microscope for (b-1, GFP) and a phase contrast microscope (b-2). (C) GFP-HEK cells-immobilized islets were cultured for 1, 3, and 5 days. Islets were observed by a phase contrast microscope (left panels) and a confocal laser scanning microscope (right panels, GFP). Scale bars: 200  $\mu\text{m}$  [140].

The new approach for surface modification of islets is living cells coating. Living cells coating can improve the histocompatibility and blood compatibility, inhibit the graft

rejection, and decrease the destruction of implanted islets resulting from blood-mediated inflammatory reactions. Pollok et al. [137] first attempted to microencapsulate rat islets with a porcine chondrocyte membrane. Kim et al. [138] also macroencapsulated islets with a chondrocyte membrane using the cell sheet engineering technique. Teramura et al. [139, 140] used amphiphilic PEG-lipid and the biotin/streptavidin reaction to immobilize HEK293 cells on the surface of islets (Figure 2.5). The function of insulin secretion was well maintained after HEK293 cell encapsulation.

#### 2.3.2.2 Islets functional modification

There has been growing attention in modifying islets with growth factors or peptides to confer biological functionality.

##### 2.3.2.2.1 Growth factors

In pancreatic islet transplantation, early revascularization is necessary for long-term graft function. Cabric et al. [141] has shown in *in vitro* and *in vivo* models that modification with surface-attached heparin protected the islets from acute attack by the innate immune system of the blood following intraportal islet transplantation. Furthermore, vascular endothelial growth factor-A was conjugated to heparin as a means of attracting endothelial cells to induce angiogenesis and revascularization to improve islet engraftment in pancreatic islet transplantation.

#### 2.3.2.2.2 Peptides

Islet transplantation has the potential to treat type I diabetes; however, its widespread clinical application is limited by the massive apoptotic cell death and poor revascularization of transplanted islet grafts. Wu et al. [142] constructed a surface-modified adenoviral vector with Arg-Gly-Asp (RGD) sequences encoding a human X-linked inhibitor of apoptosis and hepatocyte growth factor (RGD-Adv-hHGF-hXIAP). *In vivo* transduction of islets with RGD-Adv-hHGF-hXIAP decreased apoptotic islet cell death, improved islet revascularization, and eventually might improve the outcome of human islet transplantation.

#### 2.3.3 Beta cells transplantation

Within islets, there are five endocrine cell types that work as a micro-organ to maintain glucose homeostasis. Insulin is normally produced in and secreted by the  $\beta$ -cells of islets. Because of difficulties associated with the use of primary islets, such as limited human pancreas donation, the risk of zoonosis in case of an animal source, low isolation yield, and preservation [143], the  $\beta$ -cells replacement through cellular transplantation to replace primary islets has the promise of providing a long-term cure for type 1 diabetes. To achieve this goal,  $\beta$ -cells have been transplanted with hollow fibers, diffusion chambers, hydrogels, macrocapsules, or composites of them. These carriers have been proposed to protect cells from attack by the host immune system and to enhance  $\beta$ -cell survival and function *in vivo*.

### 2.3.3.1 Hollow fibers

The blood perfusion hollow fiber is similar to dialysis. Blood is perfused in the hollow fiber and  $\beta$ -cells are placed around the fibers. The advantage of the hollow fibers device is to enhance the diffusive exchange rate between  $\beta$ -cells and blood [144]. For example, the poly (ethylene-co-vinyl alcohol) (EVAL) hollow fibers were designed to develop a new type of bioartificial pancreas [100]. As Figure 2.6 shows, the device includes EVAL hollow fibers and poly (amino unrethane) coated, non-woven poly (tetrafluoroethylene) (PTFE) fabrics. Beta cells attached to the surface of the PTFE fabric, but not to the surface of the EVAL hollow fibers, allowing nutrient and oxygen exchange between blood flowing inside the fibers and cells outside.

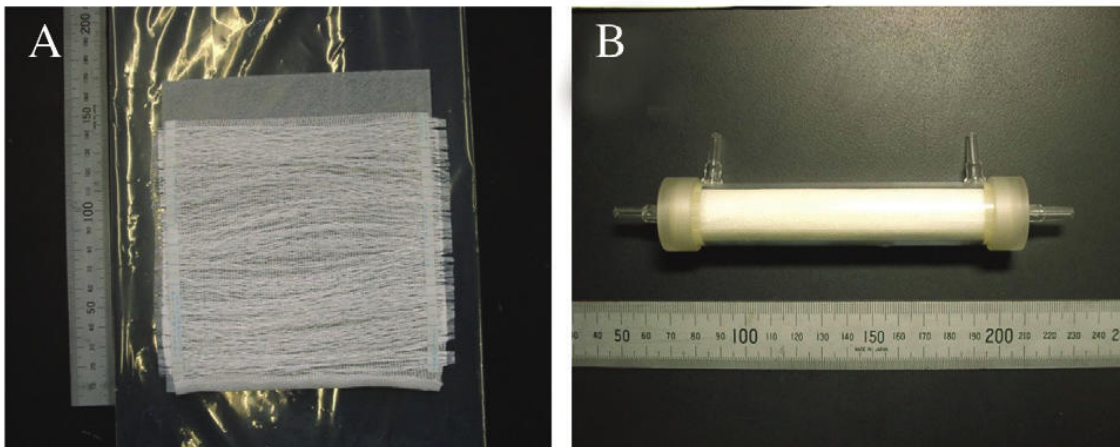


**Figure 2. 6** Construction of a bioartificial pancreas module. (A) A piece of non-woven fabric with a backing of rayon cloth was covered with 550 hollow fibers. (B) The fibers and cloth were rolled together and the spaces between the hollow fibers were sealed with urethane, and the roll was inserted into a polycarbonate casing with dimensions as shown [100].

### 2.3.3.2 Diffusion chambers

The macroencapsulation of  $\beta$ -cells includes a diffusion chamber in which  $\beta$ -cells are contained in a space surrounded by a semi-permeable membrane [145]. The advantage is that this chamber can be easily implanted into an intraperitoneal or subcutaneous space and is also easy to remove [146, 147]. Typically,  $\beta$ -cells are entrapped between two semi-permeable membranes placed on both sides of a ring-like structure. A PTFE device was used to encapsulate human fetal pancreatic islet-like cell clusters and transplanted into immunodeficient mice. After one month, encapsulated cell clusters survived, replicated, and acquired a level of glucose responsive insulin secretion sufficient to ameliorate hyperglycemia in diabetic mice [145, 148, 149].

Alumina biocapsule can be regarded as a particular type of diffusion chamber. These devices [150-152] have robust membranes and their pore size and pore size distribution can be easily controlled. The capsules were fabricated out of aluminum and aluminum oxide using a two-step anodization procedure, and the pore size is about 72 nm. PEG immobilization on the alumina surface was achieved using a covalent coupling agent silicon tetrachloride. *In vivo* study has demonstrated that implantation of these capsules into the peritoneal cavity of rats induces a transient inflammatory response, and that PEG was useful in minimizing the host response to the material.

### 2.3.3.3 Hydrogels

Encapsulation of  $\beta$ -cells within hydrogels is a potential transplantation therapy independent of immune suppression for type 1 diabetes. Hydrogels as semi-permeable

barriers allow the passage of insulin, nutrients and waste, while preventing cell-cell contact between host immune cells and encapsulated  $\beta$ -cells and the penetration of large immune cell-secreted antibodies. Several hydrogels have been developed toward this application, such as PEG, agarose [153, 154], collagen-alginate [155], collagen-gelatin [156, 157], and polyurethane-polyvinylpyrrolidone [158].

#### 2.3.3.3.1 PEG hydrogels

PEG hydrogels provide a highly biocompatible niche for  $\beta$ -cells because of their high water content, simple chemical modifications to incorporate biomolecules, and limited immunogenicity *in vivo* [159-162]. A photopolymerization PEG hydrogels was developed to test the effects of microenvironmental culture parameters on survival and function of encapsulated  $\beta$ -cells [163]. The results showed that the different hydrogel crosslinking density did not affect  $\beta$ -cells survival, and encapsulated  $\beta$ -cells transplanted into diabetic mice decreased blood glucose levels to normal levels. Furthermore, different matrix proteins, including collagen type I and IV, fibrinogen, fibronectin, laminin, and vitronectin, were mixed into PEG hydrogels to investigate the effects of matrix proteins on  $\beta$ -cells survival and function [164]. Apoptosis in encapsulated  $\beta$ -cells was less in the presence of each matrix protein, suggesting the ability of individual matrix interactions to prevent matrix signaling-related apoptosis (anoikis). Beta cell function in hydrogels presenting both collagen type IV and laminin revealed synergistic interactions.

PEG hydrogels provide a blank platform on which defined bioactive/functional motifs, such as peptides, can be easily incorporated without significantly affecting the



bulk material properties [165]. Cell-adhesive peptides (e.g., RGD, IKVAV, YIGSR, etc.) have been routinely conjugated within synthetic PEG hydrogel networks to promote survival of  $\beta$ -cells [166, 167]. The different peptides conjugated on PEG hydrogels and their effects on behaviors of  $\beta$ -cells are given in Table 2.2.

However, encapsulation with passive barrier PEG alone is generally insufficient to protect  $\beta$ -cells from rejection, because small cytotoxic molecules produced by activated T cells can diffuse readily into the capsule and mediate allograft death. As a means to provide bioactive protection for polymeric encapsulation devices, Hume et al. [168, 169] investigated a functionalized polymeric coating that mimics a natural T cell regulation pathway. Anti-Fas antibodies capable of inducing T cell apoptosis were covalently incorporated PEG hydrogels. Figure 2.7 shows how the functionalized PEG was formed. Glucose oxidase-initiated dip coatings enabled the rapid formation of uniform PEG-based coatings which incorporate anti-Fas antibody on the surfaces of PEG hydrogels.

**Table 2. 2** Peptide conjugated PEG hydrogels for  $\beta$  -cells encapsulation.

Conjugated peptides	Results	References
IKLLI, IKVAV	Preserved viability, reduced apoptosis, and increased insulin secretion	[166]
GRGDS	Promoted cell spread	[168]
LRE, PDSGR, RGD, YIGSR	Improved viability	[166]
Immobilized fusion proteins (EphA5-Fc and EphrinA5-Fc)	Increased viability	[167]
GRGDSPG, FEWTPGWYQPY	Exerted a protective effect on cells from damage induced by pro-inflammatory cytokines	[169]
Glucagon-like peptide 1	Enhanced the survival and insulin secretion	[170]

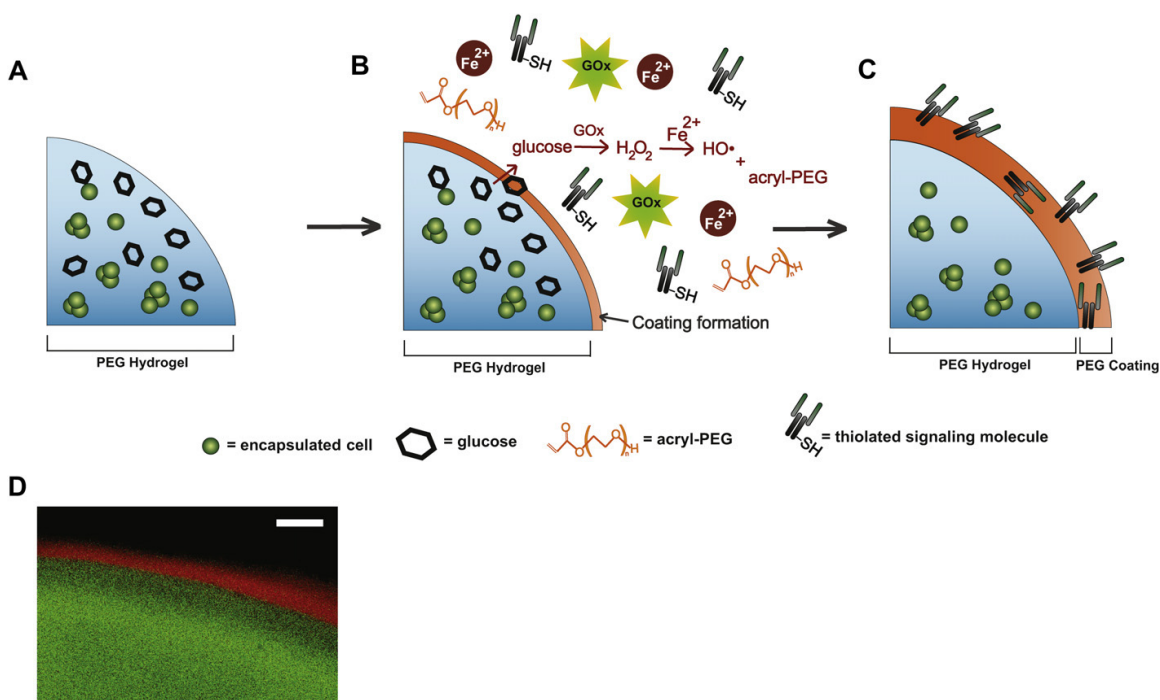


**Figure 2. 7** Schematic illustrating the formation of polymer coatings initiated by glucose oxidase (GOx). (A) Cell-laden PEG hydrogels are swollen in a glucose-containing media and then (B) dipped into a pre-polymer solution containing acryl-PEG, GOx, Fe<sup>2+</sup>, and thiolated signaling molecules. Glucose diffuses out of the gel, reacts with GOx and initiates polymerization at the surface of the hydrogel. (C) Reactive coating results in conformal PEG layers. (D) Confocal micrograph of PEG hydrogel (green) with GOx mediated polymer coating (red). Scale: 200  $\mu\text{m}$  [169].

#### 2.3.3.3.2 Glucose-responsive hydrogels

A glucose-responsive hydrogel including concanavalin A was suggested to control the release insulin through  $\beta$ -cells entrapped in hydrogels [170, 171]. At low glucose concentrations, the materials were in a gel state that exhibited low insulin permeability, while at high glucose levels, the materials became a solution that exhibited

a higher permeability to insulin. Thus, at low glucose concentrations, a higher fraction of the insulin secreted by cells accumulated within the construct, and the insulin release rate was relatively low. When the construct was exposed to high glucose, the material became a more permeable solution, and the insulin release rate from the construct was higher.

#### 2.3.3.3.3 Collagen-alginate hydrogels

Lee et al. [155] formed islets cell spheroids by using concave wells, and then encapsulated spheroids into alginate and collagen-alginate composite (CAC) hydrogels. Figure 2.8 shows the fabrication process. Alginate or CAC was covered on a concave microwell model containing islets spheroids, and  $\text{CaCl}_2$  solution was diffused through a nano-porous dialysis membrane to achieve uniform polymerization, forming convex structures. The *in vitro* and *in vivo* data showed that the collagen-alginate microencapsulation method enhanced the viability and function of islet spheroids, and protected these spheroids from immune attack.

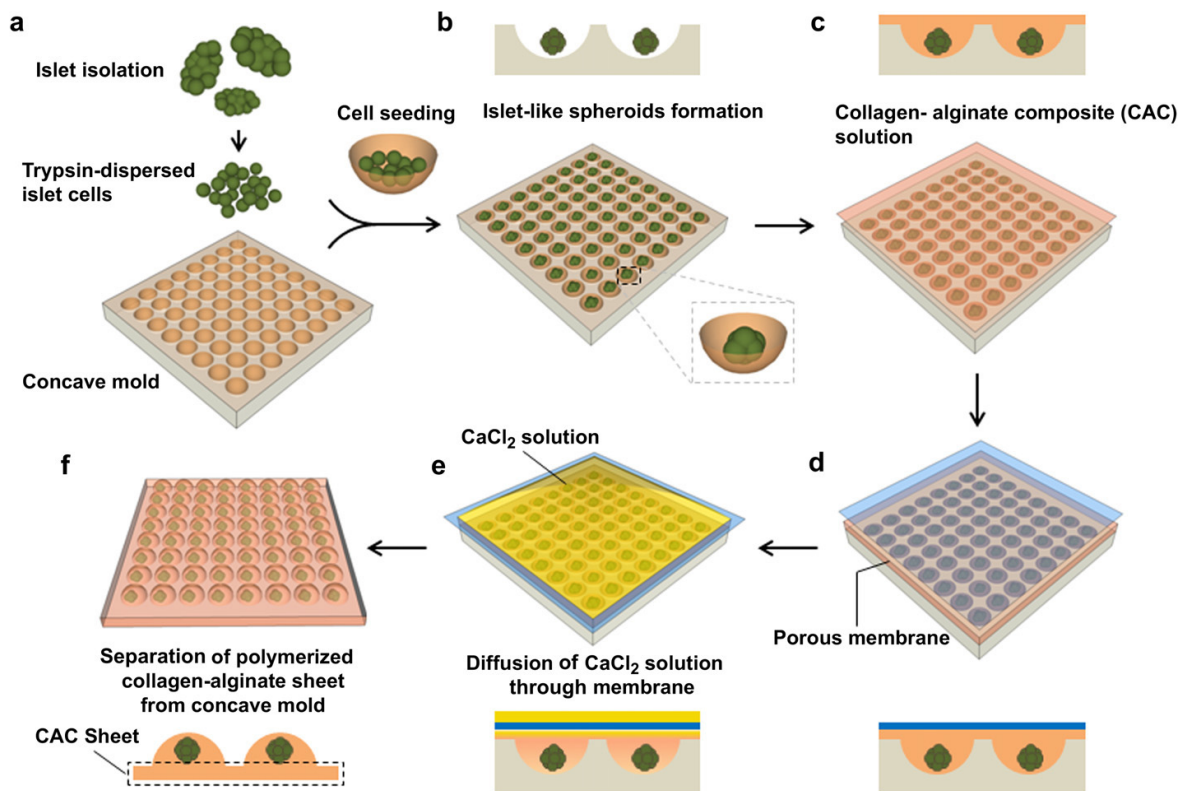


**Figure 2. 8** Schematic depiction of the *in vitro* cultivation of dispersed islet single cells, formation of islet cell-spheroids using concave microwell arrays, and the process of spheroids encapsulation within collagen-alginate composite [155].

#### 2.3.3.4 Microcapsules

Encapsulation of  $\beta$ -cells in micro scale capsules has been suggested as an alternative approach compared to macroencapsulation. Microencapsulation increases surface-area-to-volume ratio, which enhances transport properties. The most popular biomaterials used to encapsulate  $\beta$ -cells are alginate and agarose.

#### 2.3.3.4.1 Alginate

Traditional microencapsulation involves entrapping  $\beta$ -cells in a alginate/polylysine capsule [172-174]. For monitoring the fate of transplanted  $\beta$ -cells, gold nanoparticles treated with dithiolated diethylenetriamine-pentaacetic acid and gadolinium chelates (GG) were co-encapsulated in alginate capsules [173, 174]. Figure 2.9 shows a three-dimensional structure of an alginate/polylysine microspheroid encapsulating  $\beta$ -cells and GG. The micro spheroid allowed diffusion of oxygen, nutrients, glucose, and insulin, and blocked the passage of immune cells and antibodies. Gold nanoparticles enabled multimodal cellular imaging of transplanted islet cells such as magnetic resonance imaging, micro-computed tomography, and 40-MHz ultrasonography.

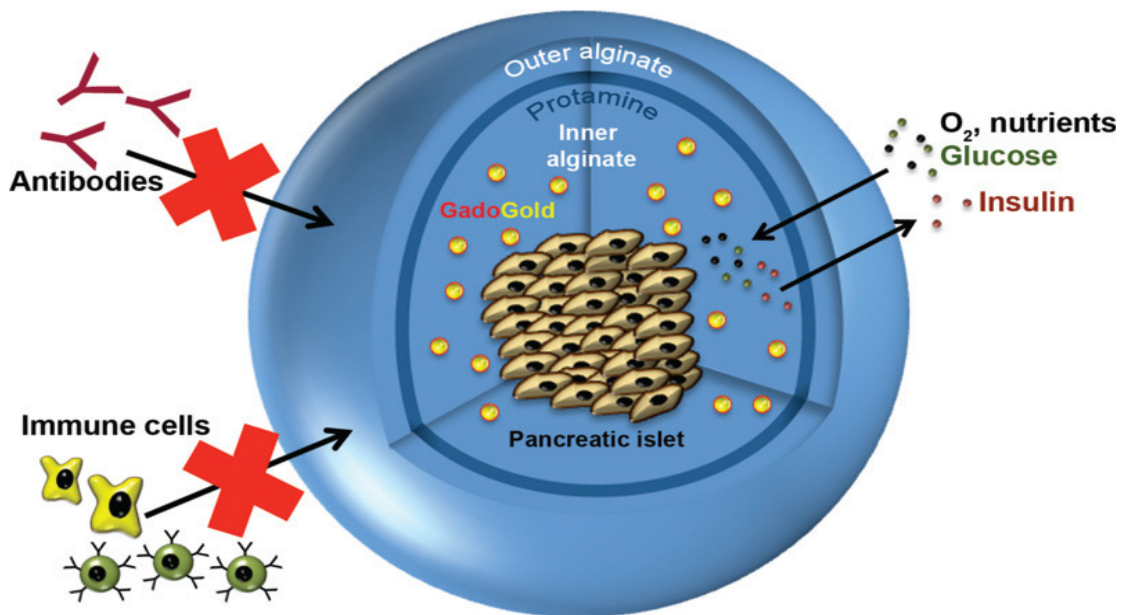


**Figure 2. 9** Three-dimensional structure of alginate/polylysine microspheroid encapsulating  $\beta$ -cells and gadolinium chelates [174].

To improve the passage of oxygen, nutrients, glucose, and insulin, some groups tried to decrease the size of microcapsules through conformal encapsulation [175] or nanofilm encapsulation technique [176]. An electrostatic layer-by-layer (LBL) technology was developed to form a chitosan/alginate nanocoating film on the surface of MIN-6  $\beta$ -cell clusters [176]. A phosphorylcholine-modified chondroitin-4-sulfate layer was coated on the surface of  $\beta$ -cell microcapsules to reduce nonspecific protein adsorption of the chitosan/alginate nanofilm and to enhance biocompatibility of the nanocoating.

For fabricating homogenous and asymmetric microencapsulation, Dang et al. [177] developed a new fabrication method by using micromolding systems. The rat insulinoma cell line (INS-1) was used and encapsulated with alginate in a polypropylene mesh mold. After cross-linking by  $\text{CaCl}_2$ , Alginate hydrogel microcapsules were formed. Beta cells encapsulated in alginate microcapsules maintained desirable viability and preserved their ability to proliferate and secrete insulin in a glucose-responsive manner.

#### 2.3.3.4.2 Poly (N-isopropylacrylamide)

Liu et al. [178] reported that the encapsulation of MIN6 cells was investigated by using thermally induced gelable materials based on poly (N-isopropylacrylamide). A vertical co-extrusion was used and a 37 °C collection bath was settled with a paraffin layer above media. The size of microcapsules ranged from 500 to 900  $\mu\text{m}$ . Encapsulated  $\beta$ -cells exhibited high viability after 5 days and a static glucose challenge showed glucose-dependent insulin secretion.

### 2.3.3.5 Composites

#### 2.3.3.5.1 Hollow fibers/microcapsules

To start, people encapsulated single  $\beta$ -cells into microcapsules to fabricate artificial islets, and then entrapped artificial islets in chambers of hydrogels for *in vivo* transplantation. A blood perfusion composite was fabricated based on  $\beta$ TC3/agarose microspheres encapsulated in a polysulfone hollow fiber [179]. The *in vitro* results showed that encapsulated  $\beta$ TC3 exhibited high viability and functionality compared to islets. Yang et al. [180] designed a bioartificial pancreas based on a calcium phosphate cement chamber used to encapsulate  $\beta$ -cells/agarose microspheres. *In vitro* results exhibited that encapsulated  $\beta$ -cells had normal viability, cell survival and insulin secretion. *In vivo* study showed that the bioartificial pancreas implanted in the bone marrow cavity for the spontaneous diabetic was effective [181, 182].

#### 2.3.3.5.2 Hydrogels/microcapsules

For early research,  $\beta$ -cells/agarose microspheres were entrapped in chitosan/gelatin hydrogel as an immunoisolative matrix [156]. Microencapsulated  $\beta$ -cells/agarose microspheres kept functional activity and secreted insulin continually for 60 days *in vitro*. Chitosan/gelatin hydrogels revealed cytoprotective effects against cytokine-mediated cytotoxicity. After being injected with chitosan/gelatin containing  $\beta$ -cells/agarose microspheres at the subcutaneous tissue, the non-fasting blood glucose concentrations of diabetic rats injected was decreased to euglycemic status albeit hyperglycemia within 10 days and was maintained at less than 200 mg/dL for 25 days

[157].

#### 2.3.4 Cell sources for $\beta$ -cell regeneration

Although transplantation of human islets has the potential to treat type 1 diabetes, the limitations of donors and immunosuppression therapy restrict the application. Thus, alternative sources of  $\beta$ -cells need to be found. There have been two major approaches for  $\beta$ -cell regeneration in recent years: the *in vitro* generation of renewable  $\beta$ -cells suitable for transplantation and the *in vivo* regeneration of  $\beta$ -cells from undefined progenitors or adult stem cells.

##### 2.3.4.1 *In vitro* generation of $\beta$ -cells

As for *in vitro* regeneration,  $\beta$ -cells can be obtained from different sources, such as embryonic stem cells (ESCs), induced pluripotent stem cells, and so on. The details about how to regenerate  $\beta$ -cells from these stem cells have been thoroughly investigated and can be referred to reviews: [183-185]. However, the conditions under which the pancreatic stem cells mature into insulin-producing cells still need to be well defined. Of the safety concerns associated with the transplantation of stem cell-derived tissues, one main issue is tumorigenicity. Moreover, the use of immunosuppressive drug regimens concurrent with the use of allogenic or xenogenic cells for transplantation will need to be elucidated, tested and standardized. At present, the effect of immunosuppressive drugs on the insulin-producing capacity of pancreatic stem cells is unknown.



For *in vitro* regeneration, various types of bioengineering approaches have been used to offer a microenvironment mimicking the niche. The niche plays an important role in promoting cell-to-cell interaction, cell proliferation and differentiation into specific lineages, as well as tissue organization [186, 187]. The study of  $\beta$ -cell regeneration based on bioengineering approaches is mainly focused on the cell sources of embryonic stem cells, embryonic pancreatic precursor cells, fetal pancreatic precursor cells, and mesenchymal stem cells [188].

#### 2.3.4.1.1 Embryonic stem cells (ESCs)

Embryonic stem cells have been investigated as a potential renewable source of cells in replacement therapies for type 1 diabetes. The five step protocol for *in vitro* generation of pancreatic cells from ESCs was reported in which cells were transitioned through mesendoerm, definitive endoderm, foregut endoderm, pancreatic endoderm, and the endocrine precursor stage, until mature  $\beta$ -cells were obtained [189].

Calcium alginate microspheres were used to encapsulate human embryonic stem cells (hESCs). The three dimensional model promoted cellular interactions. These encapsulated hESCs were differentiated to definitive endoderm [190]. Hoof et al. [191] tried to adjust the differentiation of hESCs into pancreatic endoderm through culturing hESCs in glass cover slips patterned by the covalent microcontact-printing of laminin in circular patches of 120  $\mu\text{m}$  in diameter. These hESCs formed clusters and differentiated to pancreatic endoderm-like cells. Moreover, mouse ESCs (mESCs) were encapsulated in collagen gel to form a three dimensional ES cell pancreatic differentiation system. The

encapsulated mESCs can assemble into an islet-like tissue structure. Nearly 50-60% of the cells formed cell clusters expressed insulin.

#### 2.3.4.1.2 Pancreatic precursor cells

Pancreatic precursor cells are isolated from the developing pancreatic bud. These cells have been investigated as an unlimited source of  $\beta$ -cells, as they have been directed down the early stages of pancreatic development but remain proliferative and have the innate ability to differentiate into insulin-producing  $\beta$ -cells [192].

Previous research has shown that embryonic pancreatic precursor cells encapsulated in unmodified PEG selectively after 7 days differentiated into pancreatic  $\beta$ -cells which were immature and unable to release insulin in response to changes in media glucose concentration [193]. For functional  $\beta$ -cell regeneration, collagen type 1 was entrapped in a PEG culture system [194]. Collagen type 1, which promotes mature cell viability and function, entrapped in PEG hydrogels could improve the differentiation of precursor cell clusters to form mature, glucose-responsive, islet-like structures. Concerted differentiation of pancreatic precursor cell aggregates into functionally mature islet-like clusters can be achieved in PEG culture system by blocking cell contact-mediated Notch signaling with a gamma-secretase inhibitor [195].

For *in vivo* regeneration, porcine neonatal pancreatic cell clusters microencapsulated in barium alginate were transplanted into streptozotocin-induced diabetic severe combined immunodeficient mice [196, 197]. These results exhibited that cells/alginate microspheres transplanted into immunocompetent mice could differentiate

into  $\beta$ -cells and reverse high blood glucose levels without immunosuppression for above 20 weeks. Montanucci et al. [198] encapsulated human islet-derived stem/precursor cells within alginate microspheres for transplantation. Alginate-based microspheres acted as three-dimensional niches to promote post-transplant precursor differentiation and acquisition of stem cells into immunodeficient (SCID) mice.

#### 2.3.4.2 *In vivo* regeneration of $\beta$ -cells

Recently, *in vivo* neogenesis of  $\beta$ -cells from pancreatic and non-pancreatic cells has been reported in adults. Evidence to support the presence in adult pancreas of a population of undifferentiated stem/progenitor cells that can give rise to all pancreatic cell types has still not been found. It has been shown that replication of differentiated  $\beta$ -cells contributed to new  $\beta$ -cells during normal adult life. However, neogenesis of islets also occurred during normal development (at least during the first month) and in response to physical and physiological stress. Recently, Xu et al. [199] demonstrated that the neogenesis of  $\beta$ -cells accompanied the induction of Ngn3-expressing endocrine progenitors in the ductal lining in the regenerating portion but not in the non-injured pancreas. Also, the liver represents an attractive *in vivo* source for generating  $\beta$ -cells due to its related developmental origin to the pancreas and its ease of genetic and surgical manipulation.

## 2.4 Conclusion remarks

Although various delivery systems such as hydrogels and microspheres have proved to be effective for insulin release, and non-injectable methods of insulin delivery have resulted in some clinical researches [200], frequent blood glucose monitoring and multiple daily insulin injections are still the common treatment for type 1 diabetes. This treatment can not provide sustained release and the insulin amount is not finely tuned to glycemia, so it can not prevent long-term complications such as cardiovascular disease, retinopathy, and nephropathy [201]. The development of a fully automated glucose-responsive device is the ultimate aim for type 1 diabetes treatment.

Pancreatic islet transplantation is a potential approach for patients not only to avoid insulin injection, but also to avoid complications. The limitations of islet transplantation are the significant shortage of donor pancreases and the long-term immunosuppressive therapy after transplantation. The development of a bioartificial pancreas based on bioengineering approaches has been considered to solve these problems.

The bioartificial pancreas based on bioengineering strategies protects transplanted islets from the immune system, but the next problem is how to improve long-term survival and function of transplanted pancreatic islets. It would be beneficial to mimic the  $\beta$ -cell interactions within its native environment and create this islet niche as best as possible in a carrier or capsule. The environment would include not only the islets, but accessory cells, proteins, and possibly local immunosuppression housed within a biocompatible materials. This microenvironment can also provide an alternative for the

regenerative cell-based therapy, so that other sources of  $\beta$ -cells can find their way to clinical therapy.

## 2.5 References

1. Silva, A.I., et al., *An overview on the development of a bio-artificial pancreas as a treatment of insulin-dependent diabetes mellitus*. Med Res Rev, 2006. **26**(2): p. 181-222.
2. Ludwig, B., et al., *Islet Versus Pancreas Transplantation in Type 1 Diabetes: Competitive or Complementary?* Current Diabetes Reports, 2010. **10**(6): p. 506-511.
3. Fioretto, P. and M. Mauer, *Effects of pancreas transplantation on the prevention and reversal of diabetic nephropathy*. Contrib Nephrol, 2011. **170**: p. 237-46.
4. Vaithilingam V, T.B., *Islet transplantation and encapsulation: an update on recent developments*. Rev Diabet Stud., 2011. **8**(1):51-67.
5. Wagner, R.T., et al., *Stem cell approaches for the treatment of type 1 diabetes mellitus*. Transl Res, 2010. **156**(3): p. 169-79.
6. Noguchi, H., *Pancreatic stem/progenitor cells for the treatment of diabetes*. Rev Diabet Stud, 2010. **7**(2): p. 105-11.
7. Korsgren, O. and B. Nilsson, *Improving islet transplantation: a road map for a widespread application for the cure of persons with type 1 diabetes*. Curr Opin Organ Transplant, 2009. **14**(6): p. 683-7.
8. Matsumoto, S., *Islet cell transplantation for Type 1 diabetes*. J Diabetes, 2010. **2**(1): p. 16-22.
9. Esther S. O'Sullivan, A.V., Daniel G. Anderson, and Gordon C. Weir, *Islets transplanted in immunoisolation devices: a review of the progress and the challenges that remain*. Endocrine Reviews, 2011. **32**(6): p. 827-844.
10. Wilson, J.T. and E.L. Chaikof, *Challenges and emerging technologies in the immunoisolation of cells and tissues*. Advanced Drug Delivery Reviews, 2008. **60**(2): p. 124-145.

11. Sumi, S., *Regenerative medicine for insulin deficiency: creation of pancreatic islets and bioartificial pancreas*. Journal of Hepato-Biliary-Pancreatic Sciences, 2011. **18**(1): p. 6-12.
12. Kilpatrick, E.S., A.S. Rigby, and S.L. Atkin, *For debate. Glucose variability and diabetes complication risk: we need to know the answer*. Diabet Med, 2010. **27**(8): p. 868-71.
13. Galerneau, F. and S.E. Inzucchi, *Diabetes mellitus in pregnancy*. Obstet Gynecol Clin North Am, 2004. **31**(4): p. 907-933.
14. Evensen, A.E., *Update on gestational diabetes mellitus*. Prim Care, 2012. **39**(1): p. 83-94.
15. Courtney, M., et al., *In vivo conversion of adult  $\alpha$ -cells into  $\beta$ -like cells: a new research avenue in the context of type 1 diabetes*. Diabetes, Obesity and Metabolism. **13**: p. 47-52.
16. Gruessner, A.C., *2011 update on pancreas transplantation: comprehensive trend analysis of 25,000 cases followed up over the course of twenty-four years at the International Pancreas Transplant Registry (IPTR)*. Rev Diabet Stud, 2011. **8**(1): p. 6-16.
17. Boggi, U., et al., *Current perspectives on laparoscopic robot-assisted pancreas and pancreas-kidney transplantation*. Rev Diabet Stud, 2011. **8**(1): p. 28-34.
18. Rogers, J., et al., *Pancreas transplantation: lessons learned from a decade of experience at Wake Forest Baptist Medical Center*. Rev Diabet Stud, 2011. **8**(1): p. 17-27.
19. Duan, X. and S. Mao, *New strategies to improve the intranasal absorption of insulin*. Drug Discov Today. **15**(11-12): p. 416-27.
20. Robertson, R.P., *Update on transplanting beta cells for reversing type 1 diabetes*. Endocrinol Metab Clin North Am, 2010. **39**(3): p. 655-67.
21. de Kort, H., et al., *Islet transplantation in type 1 diabetes*. BMJ, 2011. **342**: p. d217.
22. Giraldo, J.A., J.D. Weaver, and C.L. Stabler, *Tissue engineering approaches to enhancing clinical islet transplantation through tissue engineering strategies*. J Diabetes Sci Technol, 2010. **4**(5): p. 1238-47.

23. Daoud, J., L. Rosenberg, and M. Tabrizian, *Pancreatic islet culture and preservation strategies: advances, challenges, and future outlook*. Cell Transplant, 2010. **19**(12): p. 1523-35.
24. Opara, E.C., et al., *Design of a bioartificial pancreas(+)*. J Investig Med, 2010. **58**(7): p. 831-7.
25. Montanya, E., *Islet- and stem-cell-based tissue engineering in diabetes*. Curr Opin Biotechnol, 2004. **15**(5): p. 435-40.
26. Burns, C.J., S.J. Persaud, and P.M. Jones, *Diabetes mellitus: a potential target for stem cell therapy*. Curr Stem Cell Res Ther, 2006. **1**(2): p. 255-66.
27. Bresson, D. and M. von Herrath, *Immunotherapy for the prevention and treatment of type 1 diabetes: optimizing the path from bench to bedside*. Diabetes Care, 2009. **32**(10): p. 1753-68.
28. Rewers, M. and P. Gottlieb, *Immunotherapy for the prevention and treatment of type 1 diabetes: human trials and a look into the future*. Diabetes Care, 2009. **32**(10): p. 1769-82.
29. Goudy, K.S. and R. Tisch, *Immunotherapy for the prevention and treatment of type 1 diabetes*. Int Rev Immunol, 2005. **24**(5-6): p. 307-26.
30. Banting, F.G., et al., *Pancreatic extracts in the treatment of diabetes mellitus: preliminary report. 1922*. CMAJ, 1991. **145**(10): p. 1281-6.
31. Damgé, C., C.P. Reis, and P. Maincent, *Nanoparticle strategies for the oral delivery of insulin*. Expert Opinion on Drug Delivery, 2008. **5**(1): p. 45-68.
32. Ramesan, R.M. and C.P. Sharma, *Challenges and advances in nanoparticle-based oral insulin delivery*. Expert Review of Medical Devices, 2009. **6**(6): p. 665-676.
33. Home, P.D., *The pharmacokinetics and pharmacodynamics of rapid-acting insulin analogues and their clinical consequences*. Diabetes, Obesity and Metabolism, 2012: p. no-no.
34. Little, S., J. Shaw, and P. Home, *Hypoglycemia rates with basal insulin analogs*. Diabetes Technol Ther, 2011. **13 Suppl 1**: p. S53-64.
35. Gordon Still, J., *Development of oral insulin: progress and current status*. Diabetes/Metabolism Research and Reviews, 2002. **18**(S1): p. S29-S37.

36. Choi, D., et al., *Effects of water-soluble tacrolimus-PEG conjugate on insulin-dependent diabetes mellitus and systemic lupus erythematosus*. Archives of Pharmacal Research, 2011. **34**(8): p. 1301-1310.
37. Zhang, R., et al., *Development and testing of solid dose formulations containing polysialic acid insulin conjugate: next generation of long-acting insulin*. J Diabetes Sci Technol, 2010. **4**(3): p. 532-9.
38. Jain, S., et al., *Polysialylated insulin: synthesis, characterization and biological activity in vivo*. Biochimica et Biophysica Acta (BBA) - General Subjects, 2003. **1622**(1): p. 42-49.
39. Thibaudeau, K., et al., *Synthesis and Evaluation of Insulin-Human Serum Albumin Conjugates*. Bioconjugate Chemistry, 2005. **16**(4): p. 1000-1008.
40. Shechter, Y., et al., *Albumin-Insulin Conjugate Releasing Insulin Slowly under Physiological Conditions: A New Concept for Long-Acting Insulin*. Bioconjugate Chemistry, 2005. **16**(4): p. 913-920.
41. Lee, E., J. Lee, and S. Jon, *A Novel Approach to Oral Delivery of Insulin by Conjugating with Low Molecular Weight Chitosan*. Bioconjugate Chemistry, 2010. **21**(10): p. 1720-1723.
42. Clement, S., et al., *Oral modified insulin (HIM2) in patients with type 1 diabetes mellitus: results from a phase I/II clinical trial*. Metabolism, 2004. **53**(1): p. 54-58.
43. DiCostanzo, C.A., et al., *Simulated first-phase insulin release using Humulin or insulin analog HIM2 is associated with prolonged improvement in postprandial glycemia*. American Journal of Physiology - Endocrinology And Metabolism, 2005. **289**(1): p. E46-E52.
44. Shechter, Y., et al., *Reversible pegylation of insulin facilitates its prolonged action in vivo*. European Journal of Pharmaceutics and Biopharmaceutics, 2008. **70**(1): p. 19-28.
45. Lee, S., et al., *A new drug carrier, Nalpha-deoxycholy-L: -lysyl-methylester, for enhancing insulin absorption in the intestine*. Diabetologia, 2005. **48**(3): p. 405-11.
46. Lee, S., et al., *Synthesis and biological properties of insulin-deoxycholic acid chemical conjugates*. Bioconjug Chem, 2005. **16**(3): p. 615-20.



47. Peth, J.A., et al., *Effects of a unique conjugate of alpha-lipoic acid and gamma-linolenic acid on insulin action in obese Zucker rats*. Am J Physiol Regul Integr Comp Physiol, 2000. **278**(2): p. R453-9.
48. Farmer, T.G., Jr., T.F. Edgar, and N.A. Peppas, *In Vivo Simulations of the Intravenous Dynamics of Submicron Particles of pH-Responsive Cationic Hydrogels in Diabetic Patients*. Ind Eng Chem Res, 2008. **47**(24): p. 10053-10063.
49. Wu, J., et al., *A thermosensitive hydrogel based on quaternized chitosan and poly(ethylene glycol) for nasal drug delivery system*. Biomaterials, 2007. **28**(13): p. 2220-32.
50. Lima, A., et al., *Synthesis of Temperature-Responsive Dextran-MA/PNIPAAm Particles for Controlled Drug Delivery Using Superhydrophobic Surfaces*. Pharm Res, 2011. **28**(6): p. 1294-1305.
51. Luo, R., H. Li, and K.Y. Lam, *Modeling the effect of environmental solution pH on the mechanical characteristics of glucose-sensitive hydrogels*. Biomaterials, 2009. **30**(4): p. 690-700.
52. Miyata, T., N. Asami, and T. Uragami, *A reversibly antigen-responsive hydrogel*. Nature, 1999. **399**(6738): p. 766-9.
53. Morishita, M., et al., *Novel oral insulin delivery systems based on complexation polymer hydrogels: Single and multiple administration studies in type 1 and 2 diabetic rats*. Journal of Controlled Release, 2006. **110**(3): p. 587-594.
54. Tuesca, A., et al., *Complexation hydrogels for oral insulin delivery: effects of polymer dosing on in vivo efficacy*. J Pharm Sci, 2008. **97**(7): p. 2607-18.
55. Nakamura, K., et al., *Oral insulin delivery using P(MAA-g-EG) hydrogels: effects of network morphology on insulin delivery characteristics*. Journal of Controlled Release, 2004. **95**(3): p. 589-599.
56. Kim, B. and N.A. Peppas, *In vitro release behavior and stability of insulin in complexation hydrogels as oral drug delivery carriers*. International Journal of Pharmaceutics, 2003. **266**(1-2): p. 29-37.
57. Perakslis, E., A. Tuesca, and A. Lowman, *Complexation hydrogels for oral protein delivery: an in vitro assessment of the insulin transport-enhancing effects following dissolution in simulated digestive fluids*. Journal of Biomaterials Science, Polymer Edition, 2007. **18**(12): p. 1475-1490.

58. Ichikawa, H. and N.A. Peppas, *Novel complexation hydrogels for oral peptide delivery: In vitro evaluation of their cytocompatibility and insulin-transport enhancing effects using Caco-2 cell monolayers*. Journal of Biomedical Materials Research Part A, 2003. **67A**(2): p. 609-617.
59. Madsen, F. and N.A. Peppas, *Complexation graft copolymer networks: swelling properties, calcium binding and proteolytic enzyme inhibition*. Biomaterials, 1999. **20**(18): p. 1701-1708.
60. Tuesca, A.D., et al., *Synthesis, characterization and in vivo efficacy of PEGylated insulin for oral delivery with complexation hydrogels*. Pharm Res, 2009. **26**(3): p. 727-39.
61. Gong, C., et al., *Biodegradable in situ gel-forming controlled drug delivery system based on thermosensitive PCL-PEG-PCL hydrogel. Part 2: sol-gel-sol transition and drug delivery behavior*. Acta Biomater, 2009. **5**(9): p. 3358-70.
62. Al-Tahami, K., et al., *Basal level insulin delivery: in vitro release, stability, biocompatibility, and in vivo absorption from thermosensitive triblock copolymers*. J Pharm Sci, 2011. **100**(11): p. 4790-803.
63. Oak, M. and J. Singh, *Controlled delivery of basal level of insulin from chitosan-zinc-insulin-complex-loaded thermosensitive copolymer*. Journal of Pharmaceutical Sciences, 2011: p. n/a-n/a.
64. Huynh, D.P., et al., *Controlled release of insulin from pH/temperature-sensitive injectable pentablock copolymer hydrogel*. Journal of Controlled Release, 2009. **137**(1): p. 20-24.
65. Shim, W.S., et al., *Biodegradability and biocompatibility of a pH- and thermo-sensitive hydrogel formed from a sulfonamide-modified poly( $\epsilon$ -caprolactone-co-lactide)-poly(ethylene glycol)-poly( $\epsilon$ -caprolactone-co-lactide) block copolymer*. Biomaterials, 2006. **27**(30): p. 5178-5185.
66. Huynh, D.P., et al., *Functionalized injectable hydrogels for controlled insulin delivery*. Biomaterials, 2008. **29**(16): p. 2527-2534.
67. Tang, M., et al., *A reversible hydrogel membrane for controlling the delivery of macromolecules*. Biotechnology and Bioengineering, 2003. **82**(1): p. 47-53.
68. Kim, J.J. and K. Park, *Modulated insulin delivery from glucose-sensitive hydrogel dosage forms*. Journal of Controlled Release, 2001. **77**(1-2): p. 39-47.

69. Damge C, M.C., Aprahamian A, et al., *Advantage of a new colloidal drug delivery system in the insulin treatment of streptozotocin-induced diabetic rats*. *Diabetologia*, 1986. **29**(531A).
70. Hodges GM, C.E., Hazzard RA, Carr KE., *Uptake and translocation of microparticles in small intestine. Morphology and quantification of particle distribution*. *Dig Dis Sci.*, 1995. **40**(5): p. 967-75.
71. Krishnankutty RK, M.A., Sedimbi SK, Suryanarayan S, Sanjeevi CB., *Alternative routes of insulin delivery*. *Zhong Nan Da Xue Xue Bao Yi Xue Ban*, 2009. **34**(10): p. 933-48.
72. Ibrahim, M.A., et al., *Stability of insulin during the erosion of poly(lactic acid) and poly(lactic-co-glycolic acid) microspheres*. *Journal of Controlled Release*, 2005. **106**(3): p. 241-252.
73. Rastogi, R., S. Anand, and V. Koul, *Evaluation of pharmacological efficacy of 'insulin-surfoplex' encapsulated polymer vesicles*. *International Journal of Pharmaceutics*, 2009. **373**(1-2): p. 107-115.
74. Jose, S., et al., *Cross-linked chitosan microspheres for oral delivery of insulin: Taguchi design and in vivo testing*. *Colloids and Surfaces B: Biointerfaces*, 2012. **92**(0): p. 175-179.
75. Ungaro, F., et al., *Insulin-loaded PLGA/cyclodextrin large porous particles with improved aerosolization properties: In vivo deposition and hypoglycaemic activity after delivery to rat lungs*. *Journal of Controlled Release*, 2009. **135**(1): p. 25-34.
76. Bilati, U., E. Allémann, and E. Doelker, *Strategic approaches for overcoming peptide and protein instability within biodegradable nano- and microparticles*. *European Journal of Pharmaceutics and Biopharmaceutics*, 2005. **59**(3): p. 375-388.
77. Qiu, Y. and K. Park, *Environment-sensitive hydrogels for drug delivery*. *Advanced Drug Delivery Reviews*, 2001. **53**(3): p. 321-339.
78. Mundargi, R.C., V. Rangaswamy, and T.M. Aminabhavi, *Poly(N-vinylcaprolactam-co-methacrylic acid) hydrogel microparticles for oral insulin delivery*. *Journal of Microencapsulation*, 2011. **28**(5): p. 384-394.
79. Kumar, A., S.S. Lahiri, and H. Singh, *Development of PEGDMA: MAA based hydrogel microparticles for oral insulin delivery*. *International Journal of Pharmaceutics*, 2006. **323**(1-2): p. 117-124.

80. Breuck, S., L. Baeyens, and L. Bouwens, *Expression and function of leukaemia inhibitory factor and its receptor in normal and regenerating rat pancreas*. *Diabetologia*, 2006. **49**(1): p. 108-116.
81. Santander-Ortega, M.J., et al., *Insulin-loaded PLGA nanoparticles for oral administration: an in vitro physico-chemical characterization*. *J Biomed Nanotechnol*, 2009. **5**(1): p. 45-53.
82. Sarmiento, B., et al., *Probing insulin's secondary structure after entrapment into alginate/chitosan nanoparticles*. *European Journal of Pharmaceutics and Biopharmaceutics*, 2007. **65**(1): p. 10-17.
83. Damge, C., P. Maincent, and N. Ubrich, *Oral delivery of insulin associated to polymeric nanoparticles in diabetic rats*. *J Control Release*, 2007. **117**(2): p. 163-70.
84. Aboubakar, M., et al., *Study of the mechanism of insulin encapsulation in poly(isobutylcyanoacrylate) nanocapsules obtained by interfacial polymerization*. *Journal of Biomedical Materials Research*, 1999. **47**(4): p. 568-576.
85. Mesiha, M.S., M.B. Sidhom, and B. Fasipe, *Oral and subcutaneous absorption of insulin poly(isobutylcyanoacrylate) nanoparticles*. *International Journal of Pharmaceutics*, 2005. **288**(2): p. 289-293.
86. Foss, A.C., et al., *Development of acrylic-based copolymers for oral insulin delivery*. *Eur J Pharm Biopharm*, 2004. **57**(2): p. 163-9.
87. Yang, J., H. Sun, and C. Song, *Preparation, characterization and in vivo evaluation of pH-sensitive oral insulin-loaded poly(lactic-co-glycolic acid) nanoparticles*. *Diabetes Obes Metab*, 2011.
88. Zhang, X., et al., *Nasal absorption enhancement of insulin using PEG-grafted chitosan nanoparticles*. *European Journal of Pharmaceutics and Biopharmaceutics*, 2008. **68**(3): p. 526-534.
89. Sonaje, K., et al., *Effects of chitosan-nanoparticle-mediated tight junction opening on the oral absorption of endotoxins*. *Biomaterials*, 2011. **32**(33): p. 8712-8721.
90. Elsayed, A., et al., *Chitosan–Sodium Lauryl Sulfate Nanoparticles as a Carrier System for the &lt;i>In Vivo Delivery of Oral Insulin*. *AAPS PharmSciTech*, 2011. **12**(3): p. 958-964.

91. Makhlof, A., Y. Tozuka, and H. Takeuchi, *Design and evaluation of novel pH-sensitive chitosan nanoparticles for oral insulin delivery*. European Journal of Pharmaceutical Sciences, 2011. **42**(5): p. 445-451.
92. Langkjær, L., et al., *Iontophoresis of monomeric insulin analogues in vitro: effects of insulin charge and skin pretreatment*. Journal of Controlled Release, 1998. **51**(1): p. 47-56.
93. Martanto, W., et al., *Transdermal Delivery of Insulin Using Microneedles in Vivo*. Pharm Res, 2004. **21**(6): p. 947-952.
94. Patton, J., *Breathing life into protein drugs*. Nat Biotech, 1998. **16**(2): p. 141-143.
95. Neumiller, J.J., R.K. Campbell, and L.D. Wood, *A review of inhaled technosphere insulin*. Ann Pharmacother, 2010. **44**(7-8): p. 1231-9.
96. Alsaleh, F.M., et al., *Insulin pumps: from inception to the present and toward the future*. J Clin Pharm Ther, 2010. **35**(2): p. 127-38.
97. Olsovsky, J., *[Modern technologies in diabetology. CSII (continuous subcutaneous insulin infusion) and CGM (continuous glucose monitoring) in clinical practice]*. Vnitr Lek, 2011. **57**(11): p. 919-22.
98. Maki, T., et al., *Successful treatment of diabetes with the biohybrid artificial pancreas in dogs*. Transplantation, 1991. **51**(1): p. 43-51.
99. Maki T, L.J., Carretta M, Ohzato H, Borland KM, Sullivan SJ, Staruk J, Muller TE, Solomon BA, Chick WL, et al., *Treatment of severe diabetes mellitus for more than one year using a vascularized hybrid artificial pancreas*. Transplantation., 1993. **55**(4):713-7.
100. Ikeda, H., et al., *A newly developed bioartificial pancreas successfully controls blood glucose in totally pancreatectomized diabetic pigs*. Tissue Eng, 2006. **12**(7): p. 1799-809.
101. CK., C., *Implantable biohybrid artificial organs*. Cell Transplant., 1995. **4**(4):415-36.
102. Scharp DW, S.C., Olack BJ, Latta PP, Hegre OD, Doherty EJ, Gentile FT, Flavin KS, Ansara MF, Lacy PE., *Protection of encapsulated human islets implanted without immunosuppression in patients with type I or type II diabetes and in nondiabetic control subjects*. Diabetes. , 1994. **43**(9):1167-70.

103. Lamb, M., et al., *Function and Viability of Human Islets Encapsulated in Alginate Sheets: In Vitro and in Vivo Culture*. Transplantation Proceedings, 2011. **43**(9): p. 3265-3266.
104. Zhi, Z.I., et al., *Nano-scale encapsulation enhances allograft survival and function of islets transplanted in a mouse model of diabetes*. Diabetologia: p. 1-10.
105. Grundfest-Broniatowski, S.F., et al., *A New Bioartificial Pancreas Utilizing Amphiphilic Membranes for the Immunoisolation of Porcine Islets: A Pilot Study in the Canine*. ASAIO Journal, 2009. **55**(4): p. 400-405  
10.1097/MAT.0b013e3181a8deba.
106. Uludag, H., P. De Vos, and P.A. Tresco, *Technology of mammalian cell encapsulation*. Advanced Drug Delivery Reviews, 2000. **42**(1-2): p. 29-64.
107. Pollok, J.M., et al., *Islets of Langerhans encapsulated with a tissue-engineered membrane of rat chondrocytes maintain insulin secretion and glucose-insulin feedback for at least 30 days in culture*. Transplantation Proceedings, 2001. **33**(1): p. 1713-1714.
108. Cruise, G.M., et al., *A sensitivity study of the key parameters in the interfacial photopolymerization of poly(ethylene glycol) diacrylate upon porcine islets*. Biotechnology and Bioengineering, 1998. **57**(6): p. 655-665.
109. Cruise, G.M., D.S. Scharp, and J.A. Hubbell, *Characterization of permeability and network structure of interfacially photopolymerized poly(ethylene glycol) diacrylate hydrogels*. Biomaterials, 1998. **19**(14): p. 1287-1294.
110. Lim, F. and A. Sun, *Microencapsulated islets as bioartificial endocrine pancreas*. Science, 1980. **210**(4472): p. 908-910.
111. Safley SA, C.H., Cauffiel S, Tucker-Burden C, Weber CJ., *Biocompatibility and immune acceptance of adult porcine islets transplanted intraperitoneally in diabetic NOD mice in calcium alginate poly-L-lysine microcapsules versus barium alginate microcapsules without poly-L-lysine*. J Diabetes Sci Technol, 2008. **2**(5):760-7.
112. Robitaille, R., et al., *Inflammatory response to peritoneal implantation of alginate-poly-L-lysine microcapsules*. Biomaterials, 2005. **26**(19): p. 4119-4127.
113. Iwata H, T.T., Kobayashi K, Oka T, Tsuji T, Ito F., *Strategy for developing microbeads applicable to islet xenotransplantation into a spontaneous diabetic NOD mouse*. J Biomed Mater Res, 1994. **28**(10):1201-7.

114. Wang, T., et al., *An encapsulation system for the immunoisolation of pancreatic islets*. Nat Biotech, 1997. **15**(4): p. 358-362.
115. Weber CJ, H.M., Chrysochoos JT, Kapp JA, Korbutt GS, Rajotte RV, Linsley PS., *CTLA4-Ig prolongs survival of microencapsulated neonatal porcine islet xenografts in diabetic NOD mice*. Cell Transplant., 1997. **6**(5):505-8.
116. Duvivier-Kali, V.F., et al., *Complete Protection of Islets Against Allorejection and Autoimmunity by a Simple Barium-Alginate Membrane*. Diabetes, 2001. **50**(8): p. 1698-1705.
117. Mørch, Y.A., I. Donati, and B.L. Strand, *Effect of Ca<sup>2+</sup>, Ba<sup>2+</sup>, and Sr<sup>2+</sup> on Alginate Microbeads*. Biomacromolecules, 2006. **7**(5): p. 1471-1480.
118. Tuch, B.E., et al., *Safety and viability of microencapsulated human islets transplanted into diabetic humans*. Diabetes Care, 2009. **32**(10): p. 1887-9.
119. Carlos, A.G., Y. Teramura, and H. Iwata, *Cryopreserved Agarose-Encapsulated Islets As Bioartificial Pancreas: A Feasibility Study*. Transplantation, 2009. **87**(1): p. 29-34 10.1097/TP.0b013e318191b24b.
120. Luan, N.M., Y. Teramura, and H. Iwata, *Immobilization of the soluble domain of human complement receptor 1 on agarose-encapsulated islets for the prevention of complement activation*. Biomaterials, 2010. **31**(34): p. 8847-8853.
121. Kobayashi, T., et al., *Indefinite islet protection from autoimmune destruction in nonobese diabetic mice by agarose microencapsulation without immunosuppression I*. Transplantation, 2003. **75**(5): p. 619-625.
122. Murad, K.L., et al., *Stealth Cells: Prevention of Major Histocompatibility Complex Class II-Mediated T-Cell Activation by Cell Surface Modification*. Blood, 1999. **94**(6): p. 2135-2141.
123. Hashemi-Najafabadi, S., et al., *A Method To Optimize PEG-Coating of Red Blood Cells*. Bioconjugate Chemistry, 2006. **17**(5): p. 1288-1293.
124. Nacharaju, P., et al., *Surface decoration of red blood cells with maleimidophenyl-polyethylene glycol facilitated by thiolation with iminothiolane: an approach to mask A, B, and D antigens to generate universal red blood cells*. Transfusion, 2005. **45**(3): p. 374-383.
125. Teramura, Y. and H. Iwata, *Bioartificial pancreas: Microencapsulation and conformal coating of islet of Langerhans*. Advanced Drug Delivery Reviews, 2010. **62**(7-8): p. 827-840.

126. Dong Yun Lee, S.J.P., Seulki Lee, Jong Hee Nam, and Youngro Byun, *Highly Poly(Ethylene) Glycolylated Islets Improve Long-Term Islet Allograft Survival without Immunosuppressive Medication* Tissue Engineering, 2007. **13**(8): p. 2133-41.
127. Teramura, Y., Y. Kaneda, and H. Iwata, *Islet-encapsulation in ultra-thin layer-by-layer membranes of poly(vinyl alcohol) anchored to poly(ethylene glycol)-lipids in the cell membrane.* Biomaterials, 2007. **28**(32): p. 4818-4825.
128. Teramura, Y., et al., *Behavior of synthetic polymers immobilized on a cell membrane.* Biomaterials, 2008. **29**(10): p. 1345-1355.
129. Totani, T., Y. Teramura, and H. Iwata, *Immobilization of urokinase on the islet surface by amphiphilic poly(vinyl alcohol) that carries alkyl side chains.* Biomaterials, 2008. **29**(19): p. 2878-2883.
130. Teramura, Y. and H. Iwata, *Improvement of Graft Survival by Surface Modification With Poly(ethylene glycol)-Lipid and Urokinase in Intraportal Islet Transplantation.* Transplantation, 2011. **91**(3): p. 271-278  
10.1097/TP.0b013e3182034fa4.
131. Wilson, J.T., et al., *Noncovalent Cell Surface Engineering with Cationic Graft Copolymers.* Journal of the American Chemical Society, 2009. **131**(51): p. 18228-18229.
132. Miura, S., Y. Teramura, and H. Iwata, *Encapsulation of islets with ultra-thin polyion complex membrane through poly(ethylene glycol)-phospholipids anchored to cell membrane.* Biomaterials, 2006. **27**(34): p. 5828-5835.
133. Contreras, J.L., et al., *A novel approach to xenotransplantation combining surface engineering and genetic modification of isolated adult porcine islets.* Surgery, 2004. **136**(3): p. 537-547.
134. Xie, D., et al., *Cytoprotection of PEG-modified adult porcine pancreatic islets for improved xenotransplantation.* Biomaterials, 2005. **26**(4): p. 403-412.
135. Lee, D.Y., et al., *Minimization of Immunosuppressive Therapy After Islet Transplantation: Combined Action of Heme Oxygenase-1 and PEGylation to Islet.* American Journal of Transplantation, 2006. **6**(8): p. 1820-1828.
136. Yun Lee, D., J. Hee Nam, and Y. Byun, *Functional and histological evaluation of transplanted pancreatic islets immunoprotected by PEGylation and cyclosporine for 1 year.* Biomaterials, 2007. **28**(11): p. 1957-1966.



137. Pollok, J.M., et al., *In vitro function of islets of Langerhans encapsulated with a membrane of porcine chondrocytes for immunoisolation*. *Dig Surg*, 2001. **18**(3): p. 204-10.
138. Kim, J.Y., et al., *Functional Evaluation of Chondrocyte Sheeting Immunodelusive Immunoisolated Bioartificial Pancreas*. *Transplantation Proceedings*, 2010. **42**(3): p. 903-906.
139. Teramura, Y. and H. Iwata, *Islet encapsulation with living cells for improvement of biocompatibility*. *Biomaterials*, 2009. **30**(12): p. 2270-2275.
140. Teramura, Y., et al., *Microencapsulation of Islets with Living Cells Using PolyDNA-PEG-Lipid Conjugate*. *Bioconjugate Chemistry*, 2010. **21**(4): p. 792-796.
141. Cabric, S., et al., *Anchoring of Vascular Endothelial Growth Factor to Surface-Immobilized Heparin on Pancreatic Islets: Implications for Stimulating Islet Angiogenesis*. *Tissue Engineering Part A*, 2009. **16**(3): p. 961-970.
142. Wu, H., et al., *RGD peptide-modified adenovirus expressing HGF and XIAP improves islet transplantation*. *The Journal of Gene Medicine*, 2011: p. n/a-n/a.
143. Park, K.H., et al., *Insulinoma cell line (MIN6) adhesion and spreading mediated by Arg-Gly-Asp (RGD) sequence conjugated in thermo-reversible gel*. *J Biosci Bioeng*, 2005. **99**(6): p. 598-602.
144. Monaco, A.P., et al., *Transplantation of islet allografts and xenografts in totally pancreatectomized diabetic dogs using the hybrid artificial pancreas*. *Ann Surg*, 1991. **214**(3): p. 339-60; discussion 361-2.
145. Ohgawara, H., et al., *Membrane Immunoisolation of a Diffusion Chamber for a Bioartificial Pancreas*. *Artificial Organs*, 1998. **22**(9): p. 788-794.
146. Edamura, K., et al., *Xenotransplantation of porcine pancreatic endocrine cells to total pancreatectomized dogs*. *J Vet Med Sci*, 2003. **65**(5): p. 549-56.
147. Hirotani, S., et al., *Bioartificial endocrine pancreas (Bio-AEP) for treatment of diabetes: effect of implantation of Bio-AEP on the pancreas*. *Cell Transplant*, 1999. **8**(4): p. 399-404.
148. Lee, S.H., et al., *Human beta-cell precursors mature into functional insulin-producing cells in an immunoisolation device: implications for diabetes cell therapies*. *Transplantation*, 2009. **87**(7): p. 983-91.

149. Hashimoto, H., et al., *Improvement of hyperglycemia and sexual dysfunction in diabetic female rats by an artificial endocrine pancreas developed from mouse beta cells*. *Exp Anim*, 2010. **59**(4): p. 515-9.
150. La Flamme, K.E., et al., *Biocompatibility of nanoporous alumina membranes for immunoisolation*. *Biomaterials*, 2007. **28**(16): p. 2638-45.
151. La Flamme, K.E., et al., *Nanoporous alumina capsules for cellular macroencapsulation: transport and biocompatibility*. *Diabetes Technol Ther*, 2005. **7**(5): p. 684-94.
152. Popat, K.C., et al., *Surface modification of nanoporous alumina surfaces with poly(ethylene glycol)*. *Langmuir*, 2004. **20**(19): p. 8035-41.
153. Wang, W., et al., *Subcutaneous transplantation of macroencapsulated porcine pancreatic endocrine cells normalizes hyperglycemia in diabetic mice*. *Transplantation*, 2003. **76**(2): p. 290-6.
154. Wang, W., et al., *Reversal of diabetes in mice by xenotransplantation of a bioartificial pancreas in a prevascularized subcutaneous site*. *Transplantation*, 2002. **73**(1): p. 122-9.
155. Lee, B.R., et al., *In situ formation and collagen-alginate composite encapsulation of pancreatic islet spheroids*. *Biomaterials*, 2012. **33**(3): p. 837-45.
156. Yang, K.-C., et al., *Chitosan/gelatin hydrogel as immunoisolative matrix for injectable bioartificial pancreas*. *Xenotransplantation*, 2008. **15**(6): p. 407-416.
157. Yang, K.C., et al., *Chitosan/Gelatin Hydrogel Prolonged the Function of Insulinoma/Agarose Microspheres In Vivo During Xenogenic Transplantation*. *Transplantation Proceedings*, 2008. **40**(10): p. 3623-3626.
158. Muthyala, S., et al., *The reversal of diabetes in rat model using mouse insulin producing cells – A combination approach of tissue engineering and macroencapsulation*. *Acta Biomaterialia*, 2011. **7**(5): p. 2153-2162.
159. Borg, D. and E. Bonifacio, *The Use of Biomaterials in Islet Transplantation*. *Current Diabetes Reports*, 2011. **11**(5): p. 434-444.
160. Lin, C.C. and K.S. Anseth, *PEG hydrogels for the controlled release of biomolecules in regenerative medicine*. *Pharm Res*, 2009. **26**(3): p. 631-43.
161. Tibbitt, M.W. and K.S. Anseth, *Hydrogels as extracellular matrix mimics for 3D cell culture*. *Biotechnology and Bioengineering*, 2009. **103**(4): p. 655-663.

162. Lin, C.-C., A. Raza, and H. Shih, *PEG hydrogels formed by thiol-ene photo-click chemistry and their effect on the formation and recovery of insulin-secreting cell spheroids*. *Biomaterials*, 2011. **32**(36): p. 9685-9695.
163. Weber, L.M., et al., *PEG-based hydrogels as an in vitro encapsulation platform for testing controlled  $\beta$ -cell microenvironments*. *Acta Biomaterialia*, 2006. **2**(1): p. 1-8.
164. Weber, L.M., K.N. Hayda, and K.S. Anseth, *Cell-matrix interactions improve beta-cell survival and insulin secretion in three-dimensional culture*. *Tissue Eng Part A*, 2008. **14**(12): p. 1959-68.
165. Kloxin, A.M., et al., *Mechanical Properties of Cellularly Responsive Hydrogels and Their Experimental Determination*. *Advanced Materials*, 2010. **22**(31): p. 3484-3494.
166. Weber, L.M., et al., *The effects of cell-matrix interactions on encapsulated  $\beta$ -cell function within hydrogels functionalized with matrix-derived adhesive peptides*. *Biomaterials*, 2007. **28**(19): p. 3004-3011.
167. Lin, C.C. and K.S. Anseth, *Cell-cell communication mimicry with poly(ethylene glycol) hydrogels for enhancing beta-cell function*. *Proc Natl Acad Sci U S A*, 2011. **108**(16): p. 6380-5.
168. Hume, P.S. and K.S. Anseth, *Inducing local T cell apoptosis with anti-Fas-functionalized polymeric coatings fabricated via surface-initiated photopolymerizations*. *Biomaterials*, 2010. **31**(12): p. 3166-3174.
169. Hume, P.S., C.N. Bowman, and K.S. Anseth, *Functionalized PEG hydrogels through reactive dip-coating for the formation of immunoactive barriers*. *Biomaterials*, 2011. **32**(26): p. 6204-6212.
170. Cheng, S.Y., J. Gross, and A. Sambanis, *Hybrid pancreatic tissue substitute consisting of recombinant insulin-secreting cells and glucose-responsive material*. *Biotechnology and Bioengineering*, 2004. **87**(7): p. 863-873.
171. Cheng, S.Y., I. Constantinidis, and A. Sambanis, *Use of glucose-responsive material to regulate insulin release from constitutively secreting cells*. *Biotechnology and Bioengineering*, 2006. **93**(6): p. 1079-1088.
172. Mukherjee, N., et al., *Effects of cryopreservation on cell viability and insulin secretion in a model tissue-engineered pancreatic substitute (TEPS)*. *Cell Transplant*, 2005. **14**(7): p. 449-56.

173. Kiessling, F.M., *Science to practice: are theranostic agents with encapsulated cells the key for diabetes therapy?* Radiology, 2011. **260**(3): p. 613-5.
174. Arifin, D.R., et al., *Trimodal gadolinium-gold microcapsules containing pancreatic islet cells restore normoglycemia in diabetic mice and can be tracked by using US, CT, and positive-contrast MR imaging.* Radiology, 2011. **260**(3): p. 790-8.
175. Park, S.J., et al., *Functional improvement of porcine neonatal pancreatic cell clusters via conformal encapsulation using an air-driven encapsulator.* Exp Mol Med, 2012. **44**(1): p. 20-5.
176. Zhi, Z.-l., et al., *Polysaccharide Multilayer Nanoencapsulation of Insulin-Producing  $\beta$ -Cells Grown as Pseudoislets for Potential Cellular Delivery of Insulin.* Biomacromolecules, 2010. **11**(3): p. 610-616.
177. Dang, T.T., et al., *Microfabrication of homogenous, asymmetric cell-laden hydrogel capsules.* Biomaterials, 2009. **30**(36): p. 6896-902.
178. Lu, H.F., et al., *Thermally induced gelable polymer networks for living cell encapsulation.* Biotechnol Bioeng, 2007. **96**(1): p. 146-55.
179. Silva, A.I. and M. Mateus, *Development of a polysulfone hollow fiber vascular bio-artificial pancreas device for in vitro studies.* J Biotechnol, 2009. **139**(3): p. 236-49.
180. Yang, K.-C., et al., *Calcium Phosphate Cement Chamber as an Immunoisolative Device for Bioartificial Pancreas: In Vitro and Preliminary In Vivo Study.* Pancreas, 2010. **39**(4): p. 444-451 10.1097/MPA.0b013e3181be2f95.
181. Yang, K.C., et al., *The in vivo performance of bioartificial pancreas in bone marrow cavity: a case report of a spontaneous diabetic feline.* Biochem Biophys Res Commun, 2010. **393**(3): p. 362-4.
182. Yang, K.C., et al., *Comparison of bioartificial pancreas performance in the bone marrow cavity and intramuscular space.* Arch Med Res, 2010. **41**(3): p. 151-3.
183. Sacco, W.P., et al., *Educational attainment moderates the effect of a brief diabetes self-care intervention.* Diabetes Res Clin Pract, 2012. **95**(1): p. 62-7.
184. Juhl, K., S. Bonner-Weir, and A. Sharma, *Regenerating pancreatic beta-cells: plasticity of adult pancreatic cells and the feasibility of in-vivo neogenesis.* Current opinion in organ transplantation, 2010. **15**(1): p. 79-85.

185. Gonez, L.J. and K.R. Knight, *Cell therapy for diabetes: stem cells, progenitors or beta-cell replication?* *Molecular and cellular endocrinology*, 2010. **323**(1): p. 55-61.
186. Dawson, E., et al., *Biomaterials for stem cell differentiation*. *Adv Drug Deliv Rev*, 2008. **60**(2): p. 215-28.
187. Elisseeff, J., et al., *The role of biomaterials in stem cell differentiation: applications in the musculoskeletal system*. *Stem Cells Dev*, 2006. **15**(3): p. 295-303.
188. GAO Feng, W.D.-q., HU Yan-hua, JIN Guang-xin, *Extracellular matrix gel is necessary for in vitro cultivation of insulin producing cells from human umbilical cord blood derived mesenchymal stem cells*. *Chinese Medical Journal*, 2010. **121**(No.9): p. 811-818.
189. Lumelsky, N., et al., *Differentiation of embryonic stem cells to insulin-secreting structures similar to pancreatic islets*. *Science*, 2001. **292**(5520): p. 1389-94.
190. Chayosumrit, M., B. Tuch, and K. Sidhu, *Alginate microcapsule for propagation and directed differentiation of hESCs to definitive endoderm*. *Biomaterials*, 2010. **31**(3): p. 505-14.
191. Van Hoof, D., et al., *Differentiation of human embryonic stem cells into pancreatic endoderm in patterned size-controlled clusters*. *Stem Cell Research*, 2011. **6**(3): p. 276-285.
192. Bouwens, L., *Beta cell regeneration*. *Curr Diabetes Rev*, 2006. **2**(1): p. 3-9.
193. Mason, M.N. and M.J. Mahoney, *Selective beta-cell differentiation of dissociated embryonic pancreatic precursor cells cultured in synthetic polyethylene glycol hydrogels*. *Tissue Eng Part A*, 2009. **15**(6): p. 1343-52.
194. Mason, M.N., C.A. Arnold, and M.J. Mahoney, *Entrapped collagen type 1 promotes differentiation of embryonic pancreatic precursor cells into glucose-responsive beta-cells when cultured in three-dimensional PEG hydrogels*. *Tissue Eng Part A*, 2009. **15**(12): p. 3799-808.
195. Mason, M.N. and M.J. Mahoney, *Inhibition of gamma-secretase activity promotes differentiation of embryonic pancreatic precursor cells into functional islet-like clusters in poly(ethylene glycol) hydrogel culture*. *Tissue Eng Part A*, 2010. **16**(8): p. 2593-603.

196. Omer, A., et al., *Survival and maturation of microencapsulated porcine neonatal pancreatic cell clusters transplanted into immunocompetent diabetic mice*. Diabetes, 2003. **52**(1): p. 69-75.
197. Foster, J.L., et al., *Differentiation of transplanted microencapsulated fetal pancreatic cells*. Transplantation, 2007. **83**(11): p. 1440-8.
198. Montanucci, P., et al., *The functional performance of microencapsulated human pancreatic islet-derived precursor cells*. Biomaterials, 2011. **32**(35): p. 9254-62.
199. Xu, X., et al., *Beta cells can be generated from endogenous progenitors in injured adult mouse pancreas*. Cell, 2008. **132**(2): p. 197-207.
200. Yadav N, M.G., Harding SE, Ang S, Adams GG, *Various non-injectable delivery systems for the treatment of diabetes mellitus*. Endocr Metab Immune Disord Drug Targets, 2009. **Mar;9**(1): p. 1-13.
201. Hogan, P., T. Dall, and P. Nikolov, *Economic costs of diabetes in the US in 2002*. Diabetes Care, 2003. **26**(3): p. 917-32.

## CHAPTER THREE

### 3. DEVELOPING HYDROGELS SYSTEMS FOR THE FORMATION OF

#### ISLETS OF LANGERHAM FROM SINGLE BETA-CELLS

##### 3.1 Introduction

The applications of cell and tissue replacement therapies are usually limited by the lack of appropriate delivery platform for cells and engineered tissues. Successfully designed biomaterials systems for cell replacement therapies often intergrate multiple factors, such as cell-extracellular matrix (ECM) interactions, biomolecules (growth factors, peptides, cytokines, etc.), and cell-cell interactions [1, 2]. A successful design will further improve the spatial and temporal presentation of these factors to the encapsulated cells [3]. Hydrogels are important biomaterials for cell encapsulation and delivery, which can offer a physical barrier or “immuno-isolation” between the host tissue and encapsulated cells. Poly (ethylene glycol) (PEG) hydrogels are often considered advantageous for engineering such synthetic microenvironments used for cell delivery. PEG hydrogels present unique advantages for cell delivery because of their high water content and quick diffusion characteristics. Further, the nonfouling properties of PEG hydrogels provide a “blank slate” on which defined bioactive/functional motifs, such as peptides and proteins, can be easily incorporated without significantly affecting the bulk material properties [4, 5].

The peptide-functionalized PEG hydrogels mimic aspects of the ECM to support the survival and function of encapsulated cells. The specific amino acid sequences present at the binding sites, which include RGD (Arg-Gly-Asp), IKVAV (Ile-Lys-Val-

Ala-Val), YIGSR (Tyr-Ile-Gly-Ser-Arg), RYVVLPR (Arg-Tyr-Val-Val-Leu-Pro-Arg), and RNIAEIIKDI (Arg-Asn-Ile-Ala-Glu-Ile-Ile-Lys-Asp-Ile), have been identified as being involved in cell-receptor interactions. RGD and IKVAV are present on  $\alpha$  laminin chain, whereas YIGSR is found on the  $\beta$  laminin chain [6-8]. Peptides, when compared to whole proteins, are more stable, easily synthesized, and are less likely to exhibit steric hindrance after biomaterial modification.

Many studies have been reported to encapsulate islets or insulin-producing  $\beta$ -cells in PEG hydrogels for cell transplantation. To date, the design of an islets or insulin-producing  $\beta$ -cells delivery barrier has been largely focused on optimizing material biocompatibility and tailoring material properties for cell encapsulation. Few strategies use material functionalities to mimic or promote cell-cell interactions in a three-dimensional (3D) microenvironment [9]. Cell-cell interactions are important for maintaining  $\beta$ -cells survival and functionality [10]. In this study, we have developed a series of functionalized hydrogels based on *in situ* gelable, non-immunogenic material, including multi-arm (4-arm) thiolated PEG and poly (ethylene glycol) tetra-acrylate (PEGTA), focused on promoting the survival and functionality of encapsulated pancreatic  $\beta$ -cells (MIN6) in 3D. PEG hydrogels were designed to encapsulate  $\beta$ -cells for forming clusters from single cells as islets, which will improve the cell-cell interactions. Using the peptide incorporation technique, PEG hydrogels were synthesized containing peptide tethers of IKVAV, YIGSR, RGD. Individual MIN6  $\beta$ -cells were encapsulated in peptide-containing hydrogels, and cell survival and glucose-stimulated insulin secretion were observed with culture time.



The central hypothesis for this study is that PEG hydrogels can be designed for the formation of artificial islets to maintain  $\beta$ -cells survival and functionality as a biomimetic cell delivery platform. Engineering PEG hydrogels with different peptides in 3D culture systems can improve the viability and functionality of  $\beta$ -cells and promote cell-cell interactions.

## 3.2 Materials and methods

### 3.2.1 Materials

4-arm poly (ethylene glycol) (MW, 10kDa) and poly (ethylene glycol) tetraacrylate (MW, 10kDa, PEGTA) was obtained from Creative PEGWorks (Winston Salem, NC). Three types of adhesive peptides, CSRARKQAASIKVAVSADR (Cys-Ser-Arg-Ala-Arg-Lys-Gln-Ala-Ala-Ser-Ile-Lys-Val-Ala-Val-Ser-Ala-Asp-Arg), GRGDSPC (Gly-Arg-Gly-Asp-Ser-Pro-Cys), and CDPGYIGSR (Cys-Asp-Pro-Gly-Tyr-Ile-Gly-Ser-Arg), were purchased from American Peptide Company (Sunnyvale, CA). Cell culture reagents and supplements were obtained from Invitrogen (Carlsbad, CA). LIVE/DEAD viability kit was obtained from Molecular Probes (Eugene, OR). Insulin enzyme linked immunosorbent assay (ELISA) kit was obtained from Millipore (Billerica, MA). All other reagents were purchased from Sigma Aldrich (St. Louis, MO).

### 3.2.2 Synthesis of thiolated multi-arm PEG

Multi-arm PEG was chain-end thiolated by esterification reaction with thioglycolic acid (TGA) using p-toluenesulfonic acid as a catalyzer [11]. Briefly, 5 g of

multiarm PEG (4-arm PEG), 0.4 g TGA, and 5 mg p-toluenesulfonic acid, were added to 100 mL of toluene preheated to 120 °C. The reaction proceeded for 24 hrs under nitrogen atmosphere. The thiolated prepolymer was purified by precipitation into anhydrous ether (200 mL) at 4 °C. This sequence was repeated three times using dichloromethane as a solvent. The product was then dried under vacuum at room temperature for 3 days.

### 3.2.3 Preparation of hydrogels

PEGTA and 4-arm thiolated PEG stock solutions (10%, w/v) were prepared by dissolving powders in phosphate buffered saline (PBS), respectively. To elucidate the influence of polymer concentration on hydrogel properties, PEGTA solutions of different concentrations (1.5%, 2%, 2.5%, 5%, 7.5%, and 10%) were mixed with 4-arm thiolated PEG of different concentrations (1.5%, 2%, 2.5%, 5%, 7.5%, and 10%) in a ratio of 1:1, respectively. Moreover, a 5% PEGTA solution mixed with a 5% 4-arm thiolated PEG aqueous solution in specific volume ratios (2:10, 3:9, 4:8, 6:6, 8:4, 9:3, and 10:2), and another 2.5% PEGTA solution mixed with a 2.5% 4-arm thiolated PEG aqueous solution in specific volume ratios (3:9, 6:6, and 9:3), were also used to determine the effect of feed ratio on the properties of hydrogels formed.

### 3.2.4 Rheological characterization of hydrogels

For rheological study, hydrogel solutions of PEGTA and 4-arm thiolated PEG were mixed on the steel plate geometry and inspected by oscillatory shear rheometry immediately [12, 13]. An AR1000 rheometer (TA Instruments Inc.) with standard

geometry of 40 mm diameter was used for the rheological characterization of all hydrogels samples. The test methods employed were oscillatory time sweep, frequency sweep and stress sweep. The time sweep was performed to monitor the *in situ* gelation of the hydrogel solutions at 37 °C. The test, which was operated at constant frequency (1 Hz) and strain (5%) and terminated after 60 minutes, recorded the temporal evolution of shear storage modulus ( $G'$ ) and the shear loss modulus ( $G''$ ). The stress sweep was set up by holding the temperature 37 °C and constant frequency (1 Hz) while increasing the stress level from 1 to 10 Pa. The applied range of 1-10 Pa was found to be safe-for-use from a prior experiment where we determined the linear viscoelastic region (LVR) profiles of the hydrogels by shearing them until structure breakdown. We also subjected hydrogels to a frequency sweep at 50% of their respective ultimate stress levels. At this fixed shear stress and temperature (37 °C), the oscillatory frequency was increased from 0.1 to 100 Hz and the  $G'$  was recorded.

Young's modulus,  $E$ , can be evaluated by  $E = 2G(1+\gamma)$ . When a material can be assumed to be incompressible, its Poisson's ratio,  $\gamma$ , approaches 0.5 and this relationship approaches  $E = 3G$ . This assumption for hydrogels is supported by a research showing that  $\nu$  for polyacrylamide hydrogels is nearly 0.5, and these hydrogels typically used under very low strain. This relationship between  $E$  and  $G$  then provides a useful tool for comparing mechanical properties of substrates and tissues that have been determined using other methods of measurement.

### 3.2.5 Swelling of hydrogels

Hydrogels of different concentrations (1.5%, 2%, 2.5%, 5%, 7.5%, and 10%), 5% hydrogels with different ratios (2:10, 3:9, 4:8, 6:6, 8:4, 9:3, and 10:2), and 2.5% hydrogels in specific volume ratios (3:9, 6:6, and 9:3), were used to determine the effects of concentrations and feed ratios on the swelling properties of hydrogels. To characterize the swelling behavior of the hydrogels, they were weighed immediately after preparation. Hydrogels were placed in 5 mL of PBS solution at 37 °C and allowed to swell. Weights were taken every 24 hours for the next 30 days. Fresh PBS, previously equilibrated at 37 °C, was replaced every 24 hours at the time of measurement. The swelling ratio was calculated by dividing the weight of the hydrogels at equilibrium swelling by their weight after gelation.

### 3.2.6 Peptide conjugated to hydrogels

Different peptides, such as IKVAV, YIGSR, and RGD of different concentrations (1 and 0.2 mM) were conjugated to PEG hydrogels through addition reaction of peptide cys thiols onto the ends of a PEGTA crosslinker as described before. Briefly, peptides containing stock solutions (3 mM) were prepared in the PEGTA stock solution (5% w/w) and stirring for 2 hrs at room temperature. Additional PEGTA solutions with lower peptide concentrations (0.6mM) were prepared by diluting the stock solution with peptide-free PEGDA solution (peptide: PEGTA=1:5). Then PEGTA solution containing different concentrations of peptides was added to 4-arm thiolated PEG (5% w/w) solutions at the ratio of 1:2 and mixed thoroughly to form hydrogels.

### 3.2.7 Cell culture and encapsulation

Murine pancreatic  $\beta$ -cells of the MIN6 cell line were a kind gift from Dr. Bryan Wolf at Children's Hospital of Philadelphia. MIN6 cells were cultured in Dulbecco's Modified Eagle Medium (DMEM, 25 mM glucose) supplemented with 1% antibiotic and antimycotic solution, 10% fetal bovine serum, and 80  $\mu$ M of 2-mercaptoethanol at 37 °C in humid conditions with 5% CO<sub>2</sub>. The culture medium was exchanged every 2 days.

For encapsulation, MIN6 cells were mixed with PEG hydrogels or peptides conjugated PEG hydrogels of different ratios before gel formation. To avoid cells precipitating onto the surface of plate during the hydrogel formation, we coated the plate with hydrogels overnight, then mixed MIN6 cells with hydrogel precursor solutions ( $1 \times 10^4$  cells/well) and seeded on the top of pre-formed hydrogels. The culture medium was changed every 2 days.

### 3.2.8 Cell viability

Viability of cells was examined using LIVE/DEAD viability kit, which is a two color fluorescent assay based on differential permeability of live and dead cells and allows preservation of the distinctive staining pattern for a couple of hours after postfixation with 4% glutaraldehyde. Live cells were stained with green fluorescent SYTO 10; and dead cells with compromised cell membranes were stained with red fluorescent ethidium homodimer-2. The Leica TCS SP5 laser scanning confocal microscope was used to capture the images of the LIVE/DEAD cell staining patterns.

### 3.2.9 Glucose-stimulated insulin secretion

At designed time points, cultures were removed from encapsulation samples for glucose-stimulated insulin secretion. Samples were first placed in a low glucose concentration (1.1 mM) for 45 min, followed by incubation in a high glucose concentration solution (16.7 mM) for 1 hr. The high glucose solutions were collected for insulin measurement by ELISA insulin kit.

### 3.2.10 Statistical analysis

Data are shown as mean  $\pm$  S.D. Statistical analyses were performed using one-way ANOVA (analysis of variance) followed by Tukey's post tests and the paired t-test where appropriate. A probability ( $p$ ) value of  $<0.05$  was considered statistically significant.

## 3.3 Results

### 3.3.1 Hydrogel characterization

#### 3.3.1.1 Mechanical properties of hydrogels

In this study, we have developed an *in situ* cross-linkable hydrogel based on 4-arm thiolated PEG and PEGTA. Hydrogels formed at physiological conditions due to conjugate addition reactions between thiols and acrylates. We achieved hydrogels with different mechanical properties by adjusting PEG concentrations or the ratios of thiolated PEG to PEGTA. Figure 3.1 shows the time sweep profiles of storage modulus ( $G'$ ) for the 10%, 7.5%, 5%, 2.5%, 2%, 1.5%, and 1% hydrogel networks within the small time

frame (60 minutes). With increase of PEG concentrations  $G'$  was increased accordingly (Figure 3.1, inserted 1). 1% PEG solution could not form hydrogel at physiological conditions. Higher PEG concentrations resulted in faster gelation (Figure 3.1, inserted 2). The frequency and stress sweeps of hydrogels of various PEG concentrations were shown in Figure 3.2 A and B, respectively.

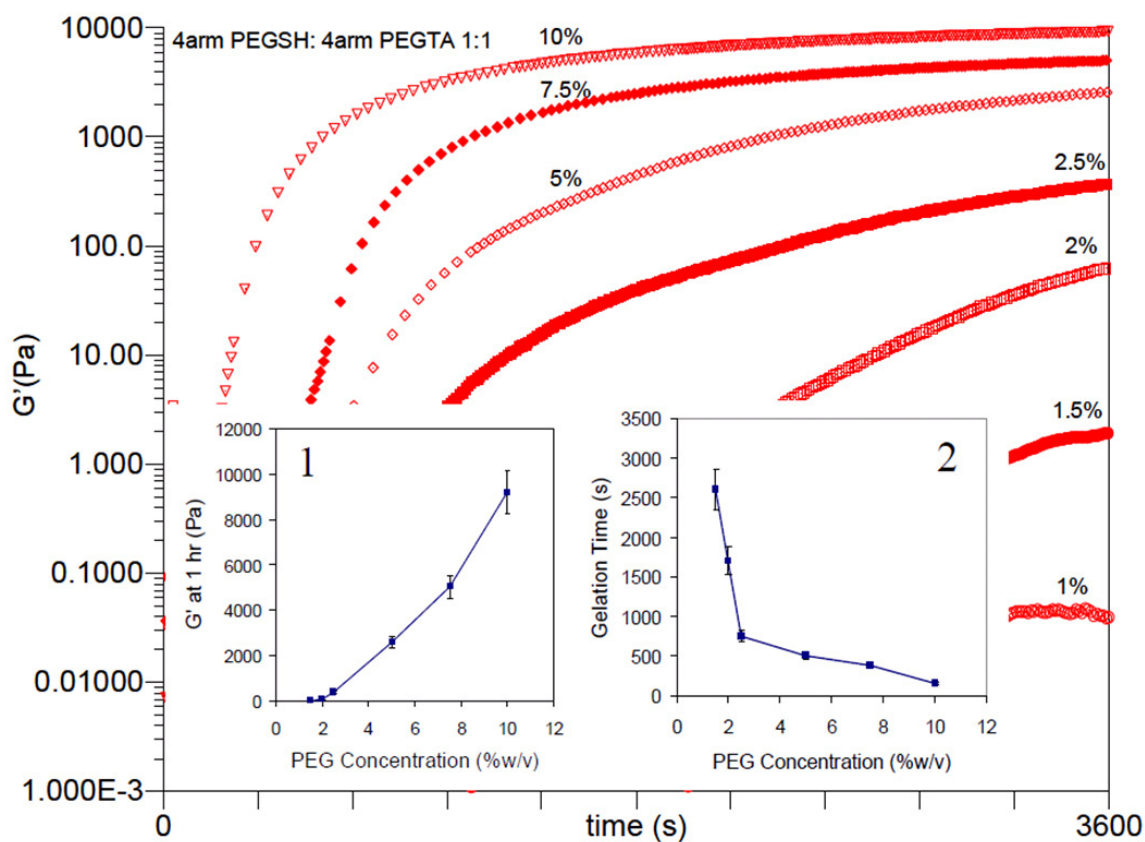


**Figure 3. 1** Evolution of shear storage moduli, ( $G'$ ) of hydrogels as a function of time. Inserted pictures: (1)  $G'$  at 1 hr and (2) gelation time as a function of PEG concentrations.

Another way to obtain hydrogels of different stiffness is to change the ratios of thiols to acrylates with the same PEG concentration. In 5% PEG solutions, the ratios of

PEGTA to 4-arm thiolated PEG were adjusted as follows: 2:10, 3:9, 4:8, 6:6, 8:4, 9:3, and 10:2. When the ratio of acrylates to thiols was kept at the stoichiometric balanced 1:1 (6:6), hydrogels formed with the largest  $G'$  (4,000 Pa, **Figure 3.3 A**). In contrast, as to ratios of 2:10 or 10:2, the biggest deviation to stoichiometric balance, PEG solutions could not form hydrogels. The gelation of hydrogels with ratios (3:9, 4:8, 6:6, 8:4, and 9:3) occurred at about 10 minutes and the ratios showed no effects on gelation time. As for 2.5% PEG solutions, hydrogels with acrylates to thiols 2:4, 3:3, and 4:2 formed within 30 minutes with  $G'$  75, 300, and 25 Pa, respectively (**Figure 3.3B**). 2.5% PEG solutions with higher deviation to stoichiometric balance (1:3 and 3:1) could not form hydrogels, either.

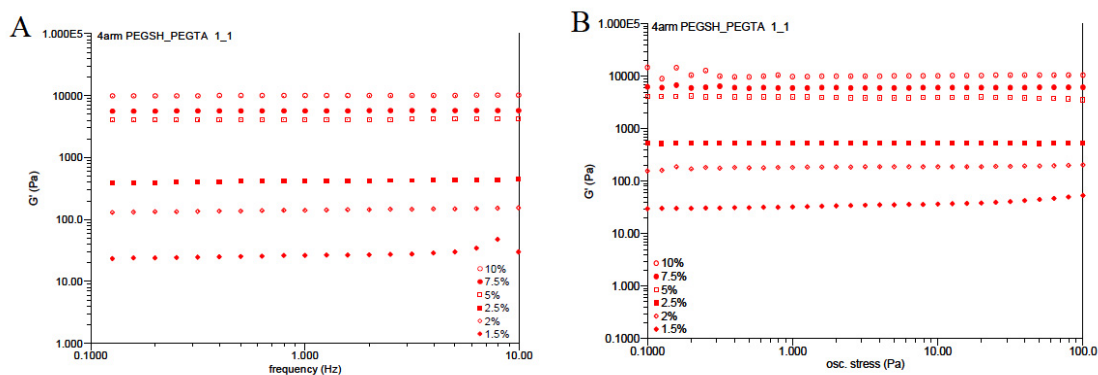


**Figure 3. 2** (A) Frequency sweep of hydrogels of various PEG concentrations. (B) Oscillatory stress sweep of hydrogels of various PEG concentrations.



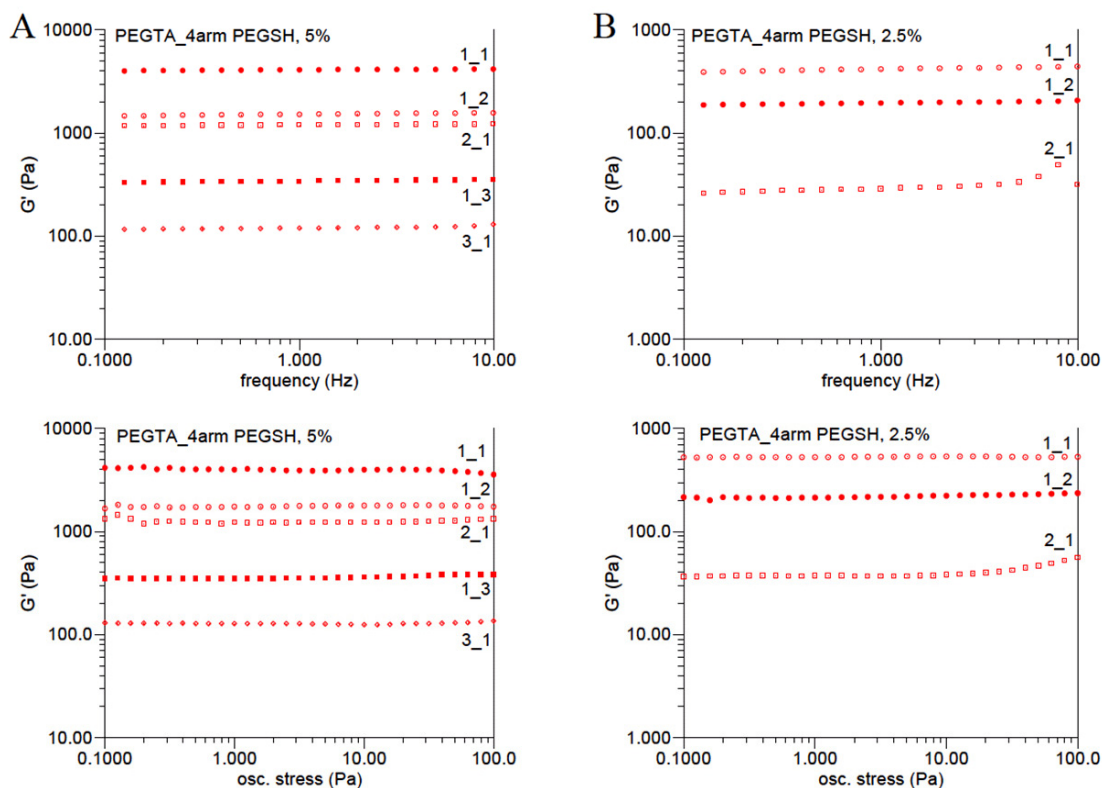
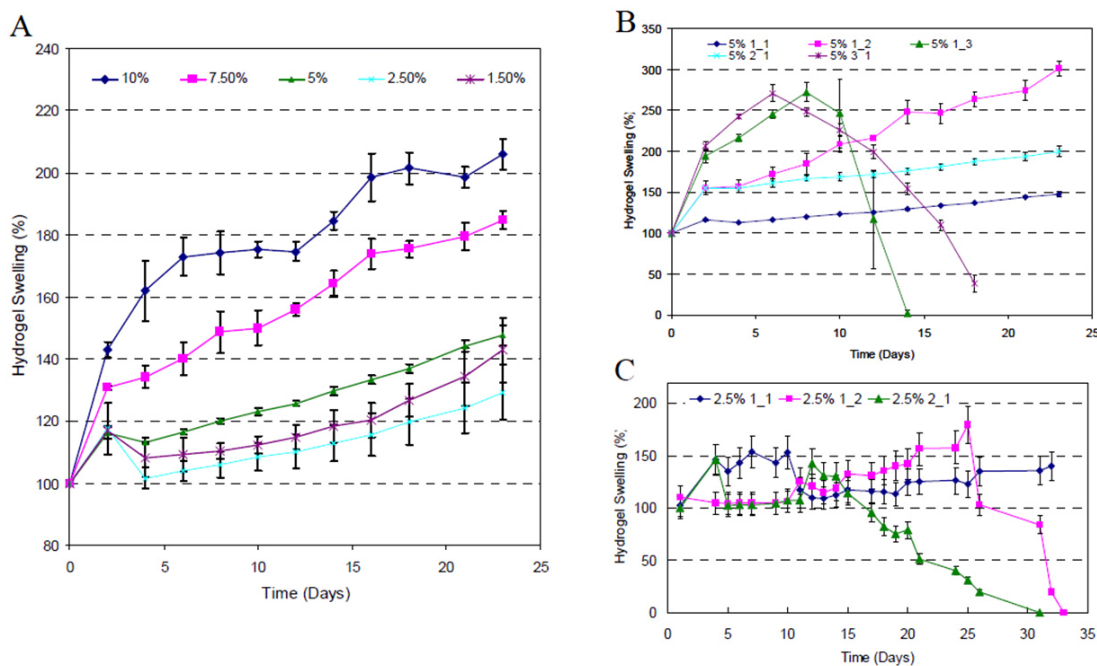


**Figure 3.3** Frequency sweep and oscillatory stress sweep of hydrogels of various ratios of different concentrations of (A) 5% and (B) 2.5%.

### 3.3.1.2 Hydrogel swelling and degradation

The swelling of hydrogels was studied by incubating them at pH 7.4 and 37 °C. Figure 3.4 A presents the dynamic swelling of the hydrogels as the function of concentration (10%, 7.5%, 5%, 2.5%, 2%, and 1.5%). Hydrogels with increasing concentrations (2.5%, 5%, 7.5%, and 10%) exhibited larger swell ratios, even though 2.5% and 1.5% showed no significant difference about their swelling ratios. All these hydrogels with stoichiometric balanced ratios were stable with steadily increased weight over the course of the study (3 weeks).

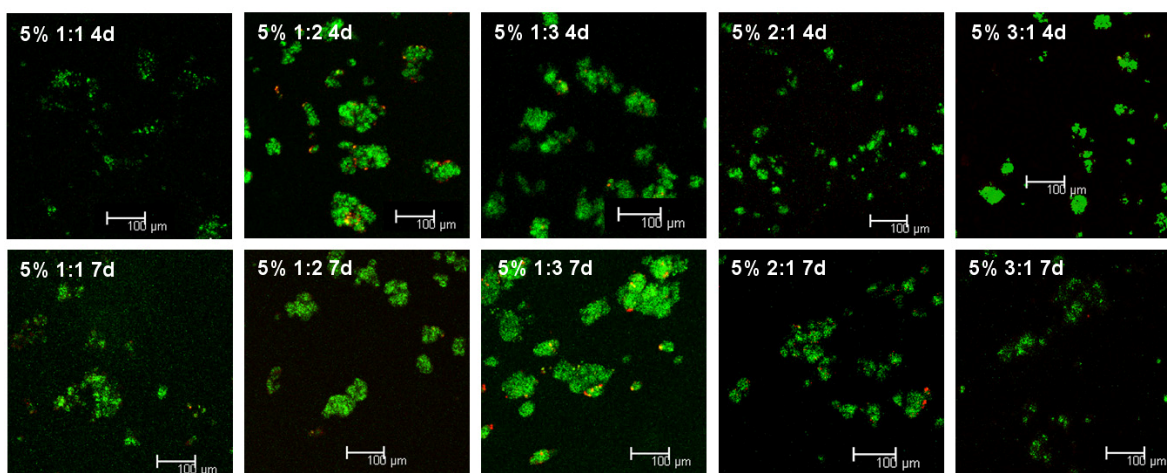
Figure 3.4 B and C shows the hydrogel swelling as the function of ratios of PEGTA to 4-arm thiolated PEG at the concentration of 5% and 2.5%, respectively. With the increase of deviation to stoichiometric balance from 6:6, 8:4 (4:8), to 9:3(3:9), hydrogels with concentration of 5% exhibited larger swell ratios. Although hydrogels with ratios of 4:8 exhibited larger swelling ratio than hydrogel of 8:4, both of them were stable over 3 weeks. In contrast, hydrogels with the ratios of 3:9 and 9:3 degraded at 14 days and 20 days, respectively. When considering 2.5% PEG hydrogels, although both of the hydrogels with ratios of 1:2 and 2:1 totally degraded at about 30 days, hydrogels with ratio of PEGTA to 4-arm thiolated PEG 2:1 began to degrade earlier than hydrogels with 1:2 ratios (16 days as opposed to 26 days).



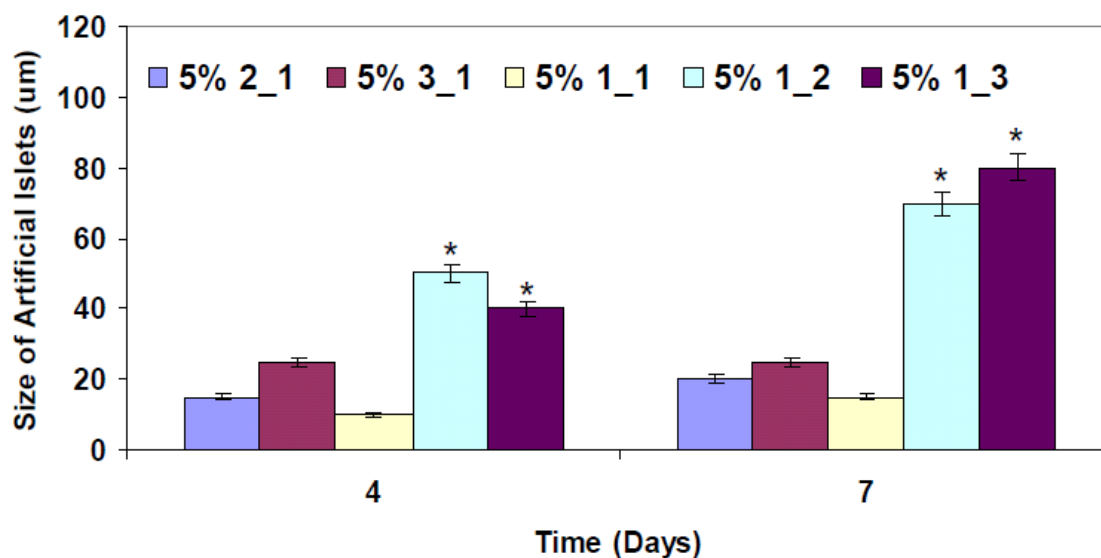
**Figure 3. 4** Dynamic swelling of the hydrogels in PBS. (A) Degree swelling of hydrogels as the function of concentration. (B and C) Degree swelling of hydrogels as the function of ratios of PEGTA to 4arm PEGSH at the concentration of (B) 5% and (C) 2.5%.

### 3.3.2 Effects of PEG hydrogels with different ratios on $\beta$ -cell clusters formation

MIN6 cells were cultured in 5% PEG hydrogels with different ratios of 4-arm thiolated PEG to PEGTA. The survival of encapsulated  $\beta$ -cells was determined by LIVE/DEAD staining. In Figure 3.5, more than 90% of cells survived in all samples up to 7 days and there was no significant difference among all samples. MIN6 cells were encapsulated as single cells, as Figure 3.5 shows, they can proliferate to form cell clusters like artificial islets, especially in the specific samples of 1:2 and 1:3. Figure 3.6 illustrates the quantity analysis of the size of cell clusters in PEG hydrogel with different ratios. Larger sizes of cell clusters especially appeared in hydrogels of 1:2 and 1:3 at both the day 4 and 7 (\*  $P < 0.05$ ).



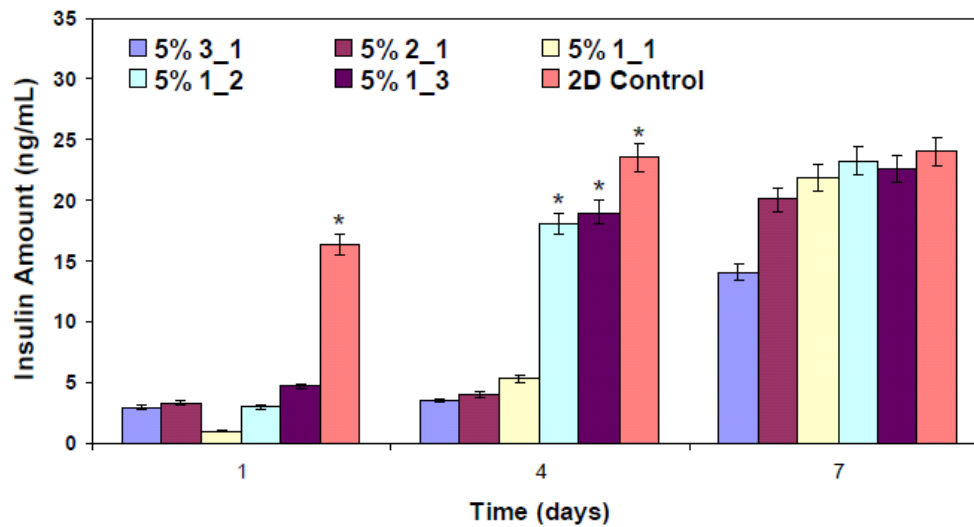
**Figure 3. 5** LIVE/DEAD (Green/Red) staining of MIN6 cells 3D cultured in 5% PEG hydrogels of different ratios of 4-arm thiolated PEG to PEGTA.



**Figure 3. 6** The size of artificial islets of MIN6 cells in 5% PEG hydrogels of different ratios of 4-arm thiolated PEG to PEGTA (\*  $P < 0.05$ ).

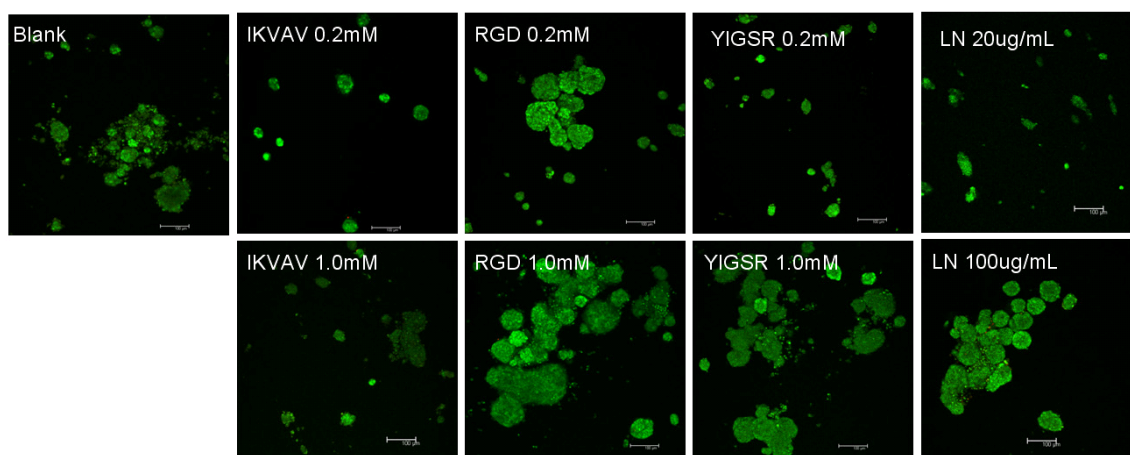
### 3.3.3 Effects of PEG hydrogels with different ratios on glucose-stimulated insulin secretion

Figure 3.7 reports insulin secretion from MIN6 cells encapsulated in PEG hydrogels with different ratios of thiolated PEG to PEGTA. On the first day, compared to MIN6 cells cultured on the plate, MIN6 cells inside hydrogels appeared to have no response to glucose stimulus. At the day 4, the cells encapsulated in the hydrogels of 1:2 and 1:3 secreted significantly higher amounts of insulin relative to those inside other hydrogel samples (\*  $P < 0.05$ ), and the amount of secreted insulin almost caught 2D control group based on glucose stimulation. At the day 7, besides the cells inside the specific hydrogel of 3:1, all the cells secreted similar amounts of insulin based on glucose stimulus when compared to 2D culture.



**Figure 3. 7** Insulin release response to glucose from MIN6 cells cultured in 5% PEG hydrogels of different ratios of 4-arm thiolated PEG to PEGTA at the day 1, 4 and 7 (\*  $P < 0.05$ ).

### 3.3.4 Effects of peptides on $\beta$ -cell survival and clusters formation



**Figure 3. 8** LIVE/DEAD (Green/Red) staining of MIN6 cells cultured in 5% PEG hydrogels of 4-arm thiolated PEG to PEGTA at the ratio of 1:2 conjugated with different peptides: IKVAV, RGD, and YIGSR at the day 4.

MIN6 cells were cultured inside 5% PEG hydrogels with the ratio of thiolated PEG to PEGTA at 1:2 conjugated with different concentrations of IKVAV, RGD and YIGSR, respectively. As Figure 3.8 shown, more than 95% of cells survived in all samples up to 7 days and there was no significant difference between all samples. As described above, the cells in the hydrogels proliferated in the format of aggregates. Peptides conjugated to hydrogels benefited aggregate formation. Higher concentrations of peptide resulted in larger sizes of cell clusters, especially in the hydrogels conjugated with RGD and YIGSR (Figure 3.9, \*  $P < 0.05$ ).

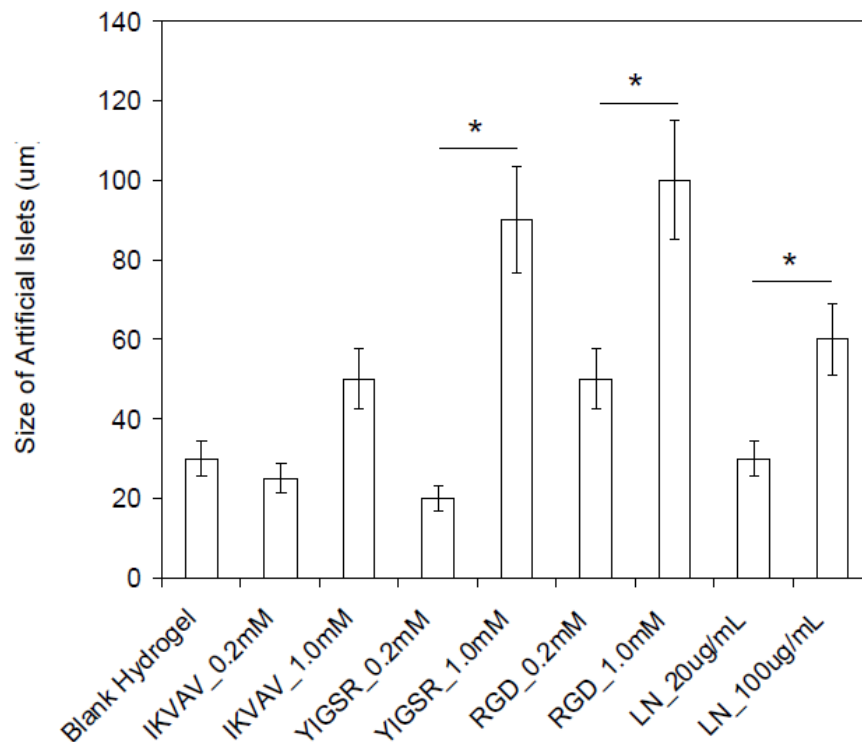


**Figure 3. 9** The size of artificial islets of MIN6 cells cultured in 5% PEG hydrogels of 4-arm thiolated PEG to PEGTA at the ratio of 1:2 conjugated with different peptides: IKVAV, RGD, and YIGSR at the day 4 (\*  $P < 0.05$ ).

### 3.3.5 Effects of peptides on $\beta$ -cell based on glucose-stimulated insulin secretion

Figure 3.10 shows insulin secretion from MIN6 cells encapsulated in PEG hydrogels conjugated with different peptides. At day 4, using YIGSR and IKVAV, higher amounts of peptides (1mM) conjugated to hydrogels resulted in larger amount of insulin secretion from cells encapsulated in the gels (\*  $P<0.05$ ). These two peptides at 1 mM benefited insulin secretion when compared to blank hydrogels. As to RGD, cells in the hydrogels with RGD at 0.2 mM have secreted the similar amount of insulin compared to those on 2D culture. Larger amount of RGD conjugation did not increase the insulin secretion further.

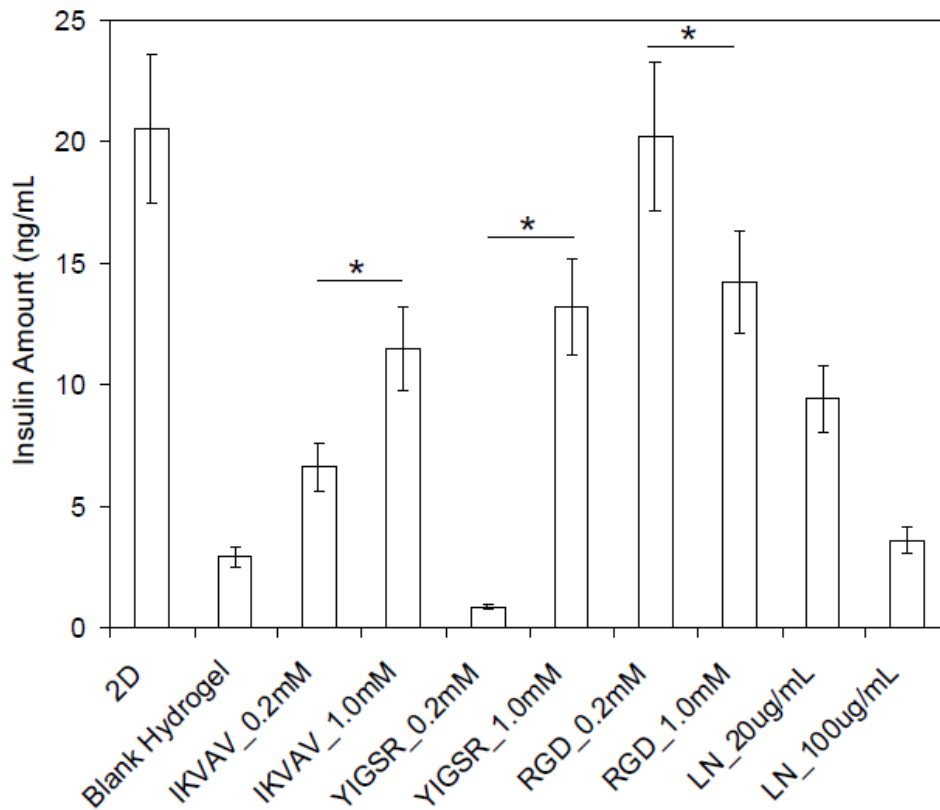


**Figure 3. 10** Insulin release response to glucose from MIN6 cells cultured in 5% PEG hydrogels of different peptides at the day 4 (\*  $P<0.05$ ).

### 3.4 Discussion

Developing bioactive hydrogels for 3D cell culture is an archetypal engineering problem. The hydrogel concentration, mechanical property, adhesive ligand and growth factor presentation, transport and degradation kinetics must be tuned to the given culture's needs a priori in a cytocompatible, reliable, and cost effective fashion. In this chapter, through adjusting the concentrations of PEG and the ratios of 4-arm thiolated PEG to PEGTA, we can achieve hydrogels with controllable mechanical properties ranging from 1 to 10,000 Pa and adjustable degradation time from 2 weeks to several months. MIN6 cells have been cultured inside hydrogels with different PEG concentrations and the ratios of thiolated 4-arm PEG to PEGTA. MIN6 cells expressed very high viability in all **the** hydrogel samples. Another study has reported that MIN6 cells encapsulated in hydrogels formed from three PEGDM macromers of varying molecular weights ( $M_n=4,000, 8,000, 10,000\text{g/mol}$ ), showed similar viability [14]. The optimal condition for the cells to form artificial islets *in vitro* is having the concentration of PEG at 5% and the ratios of 4-arm thiolated PEG to PEGTA at 1:2 (or 1:3).

The cells inside the optimal hydrogels exhibited similar insulin secretion to cells on 2D culture. Since the diffusion coefficient of agents, such as insulin, is determined by the pore size of the hydrogel matrix, the average pore size of hydrogel network is estimated based on rubber-elasticity theory according to equation 3.1 [Assuming that all chains contribute to the retraction force after deformation in a similar way (affine deformation), neglecting end effects of single chains (all chains have fixed ends towards an elastic background)] [15].



$$\xi = \left( \frac{G' N_A}{RT} \right)^{-1/3}$$

**Equation 3.1** Equation used to evaluate the mesh size of the gels [15].

**Table 3. 1** Mesh size of hydrogels with various concentrations of PEG and different ratios of 4 arm thiolated PEG to PEGTA.

PEG Concentration (% w/w)	Ratio of Thiolated 4-arm PEG to PEGTA	G' (Pa)	Mesh Size (nm)
10	1_1	9028	7.7
7.5	1_1	5026	9.5
5	1_1	2594	11.8
5	1_2	952.5	16.5
5	2_1	1248	15.1
5	1_3	112.6	33.6
5	3_1	258.5	25.5
2.5	1_1	372	22.6
2.5	1_2	25.04	55.5
2.5	2_1	75.35	38.4
1.5	1_1	21	59.2

The mesh size of hydrogels calculated from their storage modulus is shown in Table 3.1. The mesh sizes of hydrogels less than 5% are all over 10 nm. Since the size of insulin is about 10 nm, the diffusion of insulin in the hydrogels is not inhibited when the concentrations of hydrogels are less than 5%. There are different insulin secretions from cells in different hydrogels due to the cells which have been affected by the hydrogels but not to physical inhibition of hydrogels themselves.

To further optimize our hydrogel, different peptides, such as RGD, IKVAV, YIGSR, have been conjugated to hydrogel matrix through the Michael reaction. These specific amino acid sequences rather than whole proteins, are better suited for biomaterials modification. As described before, they are more stable, easily synthesized, and are less likely to exhibit steric hindrance after biomaterial modification [16]. Moreover, these ECM proteins are difficult to produce, have high batch-to-batch variability, and may cause immune response if used in clinical applications. We have found all of the peptides have benefited insulin secretion when compared to blank hydrogels. Especially, RGD at 0.2 mM can significantly promote the insulin secretion, similar to the 2D control group at the day 4.

Other investigators have reported similar results. In the absence of cell-cell and cell-matrix contacts, encapsulated MIN6  $\beta$ -cell survival diminished within one week; however, in PEG hydrogel derivatives including the laminin sequences IKLLI and IKVAV, encapsulated  $\beta$ -cells exhibited preserved viability, reduced apoptosis, and increased insulin secretion. Interactions with the laminin sequences LRE, PDSGR, RGD, and YIGSR contribute to improved viability, but insulin release from these samples was

not statistically greater than that from controls. MIN6  $\beta$ -cells were also encapsulated with various concentrations of IKLLI and IKVAV (0.05-5.0mM), individually, and the peptide combinations IKLLI-IKVAV, IKVAV-YIGSR, and PDSGR-YIGSR to explore synergistic effects [9]. Moreover, bioactive GLP-1C was efficiently immobilized within PEG hydrogels and did not alter the bulk hydrogel properties. The GLP-1 immobilized PEG hydrogels enhanced the survival and insulin secretion of encapsulated islets [17].

To further enhance cell survival in the hydrogels, a polymerizable superoxide dismutase was incorporated into PEG hydrogels to protect encapsulated cells from superoxidemediated damage, since superoxide and other small reactive oxygen species can cause oxidative damage to donor tissue encapsulated within size exclusion barrier materials [18]. Recently, Lin et al. has reported that when MIN6 cells were encapsulated in PEG hydrogels, their survival and glucose responsiveness to insulin were highly dependent on the cell-packing density. A minimum packing density of  $10^7$  cells/mL was necessary to maintain the survival of encapsulated  $\beta$ -cells without the addition of material functionalities. Thiolated EphA5-Fc receptor and ephrinA5-Fc ligand were conjugated into PEG hydrogels via a thiol-acrylate photopolymerization to render an otherwise inert PEG hydrogel bioactive. The biomimetic hydrogels provided crucial cell-cell communication signals for dispersed  $\beta$ -cells and improved their survival and proliferation. Together with the cell-adhesive peptide RGDS, the immobilized fusion proteins (EphA5-Fc and ephrinA5-Fc) synergistically increased the survival of both MIN6  $\beta$ -cells and dissociated islet cells, both at a very low cell-packing density ( $< 2 \times 10^6$  cells/mL) [10].

### 3.5 Conclusion

In this chapter, we have optimized our hydrogel systems for MIN6 cells in 3D culture. We have found that the optimal condition for the cells to form artificial islets *in vitro* is the concentration of PEG at 5% and the ratios of 4-arm thiolated PEG to PEGTA at 1:2 (or 1:3). Conjugated with RGD at 0.2 mM can significantly promote the insulin secretion, similar to the 2D control group.

### 3.6 References

1. Discher, D.E., D.J. Mooney, and P.W. Zandstra, *Growth factors, matrices, and forces combine and control stem cells*. Science, 2009. **324**(5935): p. 1673-7.
2. Seliktar, D., *Designing Cell-Compatible Hydrogels for Biomedical Applications*. Science, 2012. **336**(6085): p. 1124-1128.
3. Kloxin, A.M., et al., *Photodegradable Hydrogels for Dynamic Tuning of Physical and Chemical Properties*. Science, 2009. **324**(5923): p. 59-63.
4. Zhu, J., *Bioactive modification of poly(ethylene glycol) hydrogels for tissue engineering*. Biomaterials, 2010. **31**(17): p. 4639-56.
5. Kloxin, A.M., et al., *Mechanical Properties of Cellularly Responsive Hydrogels and Their Experimental Determination*. Advanced Materials, 2010. **22**(31): p. 3484-3494.
6. Graf, J., et al., *A pentapeptide from the laminin B1 chain mediates cell adhesion and binds the 67,000 laminin receptor*. Biochemistry, 1987. **26**(22): p. 6896-900.
7. Kleinman, H.K., et al., *Identification of a 110-kDa nonintegrin cell surface laminin-binding protein which recognizes an A chain neurite-promoting peptide*. Arch Biochem Biophys, 1991. **290**(2): p. 320-5.
8. Schense, J.C., et al., *Enzymatic incorporation of bioactive peptides into fibrin matrices enhances neurite extension*. Nat Biotechnol, 2000. **18**(4): p. 415-9.

9. Weber, L.M., et al., *The effects of cell-matrix interactions on encapsulated beta-cell function within hydrogels functionalized with matrix-derived adhesive peptides*. *Biomaterials*, 2007. **28**(19): p. 3004-11.
10. Lin, C.C. and K.S. Anseth, *Cell-cell communication mimicry with poly(ethylene glycol) hydrogels for enhancing beta-cell function*. *Proc Natl Acad Sci U S A*, 2011. **108**(16): p. 6380-5.
11. Li, X., et al., *Manipulating neural-stem-cell mobilization and migration in vitro*. *Acta Biomater*, 2012. **8**(6): p. 2087-95.
12. Ghosh, K., et al., *Rheological Characterization of in Situ Cross-Linkable Hyaluronan Hydrogels*. *Biomacromolecules*, 2005. **6**(5): p. 2857-2865.
13. Vanderhooft, J.L., et al., *Rheological properties of cross-linked hyaluronan-gelatin hydrogels for tissue engineering*. *Macromol Biosci*, 2009. **9**(1): p. 20-8.
14. Weber, L.M., et al., *PEG-based hydrogels as an in vitro encapsulation platform for testing controlled beta-cell microenvironments*. *Acta Biomater*, 2006. **2**(1): p. 1-8.
15. Freudenberg, U., et al., *A star-PEG-heparin hydrogel platform to aid cell replacement therapies for neurodegenerative diseases*. *Biomaterials*, 2009. **30**(28): p. 5049-60.
16. Hersel, U., C. Dahmen, and H. Kessler, *RGD modified polymers: biomaterials for stimulated cell adhesion and beyond*. *Biomaterials*, 2003. **24**(24): p. 4385-4415.
17. Lin, C.C. and K.S. Anseth, *Glucagon-like peptide-1 functionalized PEG hydrogels promote survival and function of encapsulated pancreatic beta-cells*. *Biomacromolecules*, 2009. **10**(9): p. 2460-7.
18. Hume, P.S. and K.S. Anseth, *Polymerizable superoxide dismutase mimetic protects cells encapsulated in poly(ethylene glycol) hydrogels from reactive oxygen species-mediated damage*. *Journal of Biomedical Materials Research Part A*, 2011. **99A**(1): p. 29-37.

## CHAPTER FOUR

### 4 AUTOMATIC ROBOTIC FABRICATION OF BETA-CELL SPHEROIDS AND MSC MICROENCAPSULATION IN A CORE-SHELL CONFIGURATION FOR IMMUNOMODULATION

#### 4.1 Introduction

In our body, most cells are organized in three-dimensional (3D) structures which allow for cell-cell and cell-extracellular matrix interactions in a very complex communication network of biochemical and mechanical signals. Knowing the cell responses to environmental cues, including biochemical and mechanical signals, is critical for the understanding development biology, disease progress, cancer biology and treatment, and tissue regeneration. However, most *in vitro* cell studies in the literature are from two-dimensional (2D) monolayer cultures. In 2D cultures, most cells lose tissue specific properties; and the physiological and pathological studies based on 2D culture may not reflect the signaling cascades in our body [1, 2]. To overcome the difficulties and issues with 2D cultures, many three-dimensional 3D culture systems have been tested, including organotypic tissue explants [3], cell seeded 3D scaffolds or hydrogels [4], multicellular spheroids [2, 5], and so on.

Multicellular spheroids have advantages over the other methods due to its simplicity, reproducibility, and similarity to physiological tissues and steer clear of the mass transport issues associated with explants and scaffolds. These multicellular spheroids have been widely used in many biological and medical applications, such as screening new drug and biologics using human spheroids before clinical trial [6, 7],

understanding developmental biology, disease progress, cancer biology and treatment, and tissue regeneration [8], and improving the survival of transplanted cells *in vivo* [5].

Although these advantages of spheroids have been widely recognized, it has been difficult to scale up spheroid culture in a high-throughput manner. Preventing cells from attaching to the culture ware substratum is the fundamental requirement for multicellular spheroid generation. The general criteria for selecting a spheroid production method include: production efficiency, spheroid size uniformity, possible damage or influence on cellular physiology, convenience and suitability for subsequent applications. Traditional fabrication methods for multicellular cell spheroids include hanging-drop [9, 10], round-bottomed well culture [11], non-adhesive surface, rotary bioreactor or spinner flasks [12], microfabricated microstructures [13-16], and so on. However, none of these methods fits the scalability criterion, either because spheroid shape and size can not be controlled during the fabrication process or because the platform does not permit fabrication of tissue spheroids in large number in a time efficient manner. The size and shape of the spheroids are very important, since uncontrolled size and shape may induce mass transport issues. Recently, a novel technique, high-throughput hydrogel microwells, has been developed to achieve mass sphere production with easy spheroid handling and diameter control [17, 18]. Mehesz and coworkers have combined this technique with automated cell seeding for scalable robotic fabrication of uniform-sized tissue spheroids [19].

The transplantation of islets of Langerhans is a potential option for curing type 1 diabetes, which can avoid the complications followed by major surgery compared to the

whole pancreas transplantation. However, islets transplantation still faces the problems of the long-term administration of immunosuppressive agents with severe side effects, and the shortage of donor tissues [20-22]. To solve these issues, the immunoisolation of islets with a semi-permeable membrane, and other cell sources for islets transplantation, has been attempted. Immunoisolation of islets is a technology being expected to overcome the immune-mediated destruction of the donor tissues without requiring toxic immunosuppression agents [23-25]. The strategy of immunoisolation means encapsulating islets within a semi-permeable membrane made of biomaterials with good biocompatibility. A variety of hydrogels have been applied to islet encapsulation. Hydrogels protect the islets from immune system but still allow pro-inflammatory cytokines and other effector molecules of low molecular weight to diffuse into the capsules and affect the function and vitality of islets [26-28]. Control of islet graft inflammation may be achieved by co-transplantation of islets with mesenchymal stem cell (MSCs). These stromal cells are connective tissue derived stem cell with immunomodulatory and regenerative properties. They also secrete anti-inflammatory proteins and suppress the activity of various immune cells such as alloantigen activated T and B lymphocytes.

Within islets, there are five endocrine cell types work as a micro-organ to maintain glucose homeostasis. Insulin is normally produced in and secreted by the  $\beta$ -cells of islets. Because of difficulties associated with the use of primary islets, such as limited human pancreas donation, the risk of zoonosis in case of an animal source, low isolation



yield, and preservation [29], the  $\beta$ -cells replacement through cellular transplantation to replace primary islets has the promise of providing a long-term cure for type 1 diabetes.

In this study, we developed a fully robotic biofabrication method to produce uniform size multi-cellular  $\beta$ -cells spheroids in large scale. Our method is the first one to allow production of cell spheroids in large number and in a time-efficient manner. The availability of this technique was assured. The size of uniform spheroids can be manipulated by adjusting the seeding concentrations of cell suspensions. Uniform sized multicellular  $\beta$ -cells spheroids can be coated with a thin layer of non-degradable hydrogel for immunoisolation. In addition, the survival of spheroids of optimized size can be further improved with a novel coating of multiple layers of MSCs to prevent graft rejection. To prevent MSC migrate away from spheroids, another layer of non-degradable hydrogel can be added. The function of  $\beta$ -cells in the spheroids with multiple layers respond to glucose to release insulin was investigated by enzyme linked immunosorbent assay.

## 4.2 Materials and Methods

### 4.2.1 Materials

Polytetrafluoroethylene (PTFE, Teflon) rods were obtained from McMaster-Carr (Atlanta, GA). Methycellulose and Agarose were purchased from Sigma (St. Louis, MO). LIVE/DEAD viability kit was purchased from Molecular Probes (Eugene, OR). Insulin enzyme linked immunosorbent assay (ELISA) kit was obtained from Millipore (Billerica, MA). Cell culture reagents and supplements were obtained from Invitrogen (Carlsbad,

CA). Alexa Fluor-543 Phalloidin, 4', 6-Diamidino-2-Phenylindole, Dihydrochloride (DAPI) was obtained from Molecular Probes (Eugene, OR). Human mitochondria antibody (MAB1273) was purchased from Millipore (Billerica, MA). Rabbit anti-insulin was purchased from Santa Cruz Biotechnology (Dallas, Texas). Fluorophore-conjugated secondary antibodies were purchased from Jackson ImmunoResearch (West Grove, PA). All other reagents were purchased from Sigma Aldrich (St. Louis, MO).

#### 4.2.2 Cell culture

Rat pancreatic  $\beta$ -cells of the RIN-m cell line were obtained from ATCC (CRL-2057). RIN-m cells were cultured in Roswell Park Memorial Institute (RPMI) 1640 medium supplemented with 10% fetal bovine serum at 37 °C in humid conditions with 5% CO<sub>2</sub>. The culture medium was exchanged every 2 days.

Human bone marrow-derived mesenchymal stem cells (hMSCs) were obtained from ScienCell (Carlsbad, CA). Human MSCs were plated in Modified Essential Medium alpha (MEM $\alpha$ ) supplemented with 10% fetal bovine serum. All the cells were incubated at 37 °C under 5% CO<sub>2</sub> and used before passage 5 in this study. The culture medium was exchanged every 2 days.

#### 4.2.3 Beta-cells spheroids fabrication

Beta-cells spheroids with uniform sizes were fabricated using a robotic fabrication system developed in our lab. Briefly, stamps with micronipple array were designed in SolidWorks and fabricated using ultra-precision lathe. The automatic spheroid fabricator

was built on a TT-C3-4040 robot (IAI Corporation, Shizuoka, Japan) with electric triggered gripper to pick up the stamp and pipette tip uptake and ejection actuator to handle liquid. Agarose solution (2% w/w) was prepared by built-in heating elements in the robot platform. The robot was programmed to first add agarose solution to culture dishes. Then the robot picked up the stamp with micronipple arrays on the bottom and pressed on the agarose solution at room temperature for 2 minutes. Then the highly uniform size microwells were formed in the agarose gel. Specific micro-mold, including 270 wells with the well diameter of 600  $\mu\text{m}$ , designed and made by ourselves, were applied to staple microwells on agarose gels. To achieve desired sizes of  $\beta$ -cells spheroids, 1 mL cell suspensions of different concentrations:  $0.1 \times 10^6$ ,  $0.8 \times 10^6$ ,  $2.4 \times 10^6$ ,  $5.6 \times 10^6$ , and  $1.2 \times 10^7$  cells/mL, were seeded into microwells. Cells in the microwells were incubated at 37 °C and 5% CO<sub>2</sub> 2 days for  $\beta$ -cells spheroids formation. The formed  $\beta$ -cells spheroids were transferred into a suspension flask on a shaker for long time culture.

#### 4.2.4 Viability of cells in microwells

Viability of the cells in agarose microwells was examined using LIVE/DEAD Viability Kit, which is a two color fluorescent assay based on differential permeability of live and dead cells and allows preservation of the distinctive staining pattern for a couple of hours after post-fixation with 4% (w/v) glutaraldehyde. Live cells were stained with green fluorescent SYTO 10; and dead cells with compromised cell membranes were stained with red fluorescent ethidium homodimer-2. A confocal laser microscope (TCS

SP5, Leica microsystem Inc., Bannockburn, IL) was used to capture the images of the LIVE/DEAD cell staining patterns.

#### 4.2.5 Morphology of spheroids

Morphology of spheroids was examined by immunocytochemistry. The spheroids were fixed with 4% (w/v) paraformaldehyde, treated with 5% goat serum in phosphate buffered saline (PBS) to block non-specific reactivity and incubated overnight at 4 °C with primary antibodies, such as insulin and human mitochondria. After washing with PBS three times, the samples were incubated with the affinity secondary antibodies at room temperature for 3 hrs. The nuclei were stained with DAPI. The samples were imaged using a Leica TCS SP5 laser scanning confocal microscope.

#### 4.2.6 Co-culture RIN-m cells and hMSCs

Mixed cell suspension of  $2 \times 10^6$  cells/mL with a ratio of RIN-m cells to hMSCs at 1:1 was seeded into microwells. Cultured 3 days, the formed spheroids were inspected by immunocytochemistry as described above and imaged by Leica TCS SP5 laser scanning confocal microscope.

#### 4.2.7 Co-culture $\beta$ -cells spheroids and hMSCs

RIN-m cells ( $1 \times 10^6$  cells/mL) in the microwells were incubated 2 days for spheroids formation. Then hMSCs ( $1 \times 10^6$  cells/mL) were seeded and co-cultured with the formed  $\beta$ -cells spheroids in the microwells for another 3 days. The morphology of co-

culture spheres was inspected through immunostaining as described before and imaged by Leica TCS SP5 laser scanning confocal microscope.

#### 4.2.8 Core/shell structure RIN-m/hMSCs complex fabrication

##### 4.2.8.1 Fabrication of hydrogel coated $\beta$ -cells spheroids

The methylcellulose coated  $\beta$ -cells spheroids were prepared as following. Briefly, hydrogel precursor solutions were prepared through mixing 1 mL 4% (w/w) methylcellulose solution and 0.1 ng/mL streptavidin. Beta-cells spheroids with hydrogel precursor solutions were poured into 10 mL of mineral oil (Sigma Aldrich, St. Louis, MO) with the magnetic stirring at 300 rpm at 37 °C. After half an hour, the  $\beta$ -cells spheroids were centrifuged at 300 rpm for 5 min, washed 3 times with culture media. The  $\beta$ -cells spheroids were fixed with 4% (w/v) paraformaldehyde, stained with DPAI for nuclei and Sulfo-Cy3 NHS ester (Lumiprobe Corp, Hallandale Beach, FL) for coated methylcellulose, and inspected by Leica TCS SP5 laser scanning confocal microscope.

##### 4.2.8.2 Human MSCs coating

Human MSCs were washed with Hank's Balanced Salt Solution (HBSS) 3 times. Human MSCs of different concentrations ( $0.4 \times 10^6$ ,  $0.8 \times 10^6$ ,  $1.6 \times 10^6$ ,  $3.2 \times 10^6$ , and  $6.4 \times 10^6$  cells/mL) were incubated in biotinylated poly(ethylene glycol)-N-hydroxysuccinimide (biotin-PEG-NHS) solution (1 mg/mL) for 30 min at 37 °C on the shaker. Human MSCs were washed 3 times with HBSS and transferred to Petrie dish with the  $\beta$ -cells spheroids for 30 min coating at 37 °C on a shaker. The formed spheroid

complex were stained by immunocytochemistry and inspected by Leica TCS SP5 laser scanning confocal microscope.

#### 4.2.8.3 Agarose hydrogel coating

Agarose hydrogels were selected for coating on the surface of RIN-m/hMSCs hybrid spheroids using the similar coating method as described before. Briefly, 1 mL 2% agarose solution was mixed with 700 to 1000 RIN-m/hMSCs spheroids and 15 mL of mineral oil (Sigma Aldrich, St. Louis, MO) was added at 40 °C. The mixture was suspended with the magnetic stirring at 200 rpm to form agarose droplets then immersed in an ice bath for 5min. The microbeads contained RIN-m/hMSCs spheroids were washed 3 times with HBSS and then cultured in medium under 5% CO<sub>2</sub> at 37 °C. The thickness of coated hydrogel was controlled through adjusting the stirring rate of mineral oil. Stirring rate was set up at 100, 200, and 500 rpm, respectively. The complexes were fixed with 4% (w/v) paraformaldehyde and inspected by the phase-contrast microscope.

#### 4.2.9 Insulin release from hMSCs coated $\beta$ -cells spheroids

$\beta$ -cells spheroids coated with different concentrations of hMSCs ( $0.4 \times 10^6$ ,  $0.8 \times 10^6$ ,  $1.6 \times 10^6$ ,  $3.2 \times 10^6$ , and  $6.4 \times 10^6$  cells/mL) were inspected for insulin release based on the glucose stimulus. Briefly, culture medium were removed from samples and washed twice with KRB solution. Samples were first placed in a low glucose concentration (1.1 mM) for 45min, followed by incubation in a high glucose

concentration solution (16.7 mM) for 1 h. The high glucose solutions were collected for insulin measurement by ELISA kit.

#### 4.2.10 Bioactivation of hMSCs to pro-inflammatory cytokines

Human MSCs were enzymatically detached from culture plates, counted, and added ( $0.4 \times 10^6$ ,  $0.8 \times 10^6$ ,  $1.6 \times 10^6$ ,  $3.2 \times 10^6$ , and  $6.4 \times 10^6$  cells/mL) to a 24-well plate with 35  $\beta$ -cells spheroids of 200  $\mu\text{m}$  compared to  $\beta$ -cells spheroids cultured alone. After 24 hrs, the insulin release based on the glucose stimulus from  $\beta$ -cells spheroids was inspected as described above.

Then these co-culture cells were exposed to a cocktail of pro-inflammatory cytokines including 100 ng/mL interferon- $\gamma$  (IFN- $\gamma$ ), 10 ng/mL tumor necrosis factor- $\alpha$  (TNF- $\alpha$ ), 0.5 ng/mL interleukin 1 $\beta$  (IL-1 $\beta$ ) for another 24 hrs. The insulin secretion based on the glucose stimulus from  $\beta$ -cells spheroids was inspected again as described above. The change of insulin release after exposing to the pro-inflammatory cytokines was calculated based on these two inspections.

#### 4.2.11 Analysis of $\beta$ -cells apoptosis by TUNEL assay

Cytokine induced  $\beta$ -cells damage was assessed by the TUNEL, a marker for cell apoptosis. After culture as 4.2.10 described above, the  $\beta$ -cells spheroids were fixed with 4% w/v paraformaldehyde. An APO-BrdU TUNEL Assay Kit (Invitrogen, Grand Island, NY) was utilized, in which an AlexaFluor 488 labeled anti-BrdU antibody was used for

detection of apoptotic cells. Propidium iodide staining was performed to detect all the cells.

#### 4.2.12 Statistical analysis

Data are shown as mean  $\pm$  S.D. Statistical analyses were performed using one way ANOVA (analysis of variance) followed by Tukey's post tests and the paired t-test where appropriate. A probability (*P*) value of  $<0.05$  was considered statistically significant.

### 4.3 Results

#### 4.3.1 Fabrication of $\beta$ -cells spheroids with uniform size

In this study, the agarose microwells were firstly fabricated by our designed computer controlled spheroid maker (Figure 4.1). Different concentrations of  $\beta$ -cells were seeded into these agarose microwells. Beta-cells survived and aggregated in these microwells (Figure 4.2 A). Beta-cells exhibited high viability ( $>95\%$ , Figure 4.2 B). The cell seeding concentration controlled the size of  $\beta$ -cells spheroids. Higher concentrations of  $\beta$ -cells resulted in the spheroids with larger diameter (Figure 4.2 A and C). These cell aggregates were transferred to a suspension flask on a shaker for long-term culture. Large amounts of uniformed  $\beta$ -cells spheroids with different sizes (100, 200, 300, 400, and 500  $\mu\text{m}$ ) have been successfully fabricated at 1 week with very high viability as shown in Figure 4.3.



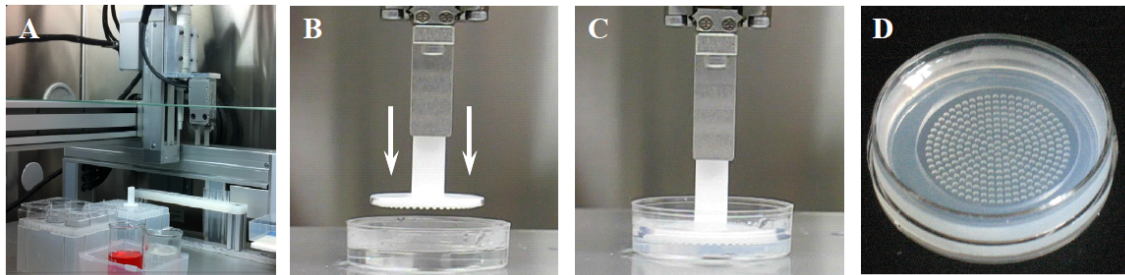


**Figure 4. 1** (A) The computer controlled spheroid maker. (B and C) The fabrication process of microwells. (D) Agarose microwells.

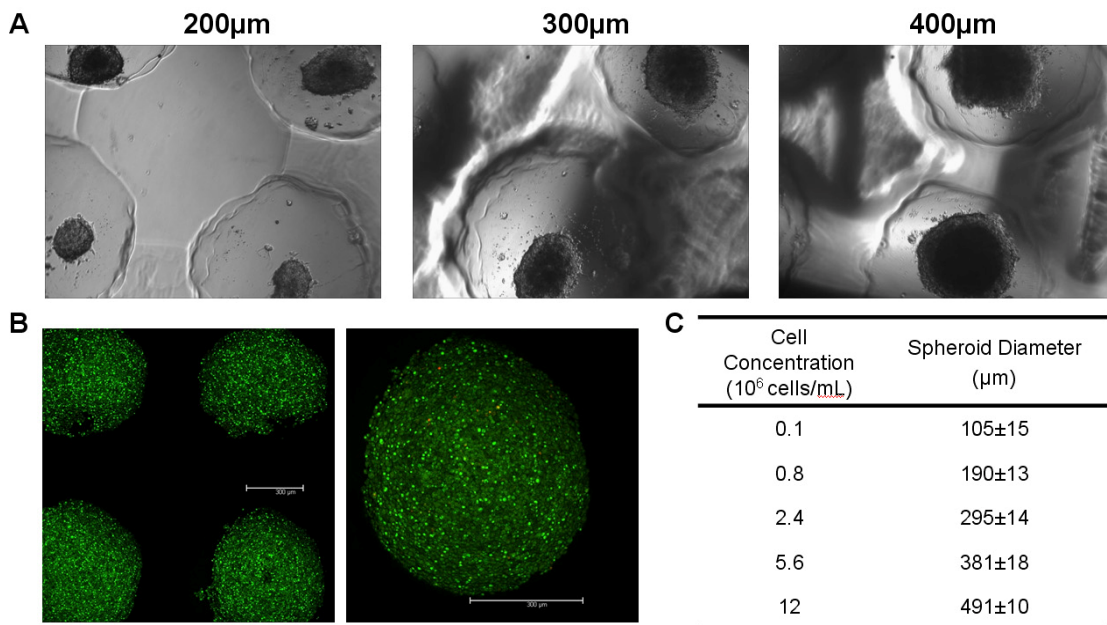


**Figure 4. 2** (A) Beta-cells formed aggregates of different diameters of 200, 300, and 400 μm in microwells. (B) LIVE/DEAD staining of β-cells aggregates in microwells. Live cells stained with green and dead with red. (C) The relationship between cell seeding concentrations and spheroid diameters.

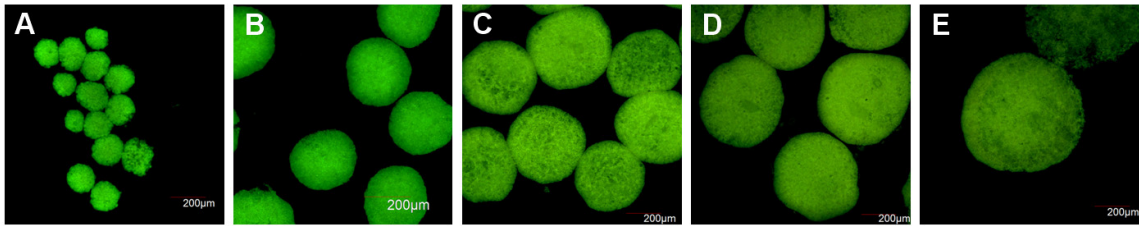


**Figure 4. 3** Beta-cells formed spheroids with different diameters of (A) 100, (B) 200, (C) 300, (D) 400, and (E) 500  $\mu\text{m}$  transferred into a suspension flask for culture 1 week with high viability. Live cells stained with green and dead with red. Scale bar = 200  $\mu\text{m}$ .

#### 4.3.2 Glucose-stimulated insulin secretion

As shown on Figure 4.4,  $\beta$ -cells in the spheroids stained strongly positive for insulin regardless of spheroid size, indicating that these cells were still capable of producing insulin after *in vitro* culture in the format of spheroids.

For stimulated insulin secretion,  $\beta$ -cells spheroids were first conditioned in Krebs Ringer Buffer (KRB) containing low glucose and then exposed to KRB containing high glucose. Figure 4.5 reports insulin secretion from  $\beta$ -cells spheroids of different sizes at high glucose level. The insulin released from the single cell was also calculated through dividing the insulin amounts by the total cells in the spheroids. The spheroids of 200  $\mu\text{m}$  released significantly larger amount of insulin than those of 100  $\mu\text{m}$  (\*  $P < 0.05$ ). And there is no significant difference about total insulin released from the spheroids of 200, 300, 400, and 500  $\mu\text{m}$ . In consideration to the capacity of the single cell for insulin secretion in the format of spheroids, the single cell from spheroids of 200  $\mu\text{m}$  released highest amount of insulin when compared to that from spheroid of 300 400, and 500  $\mu\text{m}$  (\*  $P < 0.05$ ).

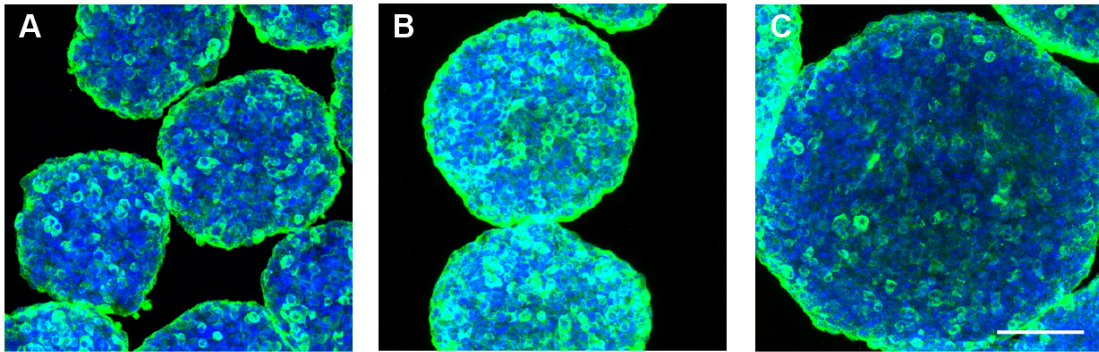


**Figure 4.4** Insulin (green) staining of  $\beta$ -cells spheroids with different diameters of (A) 200, (B) 300, and (C) 500  $\mu\text{m}$ . Nuclei were stained with DAPI (blue). Scale bar = 100  $\mu\text{m}$ .

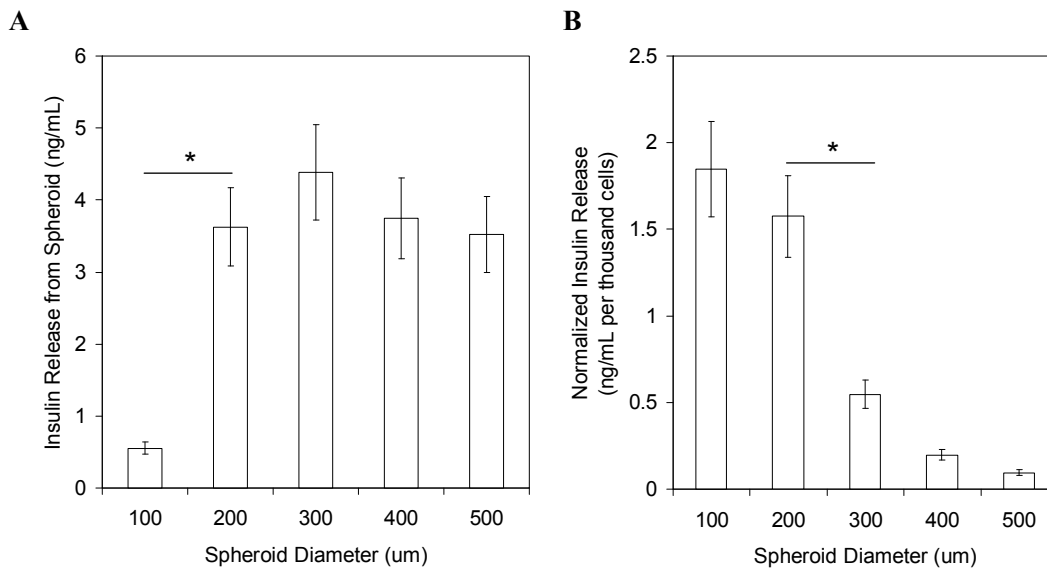


**Figure 4.5** Insulin release from  $\beta$ -cells spheroids with different diameters of 100, 200, 300, 400, and 500  $\mu\text{m}$ . (A) Insulin release from spheroids of total number of 270. Spheroids of diameter of 200  $\mu\text{m}$  released significant larger amount of insulin than those with diameter of 100  $\mu\text{m}$  (\*  $P < 0.05$ ). (B) Insulin release from the single cell in the spheroids. Cells from spheroids of 200  $\mu\text{m}$  released larger amount of insulin compared to those from spheroid of 300  $\mu\text{m}$  (\*  $P < 0.05$ ).

### 4.3.3 Human MSCs invasion into $\beta$ -cells spheroids

Human MSCs were stained with red by human specific antibody, mitochondria, and RIN-m cells were identified with green by a polyclonal antibody directed against murine insulin. When seeding these two types of cells in the microwells simultaneously, as shown on Figure 4.6A, these cells self-assembled into a spheroid in which hMSCs have integrated with each other and self-sorted to stay inside whereas  $\beta$ -cells randomly disseminated throughout the entire spheroid. Moreover, a thin layer of  $\beta$ -cells appeared to cover the whole spheroid.

When  $\beta$ -cells seeded first in the microwells, they aggregated together at the day 2. The subsequently seeded hMSCs in the same microwells did not adhere on the surface of the formed  $\beta$ -cells spheroids; instead, they invaded into  $\beta$ -cells spheroids and broke the integrity of  $\beta$ -cells spheroids regardless of the diameter of spheroid, as shown in Figure 4.6B.

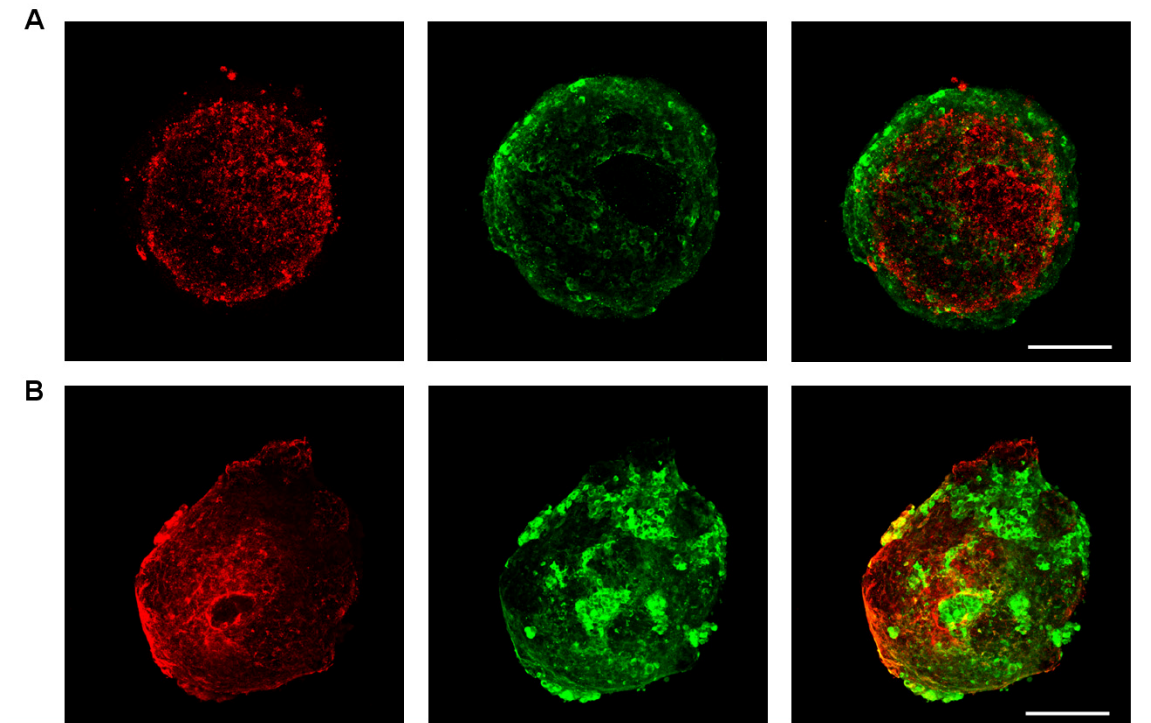


**Figure 4. 6** (A) Co-culture of  $\beta$ -cells and hMSCs. (B) Co-culture of  $\beta$ -cells spheroids with hMSCs. Beta-cells were stained with insulin with green. Human MSCs were identified by human mitochondria with red. Scale bar = 100  $\mu$ m.

#### 4.3.4 Construction of unique RIN-m/hMSCs complex with core/shell structure

To prevent the invasion of hMSCs, a physical barrier, methylcellulose hydrogel, was coated on the surface of  $\beta$ -cells spheroids. Methylcellulose hydrogel formed a nano layer on the spheroid (Figure 4.7).

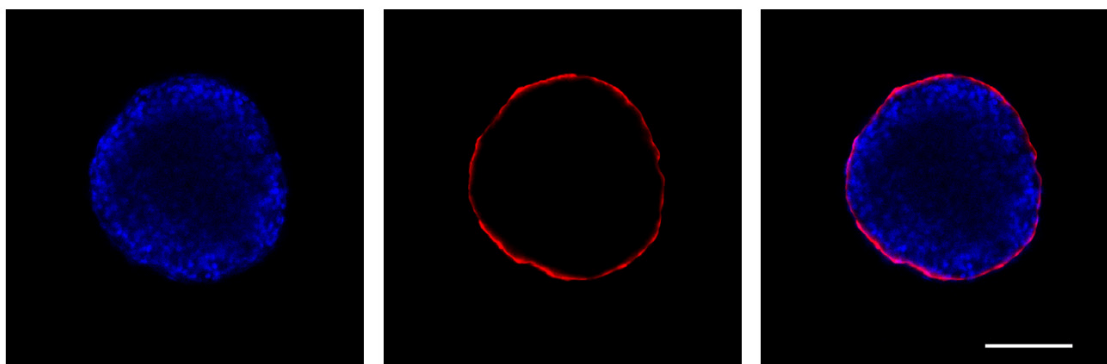


**Figure 4. 7** Methylcellulose was coated on the surface of  $\beta$ -cell spheroid. Methylcellulose was conjugated with Cy3 NHS ester (red) and DAPI for nuclei (blue). Scale bar = 100  $\mu$ m.

After nano-coating of hydrogel on the surface of  $\beta$ -cell spheroid, hMSCs attached on the  $\beta$ -cell spheroid with shell-structure. The thickness of shell can be adjusted by the concentration of hMSCs. As shown on Figure 4.8, with increasing the concentration of hMSCs, a thicker shell layer formed on the surface of  $\beta$ -cell spheroid.

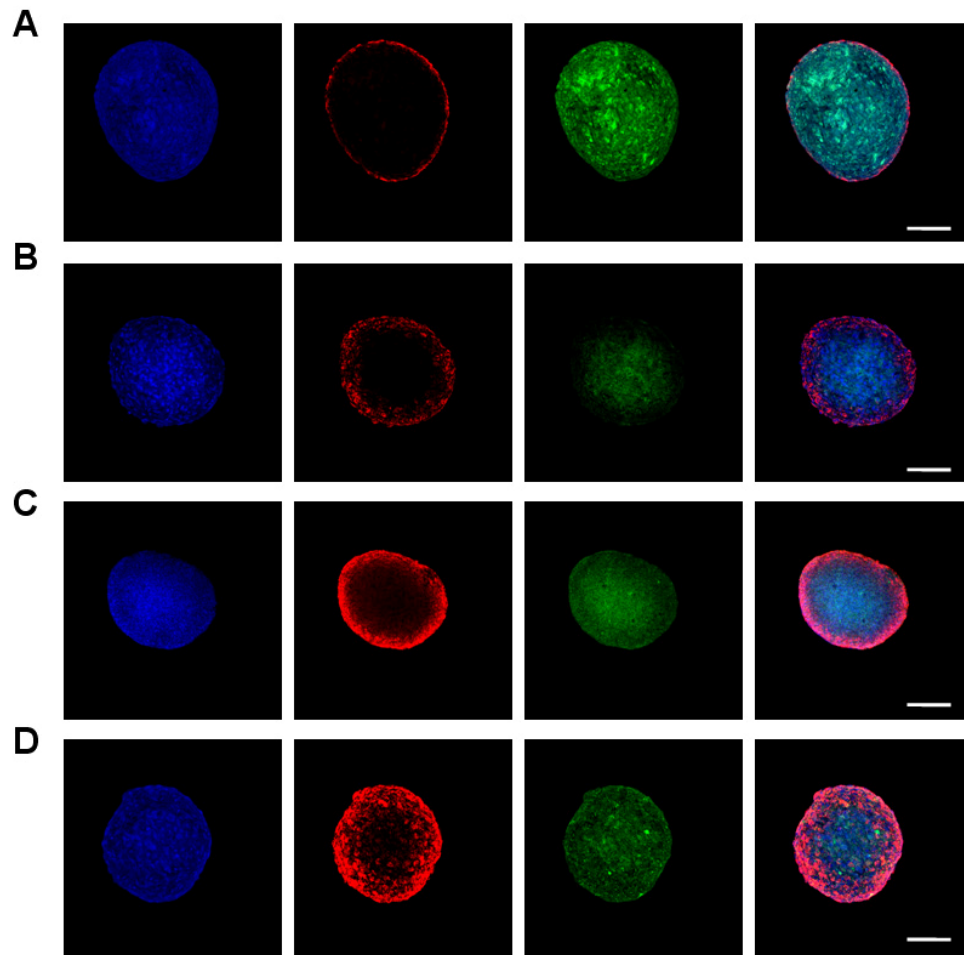


**Figure 4. 8** Human MSCs of different concentrations of (A) 0.4, (B) 0.8, (C) 1.6, and (D) 3.2 million/mL were coated on the surface of  $\beta$ -cell spheroid. Human MSCs were stained with human mitochondria antibody with red,  $\beta$ -cell spheroid was identified by insulin antibody (green) and DAPI for nuclei (blue). Scale bar = 100  $\mu$ m.

#### 4.3.5 Insulin secretion from RIN-m/hMSCs hybrid spheroids

To check the effects of coating of hMSCs on the insulin secretion from  $\beta$ -cell spheroids, RIN-m/hMSCs hybrid spheroids were first conditioned in KRB containing low glucose and then exposed to KRB containing high glucose. As shown in Figure 4.9, the

amounts of secreted insulin decreased with increasing of hMSC concentration. When the concentration caught up to  $10^6$  cells, the insulin secretion reduced significantly (\*  $P<0.05$ ).

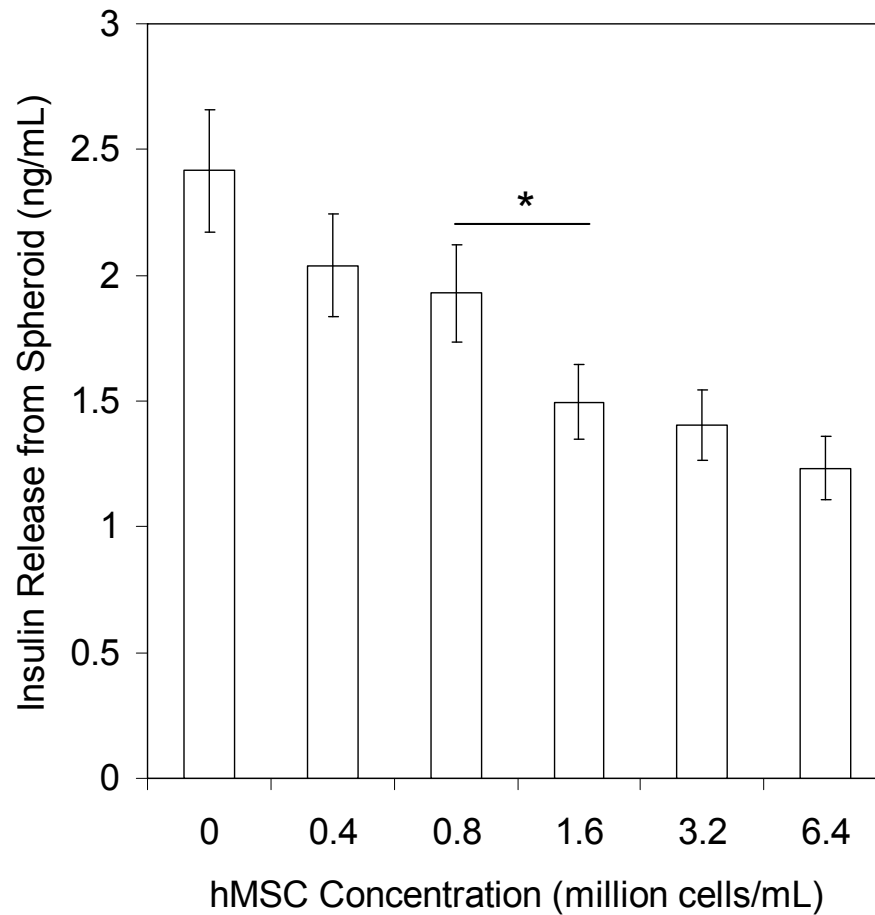


**Figure 4. 9** Insulin release from  $\beta$ -cells spheroids with diameter of 200  $\mu\text{m}$  coated with different concentrations of hMSCs. Spheroids of diameter of 200  $\mu\text{m}$  coated with the concentration of hMSCs of 0.8 million cells/mL released significant larger amount of insulin than those with 1.6 million cells/mL (\*  $P<0.05$ ).



#### 4.3.6 Effects of hMSCs on $\beta$ -cells spheroids

Before exposure of pro-inflammatory cytokines, co-culture with hMSCs for 24 hrs did not enhance glucose stimulated insulin secretion of  $\beta$ -cells regardless of hMSC concentration (Fig. 4.10 A). Without hMSCs, exposure to cytokines significantly debilitated the insulin secretion of  $\beta$ -cells (Fig. 4.10 B, 38%). Co-cultured hMSCs benefited  $\beta$ -cells to retain the insulin secretion. The protective effect of hMSCs was dose-dependent. High concentrations of hMSCs preserved  $\beta$ -cells to secrete insulin due to glucose stimulation when exposed to pro-inflammatory cytokines. Specifically, with hMSCs of  $6.4 \times 10^6/\text{mL}$ ,  $\beta$ -cells only lost 8% of insulin secretion when compared after and before exposure to pro-inflammatory cytokines

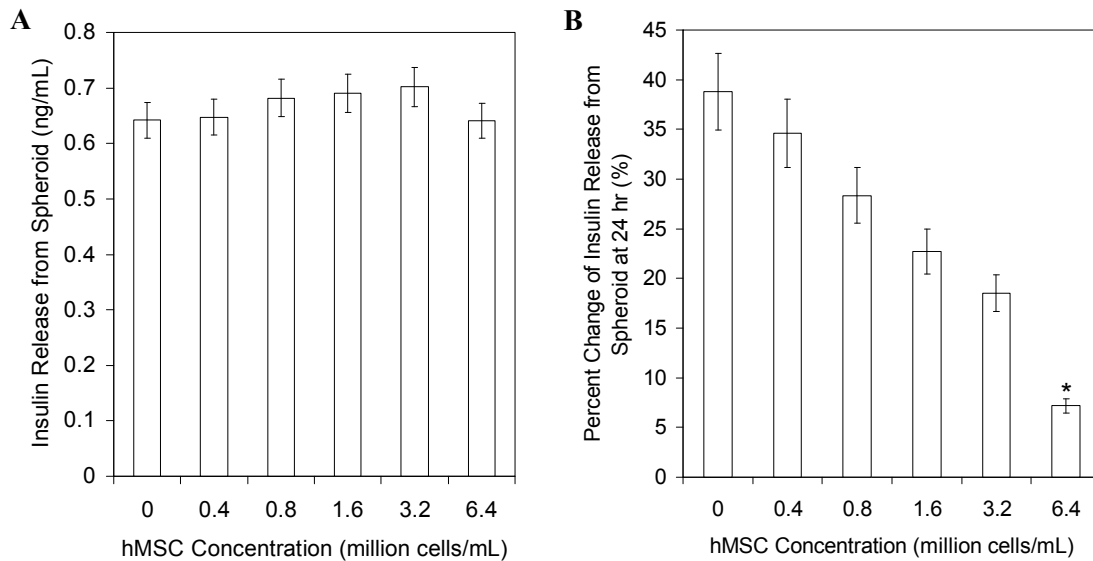


**Figure 4. 10** Beta-cells spheroids with the diameter of  $200 \mu\text{m}$  co-cultured with different concentrations of hMSCs. (A) Insulin release from  $\beta$ -cells spheroids co-culture with hMSCs of different concentrations at 24 hr. (B) Percentage change of insulin release after exposing to the pro-inflammatory cytokines after 24 hr (\*  $P < 0.05$ ).

Figure 4.11 showed apoptosis of  $\beta$ -cells co-cultured with hMSCs of different concentrations of 0, 0.4, 0.8, 1.6, 3.2, and 6.4  $\times 10^6$ /mL after exposing to the pro-inflammatory cytokines for 24 hrs. AlexaFluor 488 labeled anti-BrdU antibody was used for detection of apoptotic cells. Propidium iodide was applied to stain all the cells. With the increase of hMSC concentration, lower number of  $\beta$ -cells expressed apoptosis. Human MSCs benefited  $\beta$ -cells survival when exposed to pro-inflammatory cytokines.

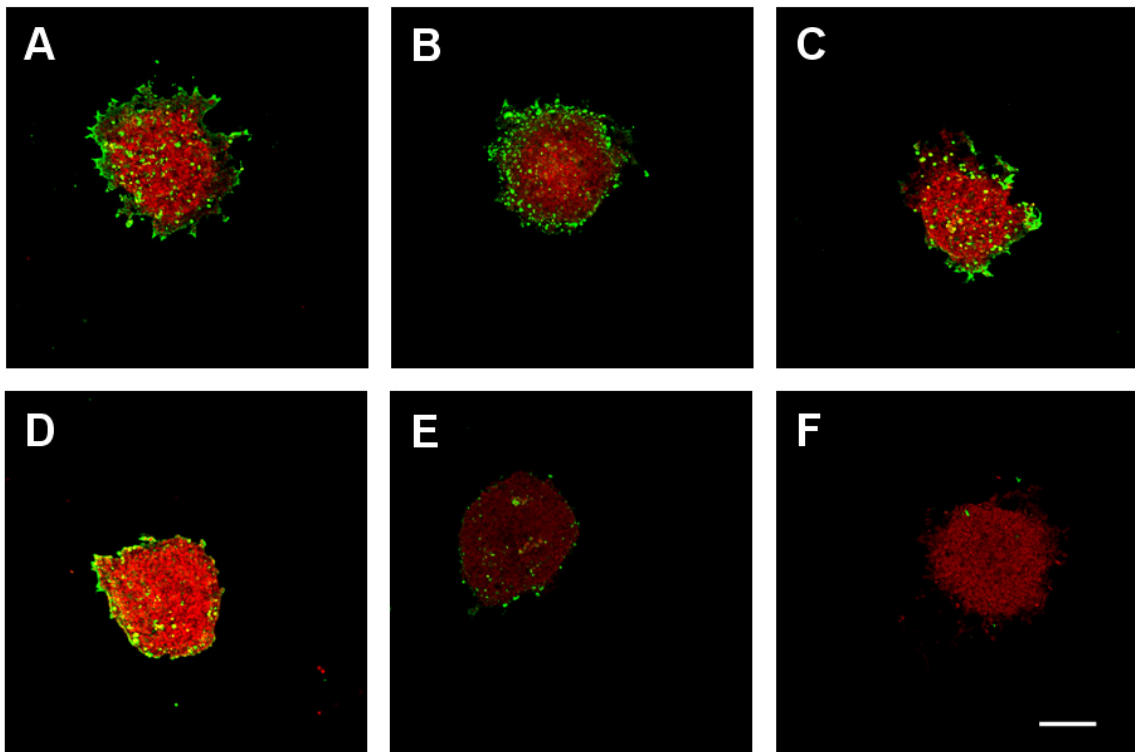


**Figure 4. 11** Apoptosis of  $\beta$ -cells with the diameter of 200  $\mu\text{m}$  co-cultured with hMSCs of different concentrations: (A) 0, (B) 0.4, (C) 0.8, (D) 1.6, (E) 3.2, and (F) 6.4 million/mL after exposing to the pro-inflammatory cytokines. AlexaFluor 488 labeled anti-BrdU antibody was used for detection of apoptotic cells and propidium iodide staining for all the cells. Scale bar = 100  $\mu\text{m}$ .

#### 4.3.7 Agarose hydrogel coating

Agarose hydrogel was coated on the surface of complex. Through controlling the stirring rate, hydrogel out layer formed on the surface of RIN-m/hMSCs hybrid spheroids with different thicknesses of 5, 20, and 60  $\mu\text{m}$ , as shown in the Figure 4.12.

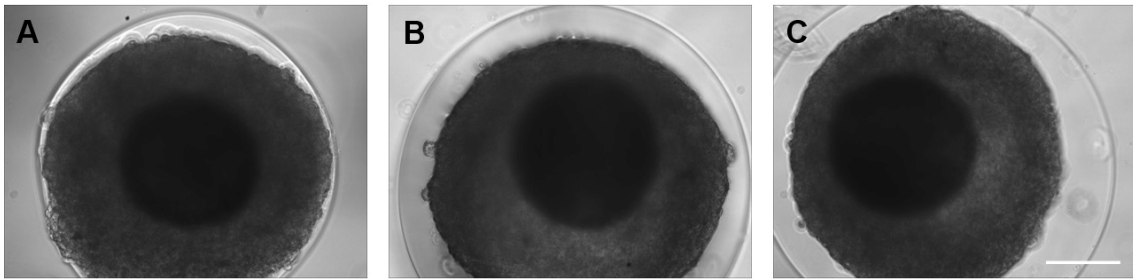


**Figure 4. 12** Agarose was coated on the surface of complex. Through controlling the stirring rate, hydrogel outlayer of different thicknesses of (A) 5, (B) 20, and (C) 60  $\mu\text{m}$  can be formed on the surface of  $\beta$ -cell spheroid-hMSCs complex. Scale bar = 100  $\mu\text{m}$ .

#### 4.4 Discussion

Isolated cells from pancreatic islets and immortalized  $\beta$ -cells lines require contact with other cells or basement membrane proteins, or mimicry of these contacts to maintain function and viability when cultured in synthetic *in vitro* systems. Recognizing this requirement, different approaches have been developed that encourage or increase cell-cell contact for  $\beta$ -cells such as cell encapsulation, cellular co-culture with MSCs, cell aggregates, and so on. For cell aggregates, typical methods are hanging drop culture, round-bottomed 96-well culture, non-adhesive plate culture, agitation culture, and so on. Non-adhesive plate and agitation culture are difficult to control sphere diameter whereas

hanging drop culture is hard to handle spheres. Recently, a novel technique, high-throughput hydrogel microwells, has been developed to achieve mass sphere production with easy spheroid handling and diameter control. In this study, we have designed a computer controlled spheroid maker, which can produce mass spheroids automatically. Uniformed  $\beta$ -cell spheroids, derived from RIN-m cells, have been successfully fabricated. The size of  $\beta$ -cell spheroids can be manipulated through adjusting the cell seeding concentrations and recess diameters of micro-molds. These spheroids were readily removed from the devices and maintained their size and shape, presumably due to strong cell-cell attachment and low cell-material adhesion.

The first relates to cell aggregates is central necrosis. Although often seen during the culture of intact islets, the re-aggregated  $\beta$ -cells did not show signs of central necrosis, as the cell-permeable viability dye were able to penetrate to the interior of the aggregates and the central cells also stained green (Figure 4.3).

The maintenance of functional expression throughout cell manipulation is important for  $\beta$ -cells. The cells preserved intracellular insulin content at high levels as evidenced by immunostaining. The model  $\beta$ -cells used in this work did not show a size-dependent effect on cellular viability, but on functional expression. The bigger spheroids released more insulin. However, the same number of cells released more insulin from smaller spheroids in the range of 100-200  $\mu\text{m}$  (Figure 4.5). It may imply that the spheroid of 300  $\mu\text{m}$  is too big, cells in the core of spheroids have limited response to glucose; and then the function of the cells in the core may be compromised.

Mesenchymal stem cells, multipotent stromal cells with the potential to give rise to cells of diverse lineages, have been noted to possess the ability to impart profound immunomodulatory effects *in vivo*. MSCs were found to down-regulate T and B lymphocytes, natural killer cells and antigen presenting cells through various mechanisms, including cell to cell interaction and soluble factor production [30]. Aggregation of MSCs into three dimensional spheroids has shown to be more effective than MSCs from adherent monolayer cultures in suppressing inflammatory responses in a co-culture system with lipopolysaccharide-activated macrophages and in a mouse model for peritonitis [30]. Furthermore, MSCs can secrete trophic molecules to enhance survival, function, and angiogenesis of isolated islets after co-transplantation of islet and MSCs [5].

To construct core/shell structured complex of RIN-m/hMSCs, first of all, we have seeded these two types of cells in microwells simultaneously, the cells self-assembled into a spheroid and self-sorted with hMSCs integrating with each other and staying inside encapsulated by a thin layer of RIN-m cells. Human MSCs and RIN-m cells have different cohesive forces (like-to-like) and adhesive forces (unlike binding). Self-sorting occurs due to these differences with hMSCs of higher cohesion in the core and RIN-m cells with lower cohesion on the outside. Moreover, the differences in cytoskeletal mediated tension between these two types of cells may also result in self-sorting.

When co-culturing hMSCs with  $\beta$ -cells spheroids, hMSCs invaded into spheroids. To successfully construct core/shell structured  $\beta$ -cells spheroids/hMSCs complex, we have to inhibit hMSCs invasion. In this study, a physical barrier, non-degradable

hydrogel, was applied between  $\beta$ -cell spheroids and hMSCs. This hydrogel effectively inhibited hMSCs invasion. The hydrogel also served as another temperately shell for  $\beta$ -cells spheroids away from the hostile destruction as immunoisolation, which may further improve the survival of  $\beta$ -cells aggregates *in vivo*.

The maintenance of functional expression throughout cell manipulation is important for  $\beta$ -cell spheroids after coating. RIN-m spheroids were shown to maintain their functional expression throughout seeding, aggregation, culture, and coating. The coating cell concentration influenced the insulin secretion from  $\beta$ -cells spheroids. While compared to the co-culture data of hMSCs and  $\beta$ -cell spheroids, hMSCs did not enhance the insulin secretion in co-culture samples, which means the coating thickness is important to maintain the function of  $\beta$ -cells spheroids. To measure the beneficial effects of this co-culture strategy, we investigated the function of  $\beta$ -cell spheroids exposed to pro-inflammatory cytokines. We found that co-culture hMSCs with  $\beta$ -cell spheroids can protect  $\beta$ -cell spheroids from pro-inflammatory cytokines.

#### 4.5 Conclusion

In this study, different sizes of uniformed  $\beta$ -cells spheroids were successfully fabricated through our automatic high-throughput spheroid maker. Single  $\beta$ -cell in the spheroid with the diameter of 200  $\mu\text{m}$  expressed strongest insulin secretion compared to other sizes of 100, 300, 400 and 500  $\mu\text{m}$ . The novel core-shell structured spheroids-hMSCs complex was achieved through coating hydrogels as physical barrier on the surface of  $\beta$ -cells spheroids to inhibit hMSCs invasion. The thickness of hMSCs coating

affected the insulin secretion. Human MSCs prevented  $\beta$ -cells spheroids apoptosis and benefited insulin secretion when exposed to pro-inflammatory cytokines. This study provides a new therapeutic approach to treat type 1 diabetes in which cell therapies may be essential.

#### 4.6 References

1. Abbott, A., *Cell culture: Biology's new dimension*. Nature, 2003. **424**(6951): p. 870-872.
2. Layer, P.G., et al., *Of layers and spheres: the reaggregate approach in tissue engineering*. Trends in Neurosciences, 2002. **25**(3): p. 131-134.
3. Berglöf, E., et al., *Inhibition of proteoglycan synthesis affects neuronal outgrowth and astrocytic migration in organotypic cultures of fetal ventral mesencephalon*. Journal of Neuroscience Research, 2008. **86**(1): p. 84-92.
4. Li, X., et al., *Engineering neural stem cell fates with hydrogel design for central nervous system regeneration*. Progress in Polymer Science, 2012. **37**(8): p. 1105-1129.
5. Li, X., et al., *Improve the viability of transplanted neural cells with appropriate sized neurospheres coated with mesenchymal stem cells*. Medical Hypotheses, 2012. **79**(2): p. 274-277.
6. Astashkina, A., B. Mann, and D.W. Grainger, *A critical evaluation of in vitro cell culture models for high-throughput drug screening and toxicity*. Pharmacology & Therapeutics, 2012. **134**(1): p. 82-106.
7. Friedrich, J., et al., *Spheroid-based drug screen: considerations and practical approach*. Nat. Protocols, 2009. **4**(3): p. 309-324.
8. Hirschhaeuser, F., et al., *Multicellular tumor spheroids: An underestimated tool is catching up again*. Journal of Biotechnology, 2010. **148**(1): p. 3-15.
9. Dang, S.M., et al., *Efficiency of embryoid body formation and hematopoietic development from embryonic stem cells in different culture systems*. Biotechnology and Bioengineering, 2002. **78**(4): p. 442-453.

10. Tung, Y.-C., et al., *High-throughput 3D spheroid culture and drug testing using a 384 hanging drop array*. Analyst, 2011. **136**(3): p. 473-478.
11. Koike, M., et al., *Characterization of embryoid bodies of mouse embryonic stem cells formed under various culture conditions and estimation of differentiation status of such bodies*. Journal of Bioscience and Bioengineering, 2007. **104**(4): p. 294-299.
12. Fok, E.Y.L. and P.W. Zandstra, *Shear-Controlled Single-Step Mouse Embryonic Stem Cell Expansion and Embryoid Body-Based Differentiation*. STEM CELLS, 2005. **23**(9): p. 1333-1342.
13. Nyberg, S.L., et al., *Rapid, large-scale formation of porcine hepatocyte spheroids in a novel spheroid reservoir bioartificial liver*. Liver Transplantation, 2005. **11**(8): p. 901-910.
14. Kelm, J.M., et al., *Method for generation of homogeneous multicellular tumor spheroids applicable to a wide variety of cell types*. Biotechnology and Bioengineering, 2003. **83**(2): p. 173-180.
15. Lin, R.-Z. and H.-Y. Chang, *Recent advances in three-dimensional multicellular spheroid culture for biomedical research*. Biotechnology Journal, 2008. **3**(9-10): p. 1172-1184.
16. Karp, J.M., et al., *Controlling size, shape and homogeneity of embryoid bodies using poly(ethylene glycol) microwells*. Lab on a Chip, 2007. **7**(6): p. 786-794.
17. Sakai, Y., et al., *Effect of microwell chip structure on cell microsphere production of various animal cells*. Journal of Bioscience and Bioengineering, 2010. **110**(2): p. 223-229.
18. Dean, D.M., et al., *Rods, tori, and honeycombs: the directed self-assembly of microtissues with prescribed microscale geometries*. The FASEB Journal, 2007. **21**(14): p. 4005-4012.
19. Mironov, A.N.M.a.J.B.a.Z.H.a.W.B.a.J.V.L.d.S.a.R.P.V.a.R.R.M.a.V., *Scalable robotic biofabrication of tissue spheroids*. Biofabrication, 2011. **3**(2): p. 025002.
20. Robertson, R.P., *Update on transplanting beta cells for reversing type 1 diabetes*. Endocrinol Metab Clin North Am, 2010. **39**(3): p. 655-67.
21. Matsumoto, S., *Islet cell transplantation for Type 1 diabetes*. J Diabetes, 2010. **2**(1): p. 16-22.



22. Ludwig, B., et al., *Islet Versus Pancreas Transplantation in Type 1 Diabetes: Competitive or Complementary?* Current Diabetes Reports, 2010. **10**(6): p. 506-511.
23. Esther S. O'Sullivan, A.V., Daniel G. Anderson, and Gordon C. Weir, *Islets transplanted in immunoisolation devices: a review of the progress and the challenges that remain.* Endocrine Reviews, 2011. **32**(6): p. 827-844.
24. Lee, S.H., et al., *Human beta-cell precursors mature into functional insulin-producing cells in an immunoisolation device: implications for diabetes cell therapies.* Transplantation, 2009. **87**(7): p. 983-91.
25. Grundfest-Broniatowski, S.F., et al., *A New Bioartificial Pancreas Utilizing Amphiphilic Membranes for the Immunoisolation of Porcine Islets: A Pilot Study in the Canine.* ASAIO Journal, 2009. **55**(4): p. 400-405  
10.1097/MAT.0b013e3181a8deba.
26. Park, S.J., et al., *Functional improvement of porcine neonatal pancreatic cell clusters via conformal encapsulation using an air-driven encapsulator.* Exp Mol Med, 2012. **44**(1): p. 20-5.
27. Thibaudeau, K., et al., *Synthesis and Evaluation of Insulin-Human Serum Albumin Conjugates.* Bioconjugate Chemistry, 2005. **16**(4): p. 1000-1008.
28. Dang, T.T., et al., *Microfabrication of homogenous, asymmetric cell-laden hydrogel capsules.* Biomaterials, 2009. **30**(36): p. 6896-902.
29. Park, K.H., et al., *Insulinoma cell line (MIN6) adhesion and spreading mediated by Arg-Gly-Asp (RGD) sequence conjugated in thermo-reversible gel.* J Biosci Bioeng, 2005. **99**(6): p. 598-602.
30. Bartosh, T., et al., *Aggregation of human mesenchymal stromal cells (MSCs) into 3D spheroids enhances their antiinflammatory properties.* Proc Natl Acad Sci U S A, 2010. **107**(31): p. 13724-9.

## CHAPTER FIVE

### 5 LIF, IL-10 AND VEGF-LOADED NANOPARTICLES COATED MSC

#### MICROENCAPSULATED BETA-CELL SPHEROIDS

##### 5.1 Introduction

Type 1 diabetes, referred to as insulin-dependent diabetes mellitus, is an autoimmune disease resulting from the destruction of  $\beta$ -cells located in the islets of Langerhans of pancreas by autoantigen-reactive T lymphocytes (T cells) which produce immune factors to attack and destroy  $\beta$ -cells of pancreas [1]. T cells specific for pancreatic islet  $\beta$ -cell constituents (auto-antigens) exist normally but are restrained by regulatory mechanisms (self-tolerant state). When regulation fails,  $\beta$ -cell specific autoreactive T cells become activated and expand clonally. The pathogenic immune response would lead to islet inflammation. This is characterized by infiltration of the islet by macrophages and T cells that are cytotoxic, both directly and indirectly by producing cytokines [e.g., interleukin 1 (IL-1), tumor necrosis factor  $\alpha$  (TNF $\alpha$ ), TNF $\beta$ , and interferon  $\gamma$  (IFN $\gamma$ )] and free radicals that damage  $\beta$ -cells. Current evidence indicates that islet  $\beta$ -cell specific autoreactive T cells belong to a T helper 1 (Th1) subset, and these Th1 cells and their characteristic cytokine products, IFN $\gamma$  and IL-2, are believed to cause islet inflammation and  $\beta$ -cell destruction [2, 3]. Several approaches are being tested or are under consideration for clinical trials to prevent or arrest complete autoimmune destruction of islet  $\beta$ -cells and insulin-dependent diabetes. Approaches for the treatment of type 1 diabetes aimed at deleting  $\beta$ -cell autoreactive Th1 cells and cytokines (IL-1,

TNF $\alpha$ , TNF $\beta$ , and IFN $\gamma$ ) and increasing regulatory Th2 cells and/or Th3 cells and their cytokine products (IL-4, IL-10 and TGF $\beta$ 1).

Th1 cells and Th2 cells secrete cytokines to lead to strikingly different T cell actions. Th1 cells produce IL-2, IFN $\gamma$ , and TNF $\beta$  which attack islet  $\beta$ -cells, while Th2 secrete IL-4 and IL-10 to inhibit the production of the Th1 cytokines. IL-10 may favor Th2 over Th1 cell differentiation and function by inhibiting expression of MHC class II molecules and the B7 accessory molecule on macrophages, a major co-stimulator of T cells. IL-10 is effective in inhibiting Th1 effector function. The cytokine milieu specifically is critical for orchestration of lineage development towards aggressive effector T cell (Teff) or tolerant Treg phenotypes. Leukemia inhibitory factor (LIF) belongs to the IL-6 family of structurally related cytokines. LIF is associated with Tregs and immune tolerance [4]. LIF can reduce the inflammatory immune response *in vivo* by promoting regulatory Treg [5]. In addition to promoting immune tolerance via Treg, LIF is also well known to promote islet cell survival and LIF regulates  $\beta$ -cell mass [6, 7].

Pancreatic islets are well vascularized throughout life. This is important for their ability to secrete insulin swiftly in response to changes in blood glucose. Reestablishment of blood flow to transplanted islets requires several days. Rapid and adequate revascularization of transplanted islets is critical for islet survival and function. Delayed and insufficient revascularization can result in islet cell death and early graft failure. Therefore, developing strategies aimed at enhancing or accelerating this process is extremely important [8].

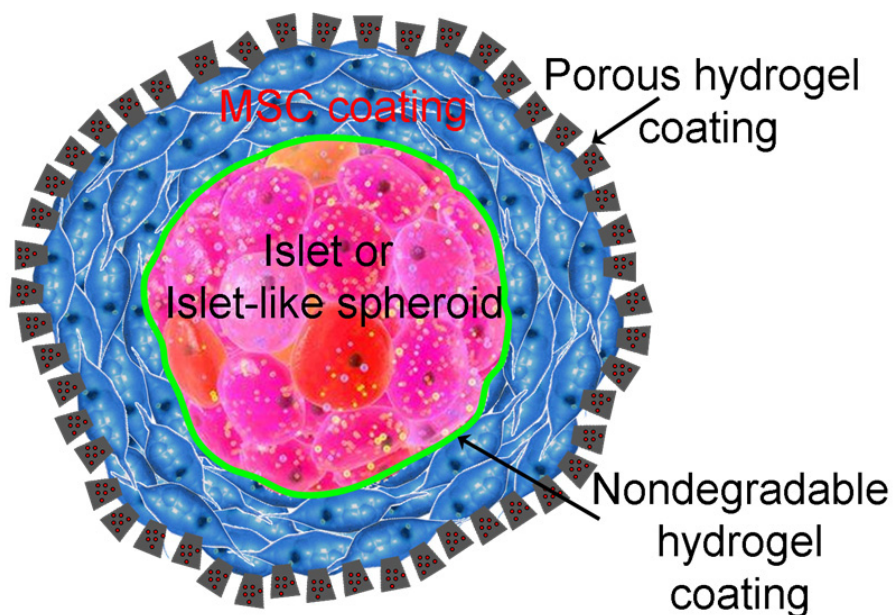


**Figure 5. 1** (A) The scheme of our core-shell structured  $\beta$ -cells/hMSCs/hydrogels complex. (B and C) The  $\beta$ -cells spheroids/hMSCs complex coated with agarose hydrogel mixed with LIF, VEGF and IL-10 loaded nanoparticles. Scale bar = 100  $\mu\text{m}$ .

To further improve the viability and suppress the immune rejection, a drug delivery system is really needed to delivery angiogenic and immune regulatory molecules like vascular endothelial growth factor (VEGF), IL-10 and LIF. Among drug delivery systems, poly (lactide-co-glycolide) (PLGA) nanoparticles have already demonstrated their potential for growth factors or immune regulatory molecules delivery in tissue equivalents. As temporally controlled systems, PLGA nanoparticles can protect the protein and release it at a specific time and for long time frames during tissue development [9-11]. In this study, we loaded IL-10, LIF, and VEGF into degradable PLGA nanoparticles and loaded nanoparticles into outside layer of agarose hydrogel, as Figure 5.1 shown, for sustained release; we then inspected the biological activities of

released IL-10 and LIF on survival and function of  $\beta$ -cells spheroids against pro-inflammatory cytokines, and the bioactivity of VEGF released from nanoparticles on the culture of human aortic endothelial cells.

## 5.2 Materials and methods

### 5.2.1 Materials

PLGA (50:50) was purchased from Sigma Chemical Co. (St. Louis, MO). Human interleukin 10 (IL-10) and rat VEGF were purchased from PeproTech (Rock Hill, NJ). Human LIF was purchased from Millipore (Billerica, MA). LIF enzyme-linked immunosorbent assay (ELISA) kit was obtained from Raybiotech, Inc. (Norcross, GA). IL-10 and VEGF ELISA kits were obtained from Sigma Aldrich. (St. Louis, MO). Transwell inserts of 8  $\mu$ m pores were purchased from Greiner Bio-One (Monroe, NC). All other reagents were purchased from Sigma Aldrich (St. Louis, MO).

### 5.2.2 Cell culture

Rat pancreatic  $\beta$ -cells of the RIN-m cell line were obtained from ATCC (CRL-2057). RIN-m cells were cultured in Roswell Park Memorial Institute (RPMI) 1640 medium supplemented with 10% fetal bovine serum at 37 °C in humid conditions with 5% CO<sub>2</sub>. The culture medium was exchanged every 2 days.

Human aortic endothelial cells (HAECs) were obtained from Sciencell (Carlsbad, CA). HAECs were maintained in endothelial cell medium supplemented with 5% fetal

bovine serum and 1% AA (Penicillin-Streptomycin). HAECs were incubated at 37 ° C under 5% CO<sub>2</sub>. Medium was changed every 3 days.

### 5.2.3 Fabrication of IL-10, LIF and VEGF-loaded PLGA nanoparticles

The IL-10, LIF, and VEGF-loaded PLGA nanoparticles were prepared using a water-in oil-in-water (W1/O/W2) solvent extraction/evaporation technique. Briefly, using LIF as an example, 2 µg LIF previously dissolved in a 1 mL 1% bovine serum albumin (BSA) buffer was emulsified by ultrasound (Branson Sonifier, CT) in 2 mL methylene chloride containing 50 mg PLGA for 5 min. This emulsion was poured into 10 mL of 1% polyvinyl acetate and emulsified by magnetic stirring at 500 rpm. After evaporation of the methylene chloride at room temperature for 4 hr, the nanoparticles were centrifuged at 14,000 rpm for 30 min, washed five times with deionized distilled water, and then lyophilized. The size and morphology of PLGA nanoparticle were inspected with Nanosizer/Particle Size Analyzer (Delsa™, Beckman Coulter, Inc.) and scanning electron microscope (SEM, JSM-5610, JEOL, Japan), respectively.

### 5.2.4 IL-10, LIF and VEGF release from PLGA nanoparticles

The release kinetics of IL-10, LIF, and VEGF from PLGA nanoparticles were examined in a phosphate buffered saline (PBS) buffer supplemented with 1% BSA and 10 µg/mL of heparin at 37 ° C, respectively. First, 3.5 mg of molecules-loaded PLGA nanoparticles was placed with 1% agarose hydrogel and then added 1 mL of buffer solutions in 15 mL tubes. The 1 mL of buffer was removed and the buffer was replaced

each time to maintain constant volume. The amount of molecules actually loaded within the PLGA nanoparticles was measured via extraction with 0.05N NaOH. Freeze-dried loaded nanoparticles (2mg, n-3) were dissolved with 1 mL of 0.05N NaOH under stirring. After 24 h, the solutions were centrifuged at 5000 rpm and the supernatant analyzed for growth factor content by ELISA. The amount of molecules released from nanoparticles was measured using ELISA kits. Cumulative release kinetics was calculated by normalizing the total release at each time point with the total loaded amount in nanoparticles.

#### 5.2.5 Bioactivity of LIF and IL-10 nanoparticles to pro-inflammatory cytokines

Thirty five  $\beta$ -cell spheroids per well were seeded to a 24 wells plate, a transwell insert was added into the well with LIF and IL-10 nanoparticles. Then these co-culture samples were exposed to a cocktail of pro-inflammatory cytokines including 100 ng/mL interferon- $\gamma$  (IFN- $\gamma$ ), 10 ng/mL tumor necrosis factor- $\alpha$  (TNF- $\alpha$ ), 0.5 ng/mL interleukin 1 $\beta$  (IL-1 $\beta$ ) for 24 hrs. Culture medium were removed from encapsulation samples for glucose-stimulated insulin secretion and washed twice with KRB solution. Samples were first placed in a low glucose concentration (1.1 mM) for 45min, followed by incubation in a high glucose concentration solution (16.7 mM) for 1 hr. The high glucose solutions were collected for insulin measurement by ELISA insulin kit.

#### 5.2.6 Analysis of $\beta$ -cells apoptosis by TUNEL assay

Cytokine induced  $\beta$ -cells damage was assessed by the TUNEL, a marker for cell apoptosis. After culture as 5.2.5 described above, the  $\beta$ -cells spheroids were fixed with

4% w/v paraformaldehyde. An APO-BrdU TUNEL Assay Kit (Invitrogen) was utilized, in which an AlexaFluor 488 labeled anti-BrdU antibody was used for detection of apoptotic cells. Propidium iodide staining was performed following to detect all the cells.

#### 5.2.7 Bioactivity of VEGF released from nanoparticles

The bioactivity of released VEGF from the PLGA nanoparticles was evaluated *in vitro* by determining the proliferative capacity of the HAECs. The CyQUANT cell proliferation assay kit was used to assess proliferation of the HAECs treated with nanoparticles supernatant and exogenous VEGF. The HAECs were plated in a density of 4000 cells/well in a 96-well plate. After 24 hours, the endothelial cell medium was removed and treated with exogenous VEGF (final concentration: 8, 16, and 32 ng/mL), and supernatant from VEGF nanoparticles (final concentration: 8, 16 and 32 ng/mL). After the 72 hrs, the contents of the assay wells were removed. Subsequent cell labeling with the CyQUANT reagent was according to the manufacturer's instructions. Microplates were read by plate reader.

#### 5.2.8 Loaded nanoparticles in RIN-m/hMSCs hybrid spheroids

The agarose hydrogel was mixed with biodegradable polyethylene glycol (PEG) hydrogel as the ratio of 1:1 to prepare hydrogel solution, and then the nanoparticles were mixed with hydrogel solution for RIN-m/hMSCs hybrid spheroids coating. The applied coating method was the same as chapter 4.2.8 described



### 5.2.9 Statistical analysis

Data are shown as mean  $\pm$  S.D. Statistical analyses were performed using oneway ANOVA (analysis of variance) followed by Tukey's post tests and the paired t-test where appropriate. A probability (*P*) value of  $<0.05$  was considered statistically significant.

## 5.3 Results and discussion

### 5.3.1 LIF and IL-10 nanoparticles

Figure 5.2 shows the morphology of LIF-loaded PLGA particles with a uniform size of approximately 400 nm (Figure 5.2 B). As Figure 5.3 shows, LIF can be released from PLGA nanoparticles in a controlled manner over 1 month. During the first 3 days, approximately 50% of total loaded LIF was released from the nanoparticles, followed by a steady release over 3 weeks. Another burst release occurred at 4 weeks due to the degradation and collapse of PLGA nanoparticles. During the first 3 days, LIF released from 3.5 mg nanoparticles was maintained at about 15 ng per day (Figure 5.3 B). Figure 5.4 reports the release profile of IL-10 from PLGA nanoparticles. IL-10 released from PLGA nanoparticles in a controlled manner about 6 weeks with a burst release of 27% during the first 3 days. These release profiles are similar to previous reports by other researchers [9, 11-13].

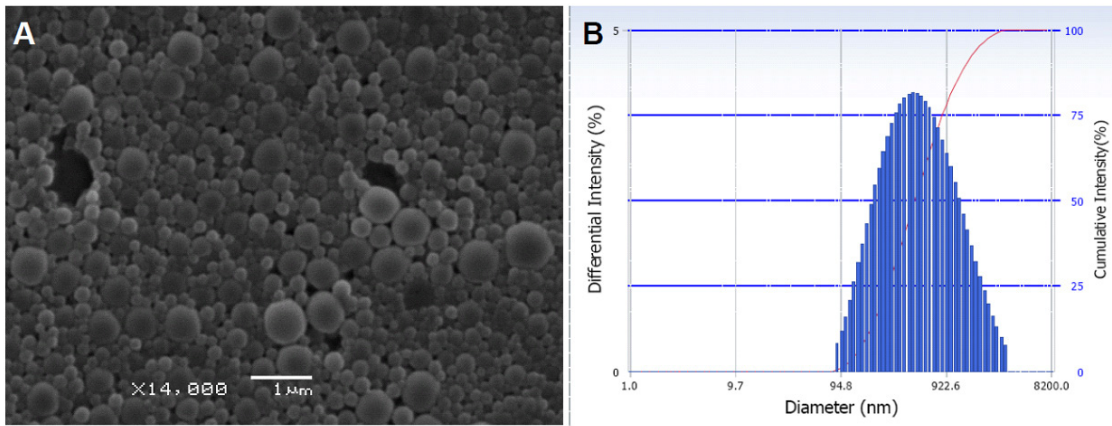


**Figure 5. 2** (A) LIF-loaded PLGA nanoparticles. (B) The average particle size is 400 nm.

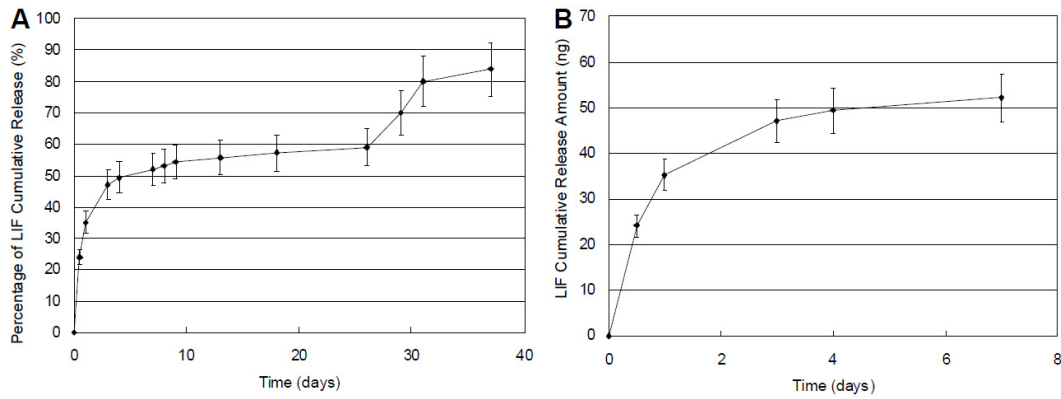


**Figure 5. 3** Cumulative *in vitro* LIF (A) percentage release from PLGA nanoparticles and (B) release amounts from 3.5 mg nanoparticles during the first 7 days.

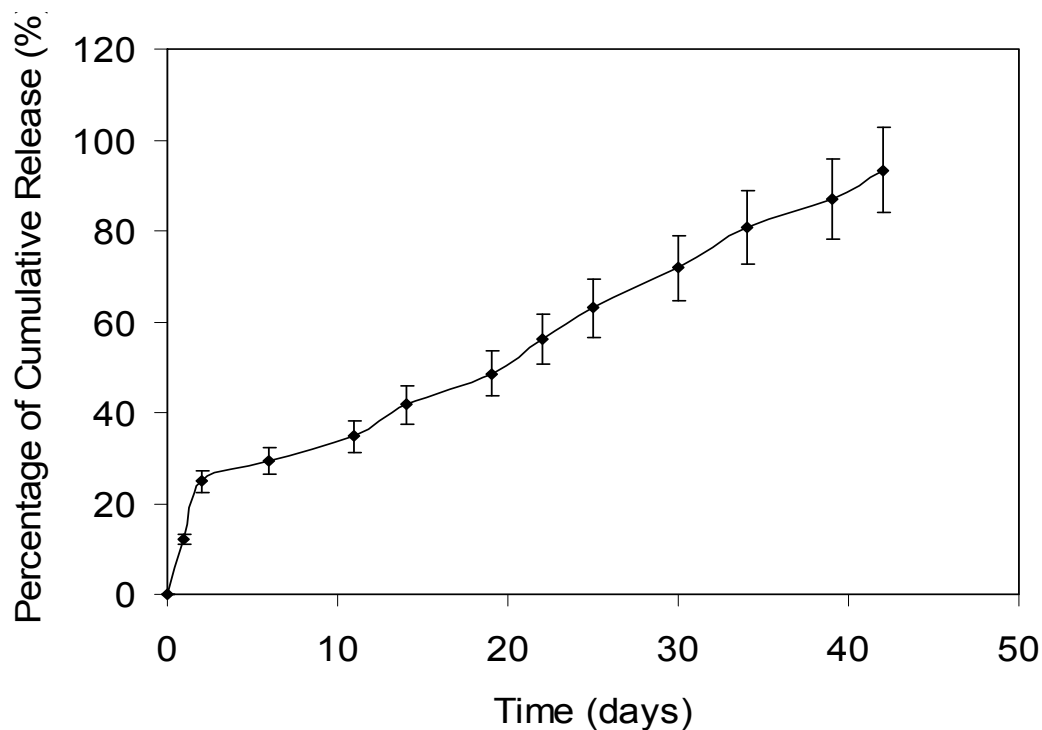


**Figure 5. 4** Cumulative *in vitro* IL-10 cumulative percentage release from PLGA nanoparticles.

### 5.3.2 Bioactivity of released IL-10 and LIF to pro-inflammatory cytokines

To investigate the effects of IL-10 and LIF on protecting  $\beta$ -cells spheroids from pro-inflammatory cytokines, such as interferon- $\gamma$ , tumor necrosis factor- $\alpha$ , and interferon  $1\beta$ , glucose stimulated insulin secretion was used to assess  $\beta$ -cell function in a two hour static incubation assay at low and high glucose concentrations. As shown in Figure 5.5, cytokine exposure significantly altered glucose stimulated insulin secretion of  $\beta$ -cells. Without nanoparticles, exposure to cytokines decreased insulin secretion of  $\beta$ -cells (38% lost when compared after and before exposure). In contrast, with nanoparticles,  $\beta$ -cells

lost 33% of insulin secretion. IL-10 and LIF loaded nanoparticles did not significantly preserve glucose stimulated insulin secretion. Apoptosis of  $\beta$ -cells cultured under these cytokines with LIF and IL-10 loaded nanoparticles or blank nanoparticles was shown in Figure 5.6. IL-10 and LIF did not prevent the apoptosis of  $\beta$ -cells. The reason lies in the facts that IL-10 is effective in inhibiting Th1 effector function whereas LIF is associated with Tregs [7, 14]. Especially, IL-10 (derived from macrophages and Th2 cells) exerts anti-inflammatory effects by inhibiting production of IL-12 and other pro-inflammatory macrophage cytokines (e.g., IL-1, IL-6, IL-8, TNF $\alpha$ ), by increasing macrophage production of IL-1 receptor antagonist, and by inhibiting the generation of oxygen and nitrogen free radicals by macrophages. Both IL-10 and LIF do not directly affect the  $\beta$ -cells. Since the situation *in vitro* (no T cells involving) is totally different from that *in vivo*, the further *in vivo* study will prove the benefits of LIF and IL-10 on survival and function  $\beta$ -cells [15, 16].

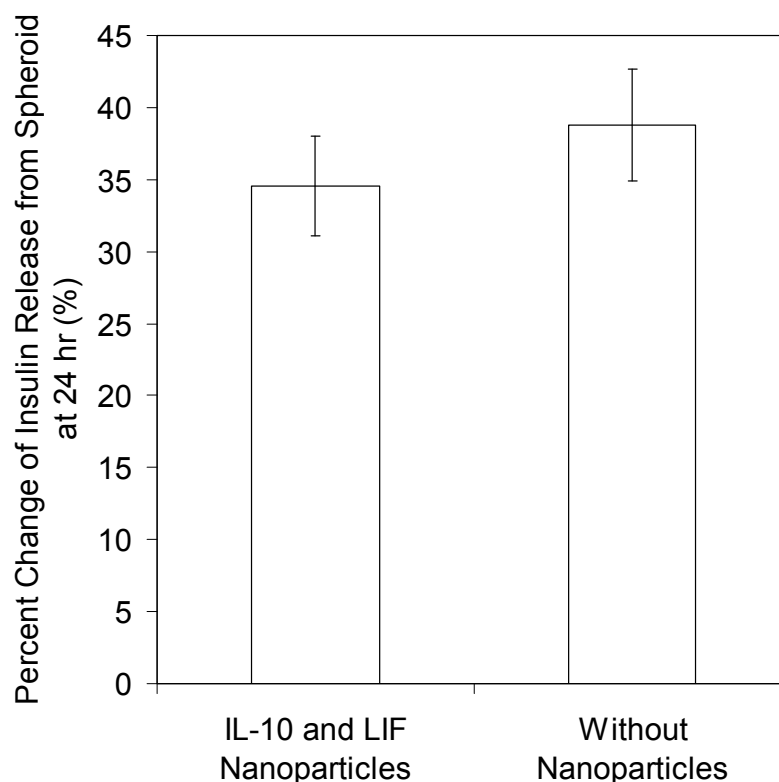
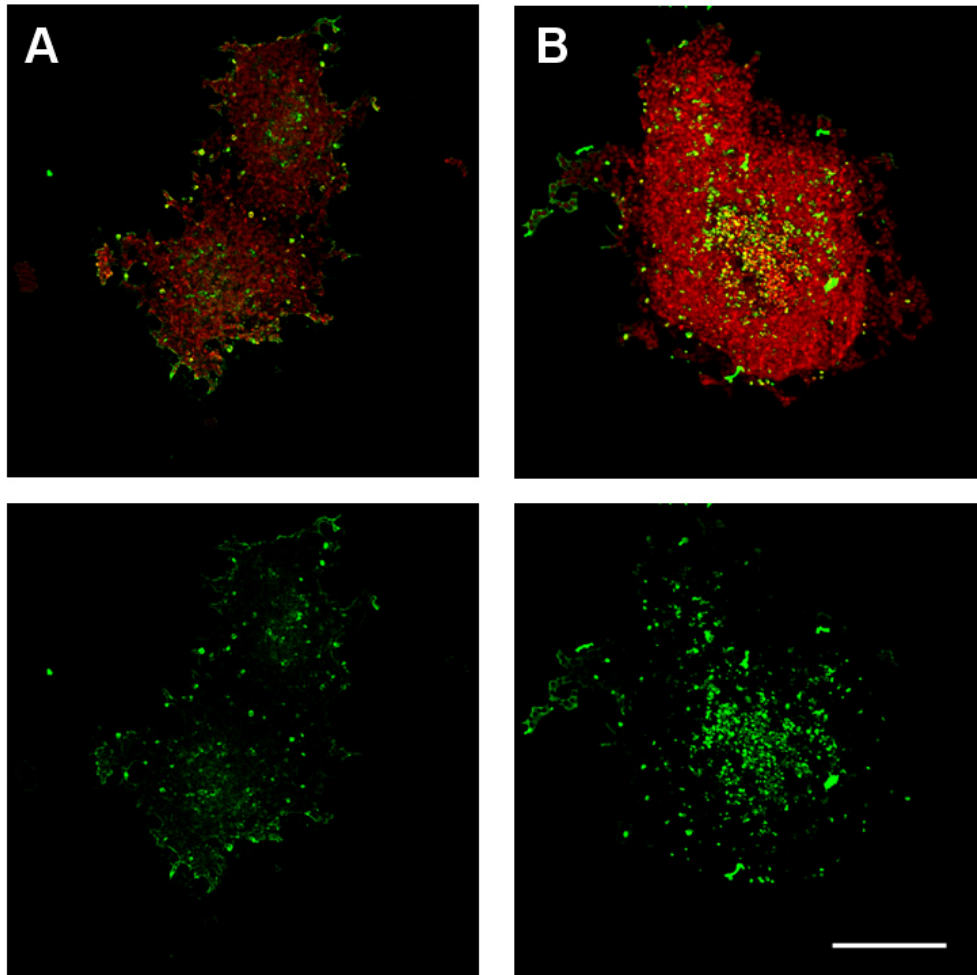


**Figure 5. 5** Beta-cells spheroids with the diameter of 200  $\mu\text{m}$  cultured with LIF and IL-10 loaded nanoparticles with a cocktail of cytokines of interferon- $\gamma$ , tumor necrosis factor- $\alpha$ , and interferon 1 $\beta$ .

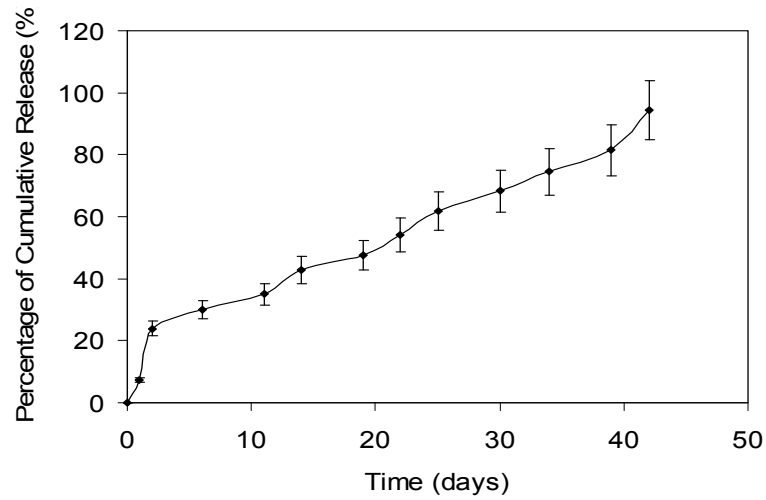
### 5.3.3 Bioactivity of released VEGF on HAECs

Figure 5.7 reports the release profiles of VEGF from PLGA nanoparticles. VEGF can be released from PLGA nanoparticles about 6 weeks in a controlled manner. The bioactivity of the VEGF released from the nanoparticles over time was assessed using an *in vitro* HAEC proliferation assay shown in Figure 5.8. Endothelial cells response to bioactive VEGF by proliferating is dose-dependent. These cells exposed to exogenous VEGF at the concentration of 16 ng/mL exhibited the highest proliferation rate when

compared to 8 and 32 ng/mL (\*  $P < 0.05$ ). In addition, the VEGF released from nanoparticles was as potent as exogenously added VEGF to enhance the proliferation of HAECs.



**Figure 5. 6** Apoptosis of  $\beta$ -cells with the diameter of 200  $\mu\text{m}$  cultured (A) with LIF and IL-10 loaded nanoparticles and (B) blank nanoparticles with a cocktail of cytokines of interferon- $\gamma$ , tumor necrosis factor- $\alpha$ , and interferon  $1\beta$ . AlexaFluor 488 labeled anti-BrdU antibody was used for detection of apoptotic cells and propidium iodide staining for all the cells. Scale bar = 100  $\mu\text{m}$ .



**Figure 5. 7** Cumulative *in vitro* VEGF cumulative percentage release from PLGA nanoparticles.

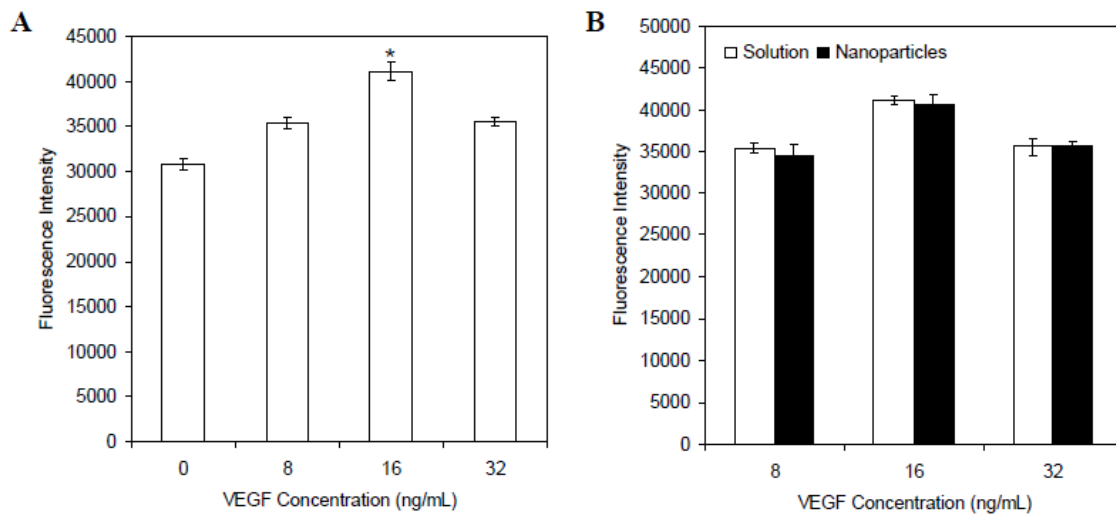


**Figure 5. 8** The bioactivity of the VEGF assessed using an *in vitro* HAEC proliferation assay. (A) The proliferation of HAEC affected by the concentration of VEGF. (B) Comparison of VEGF solution and VEGF released from nanoparticles on the proliferation of HAEC (\*  $P < 0.05$ ).

#### 5.3.4 Loaded nanoparticles in RIN-m/hMSCs hybrid spheroids

In this study, we design a hydrogel system mixed with non-degradable hydrogel (agarose) and biodegradable hydrogel (PEG). Growth factors loaded nanoparticles have been mixed with the hydrogels before the coating process. Hydrogel out layer formed on the surface of RIN-m/hMSCs hybrid spheroids with the thickness of 20  $\mu\text{m}$  was shown in the Figure 5.9.

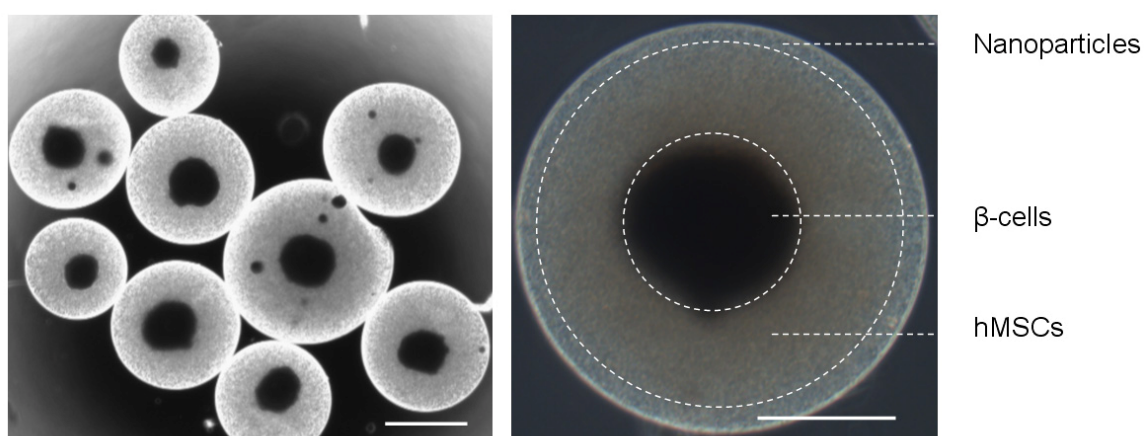


**Figure 5. 9** The  $\beta$ -cells spheroids/hMSCs complex coated with agarose hydrogel mixed with LIF, VEGF and IL-10 loaded nanoparticles. Scale bar = 100  $\mu\text{m}$ .

#### 5.4 Conclusion

In this chapter, LIF, IL-10 and VEGF loaded PLGA nanoparticles have been successfully fabricated through solvent extraction/evaporation techniques. These growth factors can be controlled release about 6 weeks. The bioactivity of released VEGF has been confirmed by the *in vitro* HAEC proliferation assay. The LIF and IL-10 did not



preserve the capacity of glucose stimulated insulin secretion of  $\beta$ -cells *in vitro* when exposure to the pro-inflammatory cytokines.

## 5.5 References

1. Padgett, L.E., et al., *The role of reactive oxygen species and proinflammatory cytokines in type 1 diabetes pathogenesis*. Ann N Y Acad Sci, 2013. **1281**: p. 16-35.
2. Johnsen-Soriano, S., et al., *IL-2 and IFN-gamma in the retina of diabetic rats*. Graefes Arch Clin Exp Ophthalmol. **248**(7): p. 985-90.
3. Rabinovitch, A. and W.L. Suarez-Pinzon, *Cytokines and their roles in pancreatic islet beta-cell destruction and insulin-dependent diabetes mellitus*. Biochem Pharmacol, 1998. **55**(8): p. 1139-49.
4. Metcalfe, S.M., *LIF in the regulation of T-cell fate and as a potential therapeutic*. Genes Immun, 2011. **12**(3): p. 157-68.
5. Park, J., et al., *Modulation of CD4+ T lymphocyte lineage outcomes with targeted, nanoparticle-mediated cytokine delivery*. Mol Pharm, 2011. **8**(1): p. 143-52.
6. Baeyens, L., et al., *In vitro generation of insulin-producing beta cells from adult exocrine pancreatic cells*. Diabetologia, 2005. **48**(1): p. 49-57.
7. Breuck, S., L. Baeyens, and L. Bouwens, *Expression and function of leukaemia inhibitory factor and its receptor in normal and regenerating rat pancreas*. Diabetologia, 2006. **49**(1): p. 108-116.
8. Bible, E., et al., *Neo-vascularization of the stroke cavity by implantation of human neural stem cells on VEGF-releasing PLGA microparticles*. Biomaterials, 2012. **33**(30): p. 7435-46.
9. Formiga, F.R., et al., *Sustained release of VEGF through PLGA microparticles improves vasculogenesis and tissue remodeling in an acute myocardial ischemia-reperfusion model*. J Control Release, 2010. **147**(1): p. 30-7.
10. Silva, E.A. and D.J. Mooney, *Spatiotemporal control of vascular endothelial growth factor delivery from injectable hydrogels enhances angiogenesis*. J Thromb Haemost, 2007. **5**(3): p. 590-8.

11. Borselli, C., et al., *Bioactivation of collagen matrices through sustained VEGF release from PLGA microspheres*. J Biomed Mater Res A, 2010. **92**(1): p. 94-102.
12. Sun, Q., et al., *Sustained vascular endothelial growth factor delivery enhances angiogenesis and perfusion in ischemic hind limb*. Pharm Res, 2005. **22**(7): p. 1110-6.
13. Ennett, A.B., D. Kaigler, and D.J. Mooney, *Temporally regulated delivery of VEGF in vitro and in vivo*. J Biomed Mater Res A, 2006. **79**(1): p. 176-84.
14. Sandler, S. and N. Welsh, *Interleukin-10 Stimulates Rat Pancreatic Islets in Vitro, but Fails to Protect against Interleukin-1*. Biochemical and Biophysical Research Communications, 1993. **195**(2): p. 859-865.
15. Yi, S., et al., *Adoptive Transfer With In Vitro Expanded Human Regulatory T Cells Protects Against Porcine Islet Xenograft Rejection via Interleukin-10 in Humanized Mice*. Diabetes, 2012. **61**(5): p. 1180-1191.
16. Dong, H., et al., *Immuno-isolation of pancreatic islet allografts using pegylated nanotherapy leads to long-term normoglycemia in full MHC mismatch recipient mice*. PLoS One, 2012. **7**(12): p. e50265.

## CHAPTER SIX

### 6 IN VIVO EVALUATION OF BETA-CELLS/MSC HYBRID SPHERIODS FOR THE TREATMENT OF TYPE 1 DIABETES

#### 6.1 Introduction

Islet transplantation, which can restore the recipients' ability to secrete insulin in a physiological manner, is the most promising approach to treat patients with type 1 diabetes. However, there are two major problems hindering this process. First, not enough donor islets are available for transplantation. Second, the function of transplanted islets is often compromised by the immune rejection response mounted to the grafts by the recipients [1-4]. Immunosuppressive agents used so far have severe toxic side effects and are sometime diabetogenic. Islet encapsulation with biocompatible materials can exert both immunoisolation and immunomodulation effects by (1) physically isolating islets from cytokines and host immune cells, and (2) delivering immune regulatory and immunomodulatory factors/cells locally to the islets to protect those islets from immune rejection [5-7]. Thus, with glycemia control well achieved by fewer donor islets, encapsulation technology not only solves the problems of limited islet supply, but also reduces/avoids the use of toxic immunosuppressants in the recipients.

The objective of this project is to develop an effective strategy for the treatment of type 1 diabetes using  $\beta$ -cells based replacement therapy. To improve the viability of transplanted  $\beta$ -cells, one novel approach is to transplant an optimal size range of  $\beta$ -cell spheroids rather than a cell suspension. Uniform sized multi-cellular spheroids can be coated with a thin layer of non-degradable hydrogel for immunoisolation. In addition, the

survival of spheroids of optimized size can be further improved with a novel coating of multiple layers of mesenchymal stem cells (MSCs), a cell type that has profound immunoregulatory effect, to prevent graft rejection [8]. To prevent MSCs from migrating away from spheroids, another layer of non-degradable hydrogel can be added. To further improve the viability and suppress the immune rejection, spheroids will be encapsulated with nanoparticles loaded with angiogenic (vascular endothelial growth factor, VEGF) [9] and immune regulatory molecules [interleukin-10 (IL-10) and leukemia inhibitory factor (LIF)] [10, 11]. By this means, the spheroid will passively evade the complications of stressors in addition to actively modulating the immune microenvironment for regulatory tolerance and long-term engraftment.

## 6.2 Materials and Methods

### 6.2.1 Materials

F40/80 and CD-31 antibodies were purchased from Abcam (Cambridge, MA). FOXP3 antibody was obtained from LifeSpan Bioscience (Seattle, WA); Insulin antibody was obtained from Santa Cruz Biotechnology (Dallas, Texas); Human mitochondria antibody was purchased from Millipore (Billerica, MA). Fluorophore-conjugated secondary antibodies were purchased from Jackson ImmunoResearch (West Grove, PA). All other reagents were purchased from Sigma Aldrich (St. Louis, MO).

### 6.2.2 Animals

Male C57BL/6 mice at 6–8 weeks of age were purchased from the Jackson Laboratory (Bar harbor, ME). All procedures were carried out using animals less than 12 weeks old and protocols were approved by the IACUC committee at Medical University of South Carolina.

### 6.2.3 Animal model and spheroids transplantation

C57BL/6 (H-2<sup>b</sup>) mice were rendered diabetic by one-time injection of streptozotocin (STZ) given intraperitoneally at 225 mg/kg as described before [12]. Five days after STZ administration, mice with two consecutive blood glucose levels exceeding 350 mg/dL were deemed diabetic and used as recipients. Beta-cell spheroids were transplanted under the kidney capsule of each recipient. There were 4 groups (n=5/group). Group I:  $\beta$ -cells spheroids; Group II:  $\beta$ -cells spheroids/hMSCs; Group III:  $\beta$ -cells spheroids/hMSCs coated with agarose hydrogel; Group IV:  $\beta$ -cells spheroid/hMSCs coated with porous hydrogel mixed with IL-10, LIF and VEGF loaded-nanoparticles. Beta cell function was monitored indirectly by measuring blood glucose levels twice per week.

### 6.2.4 Tissue processing, histology and immunohistochemistry

Beta-cells spheroid grafts including a portion of the kidney were harvested at the day 3, 9 and 30 post-transplantation. They were immediately rinsed in phosphate buffered saline (PBS), embedded in optimal cutting temperature compound, frozen, and sectioned on a cryostat according to routine histologic procedures. The sections (5  $\mu$ m thick) were

fixed with 4% (w/v) paraformaldehyde. For immunostaining, sections were permeabilized with 0.5% Triton X-100 and blocked with 4% normal goat serum in PBS for 2 hr. Primary antibodies were then applied overnight at 4 °C. The following primary antibodies were used: F40/80 to detect the expression of infiltrated macrophages inside the graft, CD-31 to identify the endothelial cells for angiogenesis, FOXP3 to inspect the regulatory T cells, and human mitochondria to check the survived human MSCs. Cy3 affinity secondary antibodies and goat anti-mouse and rabbit were used at 1:400. The specimens were imaged using a LSM 510 Meta Confocal Microscope (Zeiss, Thornwood, NY). At least 6 random fields per samples were analyzed for each group.

### 6.3 Results and discussion

#### 6.3.1 Macro-inspection of transplantation of spheroids

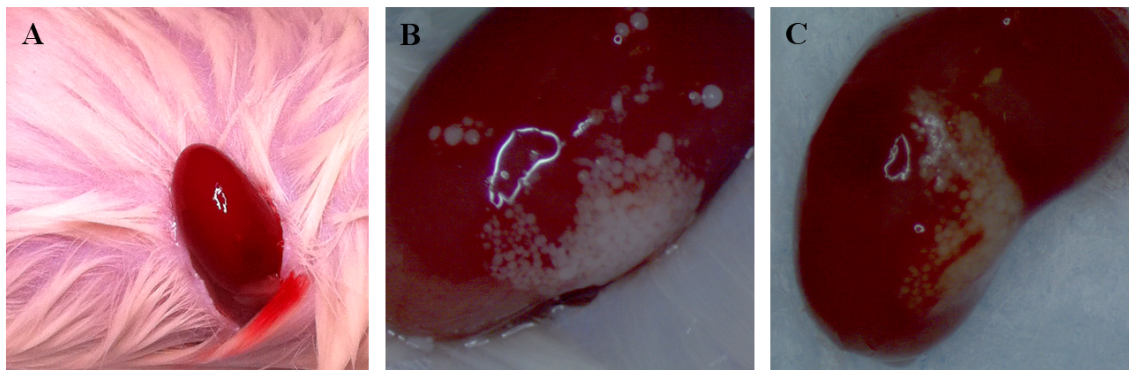


**Figure 6. 1** Macro inspection of spheroids transplantation. (A) The kidney has been exposed for  $\beta$ -cells spheroids transplantation. (B) Beta-cells spheroids have been transplanted under the kidney capsule. (C) Inspection of the  $\beta$ -cells spheroids after 3 days post-transplantation .

We have picked up the mouse as the species to construct the diabetes model since fewer cells are needed for the treatment when compared to a rat used as the model. As Figure 6.1 showed, the kidney has been exposed for spheroid transplantation. Beta-cell spheroids have been successfully transplanted under the kidney capsule. Three days later, these transplanted spheroids maintained their integrity and can be still identified.

### 6.3.2 Glucose level investigation

The function of transplanted  $\beta$ -cells was monitored indirectly by measuring blood glucose levels. As shown in Figure 6.2, during the first 2 days in the group of spheroids only, the glucose level was kept constant to that before transplantation (1.05 compared to 1). As for other three groups, all the glucose levels decreased a little bit. Without any treatment, the glucose level will increase significantly to 500 mg/dL at the day 3. All these results have implied that the transplanted  $\beta$ -cells worked with limited success to prevent the increasing of glucose level.

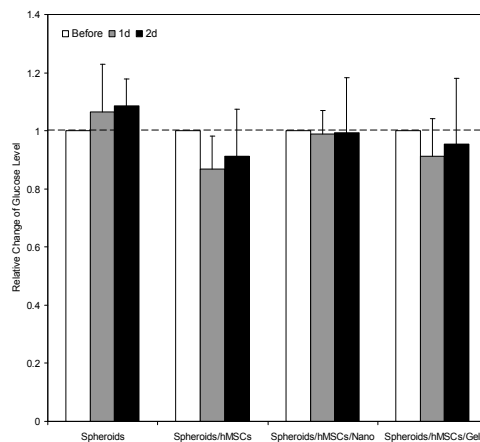


**Figure 6. 2** Glucose level after transplanted different groups of  $\beta$ -cells spheroids at the day 1 and 2.

Long-term investigation of glucose level has been recorded in the Figure 6.3. The glucose level of 500 mg/dL is assumed as failure control of the glucose condition. Based on this assumption, the control group, without any transplanted cells, the glucose level reached 500 mg/dL at the day 3 and increased with the time. During the inspection period (30 days), these four treatment groups expressed different glucose modulation times: 7 days for spheroids, 14 days for spheroids/hMSCs/nano, 30 days for spheroids/hMSCs/gel, respectively. The 7-day of glucose control time for spheroids only may imply that the survival of spheroids *in vivo* has significantly declined 7 days later after transplantation. Spheroids co-transplanted with hMSCs have maintained the glucose level during the whole period. Compared to spheroids only group, hMSCs may modulate the host immune response and enhance survival of spheroids at the transplantation site. The other two groups, both with a hydrogel out-layer, have exhibited limited success. The hydrogel out-layer has a thickness of about 20  $\mu\text{m}$ . This layer may have blocked the response of  $\beta$ -cells to host glucose or inhibited the secreted insulin free diffusion from the graft to host tissue. All these groups can not restore normoglycaemia and reduce the glucose to normal level (<200 mg/dL) [13]. This may be due to the low number of spheroids transplanted at first (just about 300) compared to the large number (>1000) of islet transplantation in other studies [14, 15].



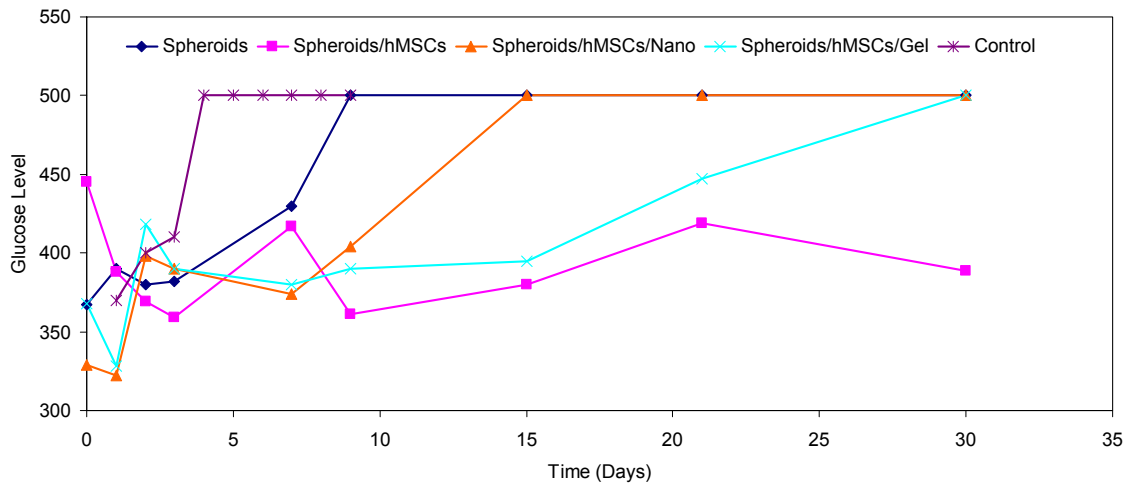


**Figure 6. 3** Glucose level after transplanted different groups of  $\beta$ -cells spheroids.

### 6.3.3 Survived hMSCs at the transplantation site

Human mitochondria have been used to identify the transplanted hMSCs shown in Figure 6.4. Especially for the group of spheroids/hMSCs, a large number of hMSCs survived at the transplantation site at day 30. In consideration to the spheroids with hydrogels, at the day 9, hMSCs still maintained the shell structure even though the encapsulated core,  $\beta$ -cells spheroids, had been lost during the histology process (Figure 6.4 G and H).

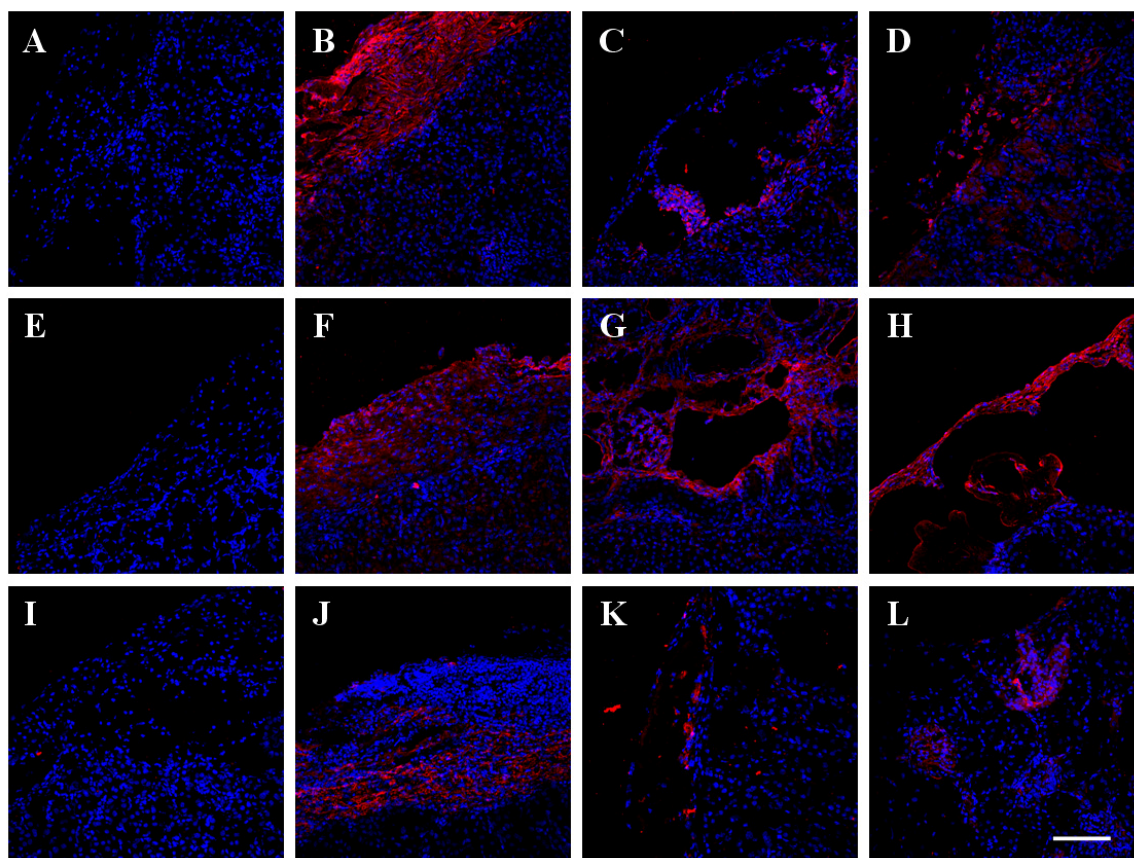


**Figure 6. 4** Human MSCs at the transplantation sites at the day of 3 (A-D), 9 (E-H) and 30 (I-L). (A, E and I) Beta-cells spheroids. (B, F and J) Beta-cells spheroids/hMSCs. (C, G and K) Beta-cells spheroids/hMSCs coated with agarose hydrogel. (D, H and L) Beta-cells spheroid/hMSCs coated with porous hydrogel mixed with IL-10, LIF and VEGF loaded-nanoparticles. Human MSCs were identified by mitochondria and nuclei by DAPI. Scale bar: 100  $\mu$ m.

#### 6.3.4 Macrophages

Figure 6.5 showed macrophages at the transplantation sites. Only in the group of spheroids, huge amounts of macrophages have existed all the time. As for the spheroids

transplanted with hMSCs, although at day 3 large numbers of macrophages appeared, at the day 9 the number of macrophages significantly decreased compared to spheroids only, and at the day 30, just few macrophages appeared at the transplantation site. All these results mean the hMSCs may suppress the inflammation at the transplantation site. Interestingly, when the spheroids were coated with an out-layer of agarose hydrogel, the spheroids did not induce an intense inflammation reaction especially at day 3. The IL-10, LIF and VEGF loaded-nanoparticles further inhibited the inflammation response at the day 3 (Figure 6.5 D compared to C). Moreover, very few macrophages existed all the time with these two groups of spheroids/hMSCs/gel and  $\beta$ -cells spheroid/hMSCs/nano. These spheroids with an out-layer of hydrogel were lost during the process of immunohistochemistry, which has been confirmed again by the empty pores on these specimens (Figure 6.5 G, H and L).

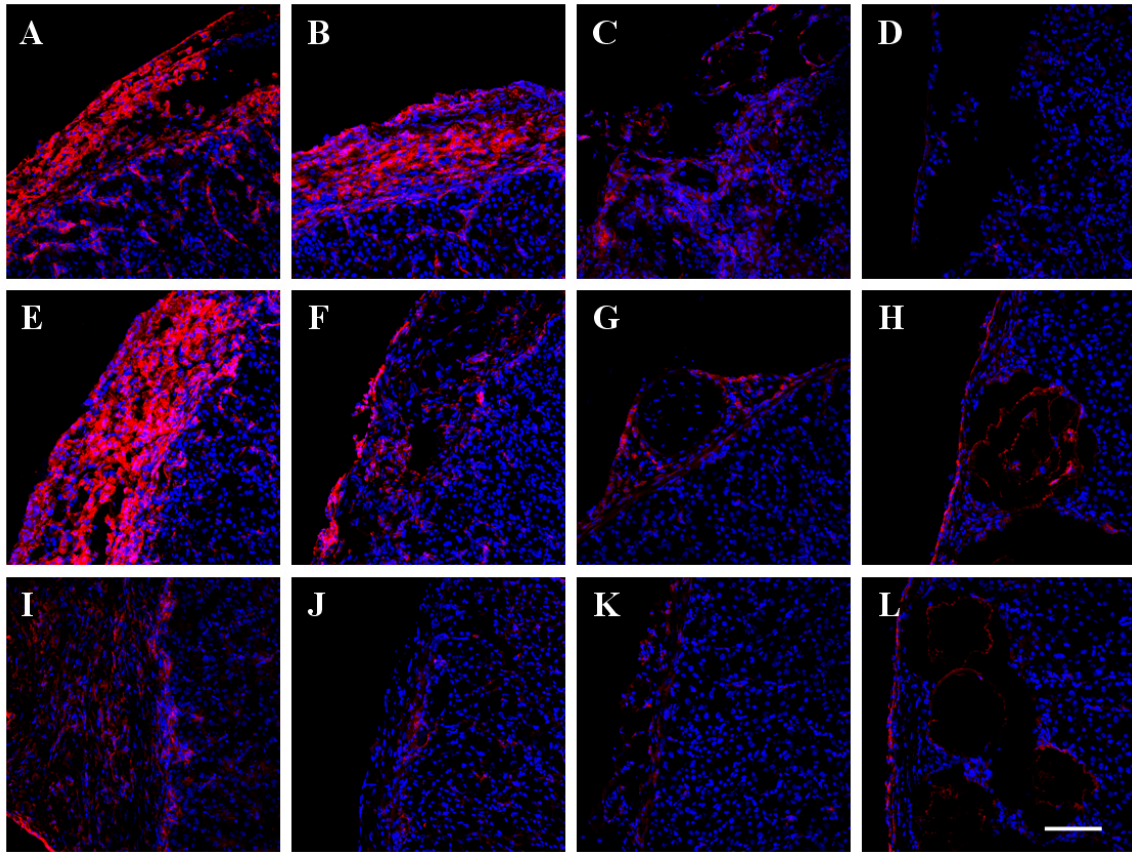


**Figure 6. 5** Macrophages at the transplantation sites at the day 3 (A-D), 9 (E-H) and 30 (I-L). (A, E and I) Beta-cells spheroids. (B, F and J) Beta-cells spheroids/ hMSCs. (C, G and K) Beta-cells spheroids/hMSCs coated with agarose hydrogel. (D, H and L) Beta-cells spheroids/hMSCs coated porous hydrogel mixed with IL-10, LIF and VEGF loaded-nanoparticles. Macrophages were identified by F40/80 and nuclei by DAPI. Scale bar: 100  $\mu\text{m}$ .

### 6.3.5 Regulatory T cells

The regulatory T cells are supposed to be activated by transplanted hMSCs to protect spheroids. As Figure 6.6 shows, no Foxp3<sup>+</sup> cells were observed in tissue sections

from all groups at 3 day following transplantation (Fig. A, B, C and D). At a later time, many more Foxp3+ cells were observed surrounding cell grafts from hMSCs group and nanoparticles loaded group, indicating that hMSCs initiated the regulatory T cells at day 9 and emphasized this activation further at day 30, and the IL-10, LIF and VEGF loaded-nanoparticles also activated regulator T cells at both day 9 and 30.

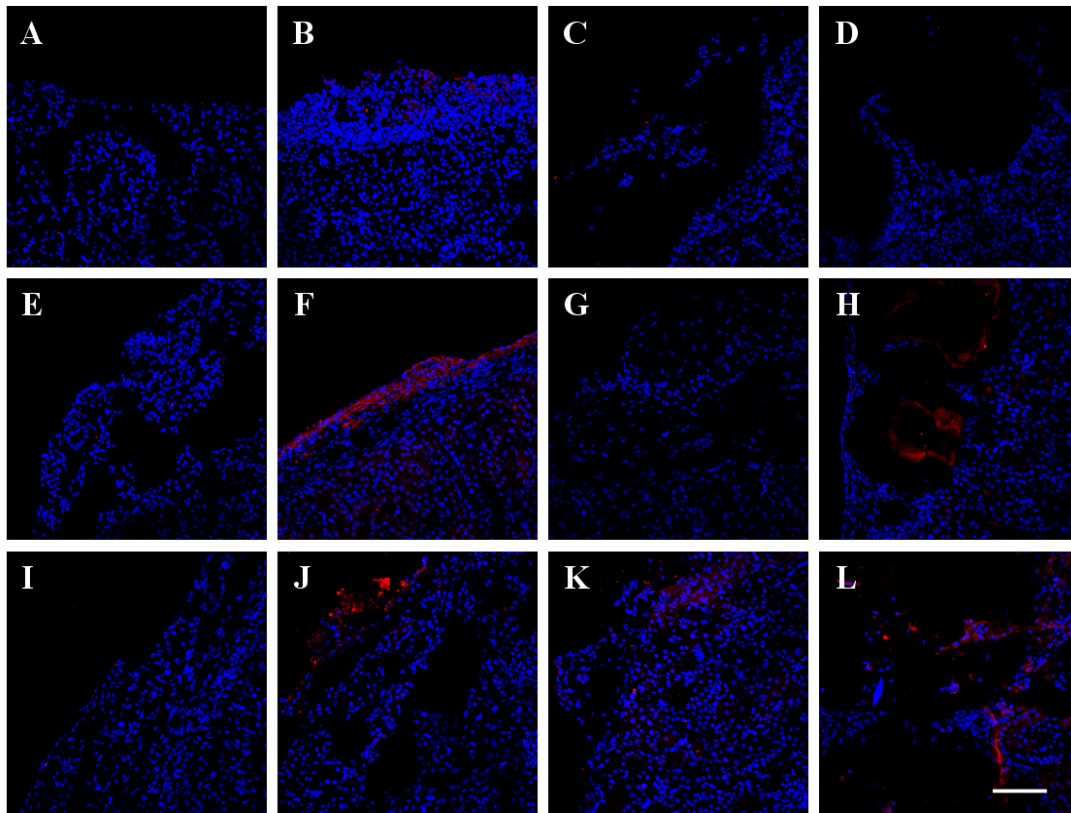


**Figure 6.6** Regulatory T cells at the transplantation sites at the day 3 (A, B, C and D), 9 (E, F, G, and H) and 30 (I, J, K and L). (A, E and I) Beta-cells spheroids. (B, F and J) Beta-cells spheroids/hMSCs. (C, G and K) Beta-cells spheroids/hMSCs coated with agarose hydrogel. (D, H and L) Beta-cells spheroids/hMSCs coated with porous hydrogel mixed with IL-10, LIF and VEGF loaded-nanoparticles. T cells were identified by FOXP3 and nuclei by DAPI. Scale bar: 100  $\mu$ m.

### 6.3.6 Blood vessels

Shown in the Figure 6.7, at day 3, there was no blood vessel formation at the transplantation sites in all groups. Compared to spheroids only, when spheroids transplanted with hMSCs, a blood vessel network had appeared at the transplantation site (Figure 6.7 F). The network became much more intense and structured at the day 30 (Figure 6.7 J). This phenomenon is consistent with other studies in which hMSCs benefited angiogenesis *in vivo* [16-18]. When considering the VEGF loaded nanoparticles in comparison to the gel group (Figure 6.7 G to H and K to L), the release of VEGF significantly enhanced the vasculature formation at the transplantation site. Well-structured blood vessel networks formed in the group of spheroids/hMSCs/nano, especially at day 30, and were consistent with other studies [19-21].



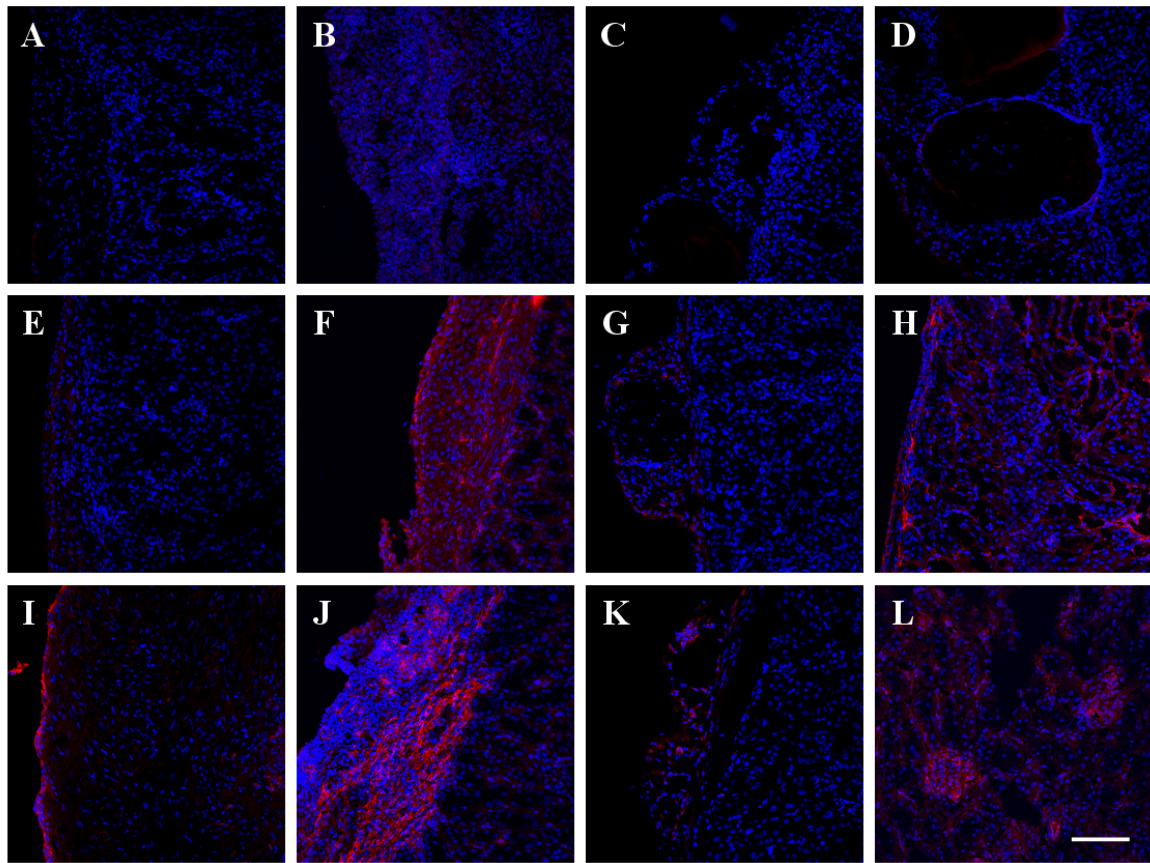


**Figure 6.** 7 Blood vessels inspected at the transplantation sites at the day 3 (A-D), 9 (E-H) and 30 (I-L). (A, E and I) Beta-cells spheroids. (B, F and J) Beta-cells spheroids/hMSCs. (C, G and K) Beta-cells spheroids/hMSCs coated with agarose hydrogel. (D, H and L) Beta-cells spheroid/hMSCs coated with porous hydrogel mixed with IL-10, LIF and VEGF loaded-nanoparticles. Blood vessels were identified by CD-31 and nuclei by DAPI. Scale bar: 100  $\mu$ m.

#### 6.4 Conclusion

In this study,  $\beta$ -cell spheroids were transplanted under the kidney capsule to treat diabetic mice. Beta-cells spheroids can keep the glucose level of diabetic mice constant.

Co-transplanted hMSCs can suppress the host inflammation response, activate the regulatory T cells and also promote angiogenesis at the transplantation sites. The  $\beta$ -cells spheroids/hMSCs/hydrogel complex initiated a mild inflammatory response. The LIF and IL-10, and VEGF loaded complex can further inhibit this response and promoted blood vessel network formation at the transplantation site. Our approach holds a great potential to treat type 1 diabetes.

## 6.5 References

1. Daoud, J., L. Rosenberg, and M. Tabrizian, *Pancreatic islet culture and preservation strategies: advances, challenges, and future outlook*. Cell Transplant, 2010. **19**(12): p. 1523-35.
2. Vaithilingam V, T.B., *Islet transplantation and encapsulation: an update on recent developments*. Rev Diabet Stud., 2011. **8**(1):**51-67**.
3. de Kort, H., et al., *Islet transplantation in type 1 diabetes*. BMJ, 2011. **342**: p. d217.
4. Matsumoto, S., *Islet cell transplantation for Type 1 diabetes*. J Diabetes, 2010. **2**(1): p. 16-22.
5. Giraldo, J.A., J.D. Weaver, and C.L. Stabler, *Tissue engineering approaches to enhancing clinical islet transplantation through tissue engineering strategies*. J Diabetes Sci Technol, 2010. **4**(5): p. 1238-47.
6. Esther S. O'Sullivan, A.V., Daniel G. Anderson, and Gordon C. Weir, *Islets transplanted in immunoisolation devices: a review of the progress and the challenges that remain*. Endocrine Reviews, 2011. **32**(6): p. 827-844.
7. Wilson, J.T. and E.L. Chaikof, *Challenges and emerging technologies in the immunoisolation of cells and tissues*. Advanced Drug Delivery Reviews, 2008. **60**(2): p. 124-145.
8. Li, X., et al., *Improve the viability of transplanted neural cells with appropriate sized neurospheres coated with mesenchymal stem cells*. Med Hypotheses, 2012. **79**(2): p. 274-7.



9. Patel, Z., et al., *In Vitro and In Vivo Release of Vascular Endothelial Growth Factor from Gelatin Microparticles and Biodegradable Composite Scaffolds*. *Pharmaceutical Research*, 2008. **25**(10): p. 2370-2378.
10. Metcalfe, S.M., *LIF in the regulation of T-cell fate and as a potential therapeutic*. *Genes Immun*, 2011. **12**(3): p. 157-68.
11. Battaglia, M., et al., *Rapamycin and Interleukin-10 Treatment Induces T Regulatory Type 1 Cells That Mediate Antigen-Specific Transplantation Tolerance*. *Diabetes*, 2006. **55**(1): p. 40-49.
12. Dong, H., et al., *Immuno-isolation of pancreatic islet allografts using pegylated nanotherapy leads to long-term normoglycemia in full MHC mismatch recipient mice*. *PLoS One*, 2012. **7**(12): p. e50265.
13. Rocuts, F., et al., *Bilirubin Promotes De Novo Generation of T Regulatory Cells*. *Cell Transplantation*, 2010. **19**(4): p. 443-451.
14. Carlos, A.G., Y. Teramura, and H. Iwata, *Cryopreserved Agarose-Encapsulated Islets As Bioartificial Pancreas: A Feasibility Study*. *Transplantation*, 2009. **87**(1): p. 29-34 10.1097/TP.0b013e318191b24b.
15. Kobayashi, T., et al., *Indefinite islet protection from autoimmune destruction in nonobese diabetic mice by agarose microencapsulation without immunosuppression*. *Transplantation*, 2003. **75**(5): p. 619-625.
16. Chen, D.Y., et al., *Three-dimensional cell aggregates composed of HUVECs and cbMSCs for therapeutic neovascularization in a mouse model of hindlimb ischemia*. *Biomaterials*, 2013. **34**(8): p. 1995-2004.
17. Lee, E.J., et al., *Potentiated therapeutic angiogenesis by primed human mesenchymal stem cells in a mouse model of hindlimb ischemia*. *Regen Med*, 2013. **8**(3): p. 283-93.
18. Lee, W.Y., et al., *Core-shell cell bodies composed of human cbMSCs and HUVECs for functional vasculogenesis*. *Biomaterials*, 2011. **32**(33): p. 8446-55.
19. Bible, E., et al., *Neo-vascularization of the stroke cavity by implantation of human neural stem cells on VEGF-releasing PLGA microparticles*. *Biomaterials*, 2012. **33**(30): p. 7435-46.
20. Sun, Q., et al., *Sustained vascular endothelial growth factor delivery enhances angiogenesis and perfusion in ischemic hind limb*. *Pharm Res*, 2005. **22**(7): p. 1110-6.

21. Chung, CW, et al., *VEGF microsphere technology to enhance vascularization in fat grafting*. *Ann Plast Surg*, 2012. **69**(2): p. 213-9.

## CHAPTER SEVEN

### 7 OVERALL CONCLUSIONS AND FUTURE DIRECTIONS

#### 7.1 Overall conclusions

The objective of this project is to develop an effective strategy for the treatment of type 1 diabetes using  $\beta$ -cell based replacement therapy. One novel approach to improve the viability of transplanted  $\beta$ -cells is to transplant an optimal size range of  $\beta$ -cell spheroids rather than a cell suspension. Uniform sized multicellular spheroids can be coated with a thin layer of non-degradable hydrogel for immunoisolation. In addition, the survival of spheroids of optimized size can be further improved with a novel coating of multiple layers of human mesenchymal stem cells (hMSCs), a cell type that has profound immunoregulatory effects, to prevent graft rejection. To prevent MSC migration away from spheroids, another layer of non-degradable hydrogel can be added. To further improve the viability and suppress the immune rejection, spheroids will be encapsulated with nanoparticles loaded with angiogenic and immune regulatory molecules. By this means the spheroid will passively evade the complications of stressors in addition to actively modulating the immune microenvironment for regulatory tolerance and long-term engraftment.

In Chapter 2, we have attempted to provide a detailed overview of bioengineering approaches for the treatment of type 1 diabetes, including insulin controlled release systems, immunoisolation of transplanted islets, and cell-based therapies, such as  $\beta$ -cells and stem cells.

In Chapter 3, we have created specific niche for  $\beta$ -cells *in vitro*. We have optimized our hydrogel systems for MIN6 cells 3D culture. We have found that the optimal condition for the cells to form artificial islets *in vitro* is the concentration of PEG at 5% and the ratios of 4-arm thiolated PEG to PEGTA at 1:2 (or 1:3). Conjugation with different peptides, especially, RGD at 0.2 mM, can significantly promote the insulin secretion, similar to the 2D control group.

In Chapter 4, we have fabricated different sizes of uniform  $\beta$ -cell spheroids through high-throughput automatic spheroids maker. Beta-cell spheroids with a diameter of 200  $\mu\text{m}$  exhibited the largest insulin secretion based on glucose stimulus when compared to others with sizes of 100, 300, 400 and 500  $\mu\text{m}$ . The novel core-shell structured spheroids-hMSCs complex was achieved through coating methylcellulose hydrogel as physical barrier on the surface of  $\beta$ -cell spheroids to inhibit invasion of hMSCs. Furthermore, hMSCs prevented apoptosis of  $\beta$ -cell spheroids and benefited insulin secretion when exposed to pro-inflammatory cytokines.

In Chapter 5, LIF, IL-10 and VEGF loaded PLGA nanoparticles were successfully fabricated through solvent extraction/evaporation technique. These growth factors can be controlled to release over about 6 weeks. The bioactivity of released VEGF has been confirmed by the *in vitro* HAEC proliferation assay. But the LIF and IL-10 did not preserve glucose stimulated insulin secretion of  $\beta$ -cells *in vitro* when exposure to the pro-inflammatory cytokines.

In Chapter 6,  $\beta$ -cell spheroids were transplanted under the kidney capsule to treat diabetic mice. Beta-cell spheroids kept the glucose level of diabetic mice constant. Co-

transplanted hMSCs suppressed the host inflammation response, activated the regulatory T cells and also promoted angiogenesis at the transplantation site. The  $\beta$ -cell spheroids/hMSCs/hydrogel complex initiated a mild inflammatory response. The LIF, IL-10, and VEGF loaded complex further inhibited this response and promoted blood vessel network formation at the transplantation site. Our approach holds a great potential to treat type 1 diabetes.

## 7.2 Future directions

### 7.2.1 Hydrogels conjugated with functional peptides

#### 7.2.1.1 Peptides with capacities of anti-immune response

In Chapter 5, we have constructed a hydrogel coated  $\beta$ -cell spheroids/hMSCs complex. The outer layer of hydrogel is supposed to accommodate nutrients, oxygen, and wastes diffusion out of the hydrogel. At the same time, the hydrogel will also permit pro-inflammatory cytokines and other effector molecules of low molecular weight, such as IL-1 $\beta$  (17.5 KD) and TNF- $\alpha$  (51 KD), to enter the capsules. Besides the benefits of hMSCs and LIF and IL-10 loaded nanoparticles to prevent the toxic effects of these-inflammatory cytokines, we want to conjugate cytokine-inhibitory peptides on the hydrogel to further exert a protective effect on cells from damage induced by pro-inflammatory cytokines that were able to permeate the capsules.

A peptide inhibitor for cell surface IL-1 receptor (IL-1R) can block the interaction between encapsulated cells and cytokines diffusing into the hydrogel. The IL-1R inhibitory peptide sequence, FEWTPGWYQPYY, has been reported [1] to conjugate to our

hydrogels. This sequence can be designed as CCRRFEWTPGWYQPYWLC and be synthesized by solid phase method.

#### 7.2.1.2 Peptides with capacities of vascularization

A synthetic 15 amino acid peptide, KLTWQELYQLKYKGI, based on a region of the vascular endothelial growth factor (VEGF) binding interface, has been shown to possess similar biological activity to that of the VEGF protein [2]. Except VEGF loaded nanoparticles, this sequence can be designed as CCRRKLTWQELYQLKYKGIWLC, be synthesized by solid phase method, and can be conjugated to our hydrogels.

### 7.2.2 Adjusting the structure of $\beta$ -cells spheroids-hMSCs complex

#### 7.2.2.1 Optimizing the size of spheroids and the thickness of shell of hMSCs

Cells in aggregates or groups can form a community to provide paracrine signaling or trophic support for neighboring transplanted cells to be able to survive in a community manner. One important parameter in the spheroid structure is the size or diameter. If the spheroid size is too big, the nutrient and oxygen support for the cells in the core of the spheroid will be limited or insufficient. If the spheroid size is too small, the beneficial impact of the multicellular community may be limited. Although we have demonstrated high viability of spheroids of different sizes *in vitro*, there is an optimal range of the spheroid size to get the highest survival rate for the transplanted  $\beta$ -cells *in vivo*. In Chapter 6, it will be our further work to inspect the effects of the size of  $\beta$ -cells on survival of transplanted cells. Moreover, the thickness of hMSCs will also affect the

survival of  $\beta$ -cells in the core of spheroids. The optimal thickness of the shell of hMSCs needs to be investigated further. Moreover, the fate of hMSCs after transplantation into the tissue is a big issue we need to address.

#### 7.2.2.2 Optimizing the hydrogel shell on the outlayer

In Chapter 5, we have selected agarose and PEG hydrogels to coat on the surface of the  $\beta$ -cell spheroids/hMSCs complex. The functions of this hydrogel out layer lie in: (1) to keep the complex intact during the transplantation process; (2) to prevent hMSCs from migrating away from the spheroids, especially at the acute and sub-acute phase (1-3 weeks) because of the capacities of anti-inflammation and immunomodulation of hMSCs. However, this layer of hydrogel definitely affects the transportation of oxygen and nutrients to encapsulated cells in complex. Even PEG hydrogel is degradable through hydrolysis *in vivo*, the optimal thickness of this out layer of hydrogel is something we need to inspect.

### 7.2.3 Clinical use of our approaches

#### 7.2.3.1 Cell source

Induced pluripotent stem cells (iPSCs) have been extensively studied in recent years as they offer the potential to generate patient-specific cells for autologous use, presumably avoiding the need for immunosuppression. The patient's own fibroblasts can be harvested and used to generate iPSCs. Induced pluripotent stem cells, as a source of  $\beta$ -cells, have years of research ahead before clinical translations. It will be our future work

to use iPSC-derived  $\beta$ -cells to fabricate spheroids and spheroids-MSCs complex for clinical use [3].

The hydrogel coated on the surface of the complex can prevent transplanted  $\beta$ -cells from host immune response. Our selected hydrogel, methyl cellulose, is biodegradable. The resorption of cellulose in human tissues does not occur, since cells are not able to synthesize cellulases [4]. The methyl cellulose is sufficiently nondegradable to enable use of xenogeneic cells.

#### 7.2.3.2 Our approaches for clinical use

As for clinical use, the spheroids will be fabricated from our robot spheroid maker and can be cultured long-term in a floating flask on a shaker. The complex of spheroids-hMSCs will be fabricated 3 days before transplantation. Sterilized hydrogel precursor solutions through 0.22  $\mu\text{m}$  filters and the complex can be transplanted into patients through syringes.

### 7.3 References

1. Su, J., et al., *Anti-inflammatory peptide-functionalized hydrogels for insulin-secreting cell encapsulation*. Biomaterials. **31**(2): p. 308-314.
2. Leslie-Barbick, J.E., et al., *The promotion of microvasculature formation in poly(ethylene glycol) diacrylate hydrogels by an immobilized VEGF-mimetic peptide*. Biomaterials, 2011. **32**(25): p. 5782-9.
3. Hua, H., et al., *iPSC-derived beta cells model diabetes due to glucokinase deficiency*. J Clin Invest, 2013.



4. Martson, M.; Viljanto, J.; Hurme, T.; Laippala, P.; Saukko, P. Is cellulose sponge degradable or stable as implantation material? An in vivo subcutaneous study in the rat. *Biomaterials* 1999, 20(21): p. 1989-95.